MODULATING CALCIUM SIGNALING PATHWAYS IN CEREBELLAR PURKINJE CELLS ALLEVIATES SPINOCEREBELLAR ATAXIA 2

APPROVED BY SUPERVISORY COMMITTEE

_____
Ilya Bezprozvanny, PhD

_____
Steve Cannon, MD PhD

_____
Robin Hiesinger, PhD

_____
Ege Kavalali, PhD

Acknowledgements

I would like to thank Ilya Bezprozvanny for the opportunity to work on such an amazing project, for giving me an avenue to put my hands to work, for the opportunity to learn a lot of techniques and above all pulling me out of my comfort zone and encouraging me to push my self-set limits. I would also like to thank my thesis committee members for direction and helpful feedback on my projects. I would like to acknowledge Dr. Rolf Joho for his expertise in cerebellar purkinje cells, helpful discussions at the start of my electrophysiology experiments and input during my thesis committee meetings. Special thanks to the past and present members of the Bezprozvanny lab for their generous direct and indirect assistance in various parts of these projects. Without their direct and indirect input, my thesis project would not have been this fruitful because they provided a nurturing environment for science. Finally, I would like to thank my loving family and friends for believing in me over the years and for supporting every educational endeavor I have embarked on.

MODULATING CALCIUM SIGNALING PATHWAYS IN CEREBELLAR PURKINJE CELLS ALLEVIATES SPINOCEREBELLAR ATAXIA 2

by

ADEBIMPE WAKILAT KASUMU

DISSERTATION

Presented to the Faculty of the Graduate School of Biomedical Sciences

The University of Texas Southwestern Medical Center at Dallas

In Partial Fulfillment of the Requirements

For the Degree of

DOCTOR OF PHILOSOPHY

The University of Texas Southwestern Medical Center at Dallas

Dallas, Texas

April, 2012

MODULATING CALCIUM SIGNALING PATHWAYS IN CEREBELLAR PURKINJE CELLS ALLEVIATES SPINOCEREBELLAR ATAXIA 2

ADEBIMPE WAKILAT KASUMU

The University of Texas Southwestern Medical Center at Dallas, 2012

Supervising Professor: Ilya Bezprozvanny, PhD

Spinocerebellar ataxia 2 (SCA2) is a neurodegenerative disorder characterized by progressive ataxia. SCA2 results from the polyglutamine expansion in the cytosolic protein ataxin-2 (Atx2). Cerebellar Purkinje cells (PC) are primarily affected in SCA2, but the cause of PC dysfunction, PC death and motor incoordination in SCA2 is poorly understood. It has been reported that mutant, but not wild type Atx2, specifically binds to the inositol 1,4,5-trisphosphate receptor ($InsP_3R$) and increases its sensitivity to activation by IP3. Thus, this toxic gain-of-function of Atx2 results in supranormal calcium (Ca^{2+}) release from the PC endoplasmic reticulum and may play a key role in the development of SCA2 pathology. The primary focus of this dissertation will be to further elucidate the

underlying mechanism of SCA2 pathogenesis, identify therapeutic targets and develop a potential treatment of SCA2. The first part of this dissertation will test the hypothesis that suppressing $InsP_3R$-mediated Ca^{2+} signaling alleviates age-dependent dysfunction, and degeneration of PCs in SCA2 mice. The second part of this dissertation will focus on testing the efficacy of novel compounds that modulate calcium-activated potassium (SK) channels in the symptomatic treatment of SCA2.

I conclude from this work that supranormal $InsP_3$--Ca^{2+} signaling plays an important role in SCA2 pathogenesis. Partial inhibition of $InsP_3$-mediated Ca^{2+} signaling or regularizing PC firing with SK channel modulators could provide therapeutic benefit for the patients afflicted with SCA2 and possibly other SCAs.

TABLE OF CONTENTS

Prior Publications

Kasumu A, Bezprozvanny I. (2010) Deranged calcium signaling in Purkinje cells and Pathogenesis of Spinocerebellar ataxia 2 and other ataxias. *The Cerebellum* PMID 20480274

Ross AP, Bruggeman EC, **Kasumu AW**, Mielke JG, Parent MB. (2012) Non-alcoholic fatty liver disease impairs hippocampal-dependent memory in male rats. *Physiology and Behavior*

Kasumu AW, Xia Liang, Polina Egorova, Daria Vorontsova, Bezprozvanny I. Chronic suppression of inositol 1,4,5-triphosphate receptor-mediated calcium signaling in cerebellar Purkinje cells alleviates pathological phenotype in spinocerebellar ataxia 2 mice (*Journal of Neuroscience*, under review)

Publications in preparation

Kasumu AW, Hougaard C, Rode F, Sabatier JM, Eriksen BL, Strøbæk D, Xia Liang, Polina Egorova, Daria Vorontsova, Christophersen P, Rønn LCB, Bezprozvanny I. Pharmacological modulation of SK channels reverts irregular cerebellar activity and improves motor function in a mouse model of spinocerebellar ataxia 2 (*Chemistry & Biology*, Awaiting submission)

LIST OF FIGURES

LIST OF TABLES

LIST OF DEFINITIONS

SCA2- Spinocerebellar ataxia 2

PC- Purkinje cell

WT- Wildtype

Atx2 – Ataxin 2

PolyQ - polyglutamine

Atx2-58Q – Polyglutamine expanded ataxin 2

58Q – SCA2-58Q mouse model

IP3- Inositol 1,4,5-triphosphate

$InsP_3R1$- Inositol 1,4,5-triphosphate receptor

IICR – IP3-induced Ca^{2+} release

CICR – Ca^{2+}-induced Ca^{2+} release

NMDA - N-methyl-D-aspartic acid

RYR – Ryanodine receptors

DCD – Dark cell degeneration

5PP – Inositol 1,4,5-triphosphate 5-phosphatase

RA – R343A mutant 5PP

DM – double R343A/R350A mutant 5PP

NI – non injected

SK – small conductance calcium-activated potassium channel

BK – big/large conductance calcium-activated potassium channel

CyPPA – Cyclohexyl-[2-(3,5-dimethyl-pyrazol-1-yl)-6-methyl-pyrimidin-4-yl]-amine. An SK modulator with high selectivity and low potency

NS13001 – (4-Chloro-phenyl)-[2-(3,5-dimethyl-pyrazol-1-yl)-9-methyl-9*H*-purin-6-yl]-amine. An SK modulator with high selectivity and potency

NS309 – 3-Oxime-6,7-dichloro-1H-indole-2,3-dione, An SK modulator with low selectivity and potency

1-EBIO – 1-ethyl-2-benzimidazolinone

DNs – dopaminergic neurons

VGCCs – voltage-gated calcium channels

CB – calbindin

CB – parvalbumin

ALS – Amyotrophic lateral sclerosis

CHAPTER ONE

General introduction

General introduction

Spinocerebellar ataxias (SCAs) constitute a heterogeneous group of autosomal-dominant genetic and neurodegenerative disorders. SCAs are generally characterized by cerebellar atrophy and a progressive incoordination of movement known as ataxia (Filla et al., 1999, Schols et al., 2004, Lastres-Becker et al., 2008). Over 30 SCAs have been identified and named in the chronological order of their discovery from SCA1 to SCA30 (Matilla-Duenas et al., 2009). Although all SCA patients present with the phenotypic overlap of cerebellar atrophy and ataxia, few other brain regions are differentially affected in each SCA. Seventeen genes have been associated with these SCAs and it is not understood how mutations in those SCA-associated genes lead to the SCA pathogenesis (Paulson, 2009). The pathogenesis of SCAs is not fully understood, however, several different pathogenic mechanisms have been studied in SCAs such as dysregulation of transcription and gene expression, alterations in calcium homeostasis and synaptic neurotransmission, mitochondrial stress and apoptosis (reviewed in (Carlson et al., 2009, Matilla-Duenas et al., 2009, Bezprozvanny and Klockgether, 2010, Kasumu and Bezprozvanny, 2010)). Currently, therapy for SCA patients is mainly supportive and directed at treating individual symptoms in each subtype (Pirker et al., 2003, Bezprozvanny and Klockgether, 2010). No disease-modifying therapy exists for any of the SCAs. In order to develop a successful treatment of SCAs, it will be important to identify a valid therapeutic target and understand the pathogenic pathways.

Emerging research suggest that a fundamental cellular pathway is disrupted by some of the mutated SCA genes, which could explain the characteristic death of Purkinje cells, cerebellar atrophy and the resulting ataxia (Lin et al., 2000, Vig et al., 2000, Serra et al.,

2006, Adachi et al., 2008, Chen et al., 2008, Hara et al., 2008, Iwaki et al., 2008, Watase et al., 2008, Liu et al., 2009). I propose that mutations in SCA genes disrupt multiple cellular pathways, but SCA pathogenesis does not begin and progress until calcium homeostasis is disrupted in cerebellar Purkinje cells (PC). This can occur either as a result of an excitotoxic increase or a compensatory suppression of PC calcium signaling, which eventually leads to cellular dysfunction and cell death. A similar hypothesis was recently proposed based on the comparison of genes involved in cerebellar plasticity and human ataxias (Schorge et al., 2010).

Calcium signaling in Purkinje cells is important for normal cellular function as these neurons express a variety of calcium channels, calcium-sensitive kinases and phosphatases, calcium sensors, calcium stores, compartments and buffers to tightly maintain intracellular calcium (Ca^{2+}) homeostasis. Glutamate, an excitatory neurotransmitter, induces a transient increase in the cytoplasmic calcium level of PCs via activating ionotropic AMPA receptors and metabotropic glutamate receptors (mGluR). Activation of AMPA receptors causes membrane depolarization, activation of voltage-gated calcium channels (VGCCs) and calcium influx into the cytoplasm. Activation of mGluR couples to Ca^{2+} release from endoplasmic reticulum stores via activating inositol 1,4,5-triphosphate receptors ($InsPR_3$) to allow a transient increase in cytoplasmic Ca^{2+} levels. Initial Ca^{2+} signals are further amplified by the Ca^{2+}-induced Ca^{2+} release mechanism (CICR), which involves activation of ryanodine receptors (RyR), another intracellular Ca^{2+} release channel. When tightly controlled, a transient change in calcium levels functions as an intracellular messenger, is important for gene transcription (Greer and Greenberg, 2008) and synaptic neurotransmission (Neher and Sakaba, 2008).

Aberrant calcium levels can uncouple neuronal plasticity and activate toxic cascades leading to cell death. Several studies have implicated deranged calcium signaling in neurodegenerative disorders culminating in the "calcium hypothesis of neurodegeneration". This hypothesis posits that as fundamental as calcium levels are to cellular functions, dysregulation of calcium homeostasis is detrimental to neuronal survival (Bezprozvanny, 2009).

Purkinje cells (PCs) are the only efferent projection from the cerebellar cortex. They modulate the activity of neurons in the deep cerebellar nuclei (DCN) via inhibitory signals; hence PC dysfunction and death in SCAs would lead to cerebellar dysfunction. Without inhibition from PCs, DCN neurons will become hyper-excitable, motor centers receiving DCN input will be affected and incoordination of movement will be the outcome (Shakkottai et al., 2004). This explains why PCs are suspected to be the likely site of onset of SCA pathogenesis. They are very sensitive to cellular changes (Potts et al., 2009), and over 75% of PCs are reported to be lost in a number of the SCAs (Table 1) (Schols et al., 2004). I will further discuss this calcium hypothesis of PC neurodegeneration outlining recent work focused on studies of the mechanisms underlying SCA2 pathogenesis.

Deranged calcium signaling in SCA2

SCA2 patients suffer from a progressive cerebellar syndrome with ataxia of gait and stance, ataxia of limb movements, and a variety of secondary symptoms including dysphagia, dysarthria, delayed saccadic eye eye-movements, peripheral neuropathy, Parkinson's disease like tremors and cognitive deficits (Filla et al., 1999, Schols et al.,

2004, Lastres-Becker et al., 2008). SCA2 is caused by an expansion and translation of unstable CAG repeats in the gene encoding ataxin-2 from the normal 22 to more than 31 extra glutamine repeats (Imbert et al., 1996, Pulst et al., 1996, Sanpei et al., 1996). The pathogenesis of SCA2 is currently not understood. Polyglutamine-expanded ataxin-2 protein, similar to wildtype ataxin-2, has a wide spread expression without severe aggregation and formation of inclusion bodies (Huynh et al., 2000). In spite of this, cerebellar PCs in SCA2 patients are preferentially lost (Table 1) (Schols et al., 2004). Genetic knockouts of ATXN2 orthologs in fly and worm resulted in embryonic lethality (Kiehl et al., 2000, Satterfield et al., 2002). ATXN2 knockout mice were viable but displayed a late-onset obesity phenotype (Kiehl et al., 2006). Mice deficient in ATXN2 did not show Purkinje cell loss or marked changes in the Purkinje cell dendritic tree (Kiehl et al., 2006). The non-essential role of Atxn2 in rodents is most likely related to the presence of orthologs and redundancy in its function (Kiehl et al., 2006). Thus, the polyglutamine expansion in ataxin-2 likely does not cause a loss of function nor a dominant negative effect but a gain of toxic function (Kiehl et al., 2006). The role of calcium signaling in the pathogenesis of SCA2 was suggested by the genetic association between polymorphisms in the CACNA1A gene and the age of disease onset in patients diagnosed with SCA2. The CACNA1A gene encodes the pore-forming α1A subunit of $Ca_V2.1$, a P/Q-type voltage-gated calcium channel. Patients with a prematurely early age of onset of SCA2 tended to have a longer CAG-repeat length in the CACNA1A gene (Pulst et al., 2005). Longer CAG-repeat lengths is the genetic basis of SCA6 (Zhuchenko et al., 1997).

The role of aberrant neuronal calcium signaling in SCA2 pathogenesis was strengthened further by a finding in our lab that $ATXN2^{exp}$ but not wildtype ATXN2 ($ATXN2^{wt}$) specifically binds type 1 Inositol (1,4,5) triphosphate receptors ($InsPR_3$s) (Liu et al., 2009). This suggested that its association would result in either a sensitization or desensitization of $InsPR_3$ to activation by Inositol 1,4,5-triphosphate (IP3) during glutamate signaling in PCs. PCs express extremely high levels of intracellular $InsPR_3$ (Furuichi et al., 1993, Sharp et al., 1999), which are present on endoplasmic reticulum (ER) membranes. $ATXN2^{exp}$ and $ATXN2^{wt}$ were found to localize and associate with ER membranes (van de Loo et al., 2009). In a lipid bilayer reconstitution experiment, the effect of $ATXN2^{exp}$ expression on $InsPR_3$ activation in single channel recordings of $InsPR_3$ co-expressed with $ATXN2^{exp}$ was examined. The presence of $ATXN2^{exp}$ substantially sensitized $InsPR_3$s to activation by IP3 (Liu et al., 2009).

To test the importance of $Ca2^{+}$ signaling in SCA2 pathogenesis, a series of experiments were performed in our lab using a SCA2 transgenic mouse model (SCA2-58Q, generated by (Huynh et al., 2000)) expressing 58 glutamine repeats ($ATXN2^{exp}$) in the ataxin-2 gene under the control of the L7/Pcp2 PC-specific promoter. These mice exhibit behavioral deficits, loss of Purkinje cell dendritic arborization and Purkinje cell death, which is progressive and akin to SCA2 patient pathology (Huynh et al., 2000). Our lab found that there was a significant increase in calcium release from ER stores via $InsPR_3$s in calcium imaging experiments in primary PCs cultured from SCA2-58Q transgenic mice, which was not observed in PCs cultured from wildtype littermates (Liu et al., 2009). When ryanodine or dantrolene were added to block ryanodine receptors and ER calcium release in PC cultures, the effect of $ATXN2^{exp}$ expression was immediately

reversed as ER calcium release returned to wildtype levels (Liu et al., 2009). In a TUNEL assay of PC death, it was found that the addition of dantrolene to block the excessive ER calcium release caused by $ATXN2^{exp}$ expression attenuated exogenous glutamate-induced PC death (Liu et al., 2009). Furthermore, long-term feeding of SCA2-58Q mice with a calcium stabilizer dantrolene alleviated the age-dependent motor coordination deficits in these mice quantified by rotarod and beam-walk behavioral assays (Liu et al., 2009). Stereological counting of PCs showed a rescue of PC death in 12-month old SCA2-58Q mice fed with dantrolene (Liu et al., 2009). The above lines of evidence supported the hypothesis that deranged calcium signaling plays a role in SCA2 pathogenesis.

Supranormal calcium signaling and Purkinje cell dysfunction in SCA2

The exact pathway(s) that is activated by excitotoxic calcium signaling and that causes PC degeneration in SCA2 is unknown. I propose that in Purkinje cells in SCA2 animals and patients, the significant increase in calcium release from the ER into the cytoplasm becomes toxic and initiates cell death via multiple pathways (Fig. 1) (Liu et al., 2009, Bezprozvanny and Klockgether, 2010). A transient increase in cytoplasmic calcium levels can be tolerated by cells and is important for many neuronal processes but if prolonged can be detrimental. Excessive cytosolic calcium is first taken up by the PC calcium buffers, calbindin (CB) and parvalbumin (PV), which as the first line of defense eventually become overwhelmed (Fig. 1) (Hof et al., 1999)**.** The important neuroprotective role of these endogenous Ca^{2+} buffers is supported by the fact that although CB knockout or PV knockout mice are only slightly ataxic (Airaksinen et al., 1997, Farre-Castany et al., 2007), the double knockout $CB^{-/-}$::$PV^{-/-}$ mice display a severe

ataxic phenotype and alterations in PC morphology (Vecellio et al., 2000). Also, when CB is depleted in a mouse model of SCA1, the ataxia and cerebellar pathology is accelerated (Vig et al., 2011). This supports the role of intracellular calcium homeostasis in the progression of disease.

Some of the excess calcium released from the ER is also taken up by mitochondria (Werth and Thayer, 1994, Nicholls et al., 2003), which can become overloaded as well, eventually creating free radicals and inducing oxidative stress, activating apoptotic cascades and necrotic cell death (Zhu et al., 2000, Bezprozvanny, 2009) (Fig. 1). Excessive cytoplasmic calcium also leads to excitotoxic glutamate release which can cause reactive oxygen species (ROS) production which damages DNA (Campisi et al., 2004). Intracellular calcium levels higher than physiological concentrations can also cause an increase in activation of multiple calcium-sensitive enzymes. These include calcium-sensitive phosphatases and kinases that alter gene transcription upon activation (reviewed in (Greer and Greenberg, 2008)), as well as proteases such as calpains, which upon activation cause degradation of intracellular substrates such as α-spectrin, actin and microtubule associated proteins (Chan and Mattson, 1999, Nixon, 2003). Excessive activation of nitric oxide synthase also abnormally increases intracellular nitric oxide levels and causes DNA damage. Thus in the absence of sufficient intracellular calcium buffering, calcium-induced excitotoxicity is detrimental to cell survival. This uncontrolled calcium burden could then fall on cerebellar plasticity mechanisms to attempt to control.

It has been suggested that cerebellar LTD could instead of or in addition to playing a role in motor learning also play a role in neuroprotection in PCs (reviewed in (Schorge et al., 2010)). Cerebellar LTD is triggered in response to an increase in intracellular calcium following coincident stimulation at both parallel and climber fiber synapses (Finch and Augustine, 1998, Miyata et al., 2000, Wang et al., 2000, Coesmans et al., 2004). This coincident and transient rise in calcium could function in coding information, which is the reason why LTD is believed to be involved in motor learning (reviewed in (Jorntell and Hansel, 2006)); (Kano et al., 2008). However, in instances where presynaptic calcium is above physiological levels, LTD could function to suppress synaptic transmission and prevent over-excitation of postsynaptic densities. Accordingly, it has been reported that blocking glutamate uptake and increasing synaptic glutamate levels increases the induction of LTD in cerebellar slices (Brasnjo and Otis, 2001), suggesting that LTD could protect PCs from detrimental effects of excitotoxic synaptic transmission. This idea that cerebellar LTD could play a separate role from motor learning in the cerebellum is supported also by evidence showing that LTD can be disrupted and uncoupled without affecting motor learning in two types of motor tasks (Kimura et al., 2005, Welsh et al., 2005). Therefore, LTD could be a mechanism that PCs use to relieve themselves from excitotoxicity by suppressing glutamatergic synaptic transmission when intracellular calcium exceeds a set threshold.

Alternatively, it is also possible that a compensatory increase in cerebellar LTD plays a direct role in the development of an ataxic phenotype (Fig. 1). This is because a complete prevention of synaptic transmission removes the inhibition of postsynaptic DCN neurons thus allowing hyper-excitability and ataxia (Shakkottai et al., 2004). In any

case, maintaining calcium homeostasis would be critical at ensuring tight regulation of synaptic transmission and cerebellar output. PCs, unlike other neurons that rely on N-methyl-D-aspartic acid (NMDA) receptors, rely heavily on $InsP_3Rs$ for plasticity mechanisms (Inoue et al., 1998). Thus, if my hypothesis for the involvement of IP3 signaling in SCA2 pathogenesis is correct, then the physiology and synaptic plasticity mechanisms are disrupted in PCs of SCA2 mice (discussed in chapter 2).

PCs fire action potentials relentlessly in the absence of synaptic inputs. It is suggested that cerebellar information is encoded in the firing rate and variability of firing of PCs (Ito, 1984). Thus, disease-mediated changes to these PC properties may underlie disease onset and/or progression (discussed in chapter 2). $InsP_3Rs$, which are required for calcium release from intracellular stores in the induction of cerebellar-LTD (Finch and Augustine, 1998, Inoue et al., 1998, Miyata et al., 2000), are excessively sensitized to activation in PCs of SCA2 mice (Bezprozvanny, 2009). Consequently, in PCs of SCA2 mice, when there is a calcium overload resulting from the sensitization of $InsP_3Rs$ to activation by IP3, it is possible that this overwhelms and uncouples synaptic plasticity mechanisms that require specific and transient changes in intracellular calcium levels. This can be tested by measuring LTD induction in cerebellar slices from SCA animal models compared to wildtype animals. These studies may also provide new insights into cerebellar plasticity. Future investigations with SCA2 mouse models will be necessary to test these ideas.

Purkinje cells in SCA2-58Q mice die by dark cell degeneration

Although a dysfunction in PC firing activity and cerebellar LTDinduction may be responsible for initial symptoms of SCA2, it is likely that the degeneration and eventual death of PCs are responsible for the symptoms of the disease in the late stages. What is a mode of PC cell death in SCA2? Previous studies in our lab demonstrated that the application of glutamate induces apoptotic cell death of SCA2-58Q PC neurons in *in vitro* culture which can be detected by TUNEL staining (Liu et al., 2009). What is a mode of cell death of PC cells *in vivo*? A number of previous studies described a characteristic mode of excitotoxic cell death of PC neurons which has been termed dark cell degeneration (DCD). DCD has been reported in PCs resulting from excitotoxicity in the form of excessive presynaptic glutamate stimulation or sensitivity to glutamate in the synapse (Barenberg et al., 2001, Strahlendorf et al., 2003, Maltecca et al., 2009). It is suggested to lie in a spectrum between classical apoptotic and passive necrotic cell death because it shares characteristics with both forms of death (Strahlendorf et al., 2003). DCD mode of PC cell death has been previously identified in mouse models of SCA5, SCA7 and SCA28 suggesting that excitotoxicity could be central for pathogenesis of these disorders (Custer et al., 2006, Maltecca et al., 2009, Perkins et al., 2010). DCD in SCA7 PCs is induced by the absence of Bergmann glia, which ensheath PCs and re-uptake glutamate from synapses (Custer et al., 2006). In SCA28, DCD appears to be mitochondria-mediated (Maltecca et al., 2009).

Typically, DCD is evaluated by the analysis of transmission electron microscopy (TEM) images of cerebellar sections. The rationale behind this method is that unlike healthy PCs, as unhealthy PCs degenerate as a result of excitotoxicity-induced cell death cascades, the cytoplasm fills with cellular aggregates and debris. The compounds used for

TEM processing form an extensive complex that bind to cellular protein structures. Once processed for TEM, the DCD PCs appear to have higher intracellular electron density and appear darker than healthy PCs.

Consistent with my predictions, TEM of 10-month old SCA2-58Q mice and age-matched nontransgenic mice confirmed a continuous process of DCD in SCA2-58Q mice cerebellum (Fig. 2). PCs in nontransgenic mice appear normal with a regular alignment in the PC monolayer, spherical shape with clearly distinct nuclei and cytoplasm (Fig. 2*A*,*C*). PCs in SCA2-58Q mice show defects in spatial alignment resulting in PCs residing outside of the defined PC monolayer, evident shrinkage and darkened cytoplasm (Fig. 2*B*,*D*). For quantification of obtained results, PCs observed on TEM images were divided into 3 groups: normal (spherical, no darkening at all); moderately degenerated (slight shrinkage, moderately electron-dense cytosol not as dark as nucleus); or severely degenerated (markedly shrunken and electron-dense cytosol with similarly darkened nucleus). Quantitative analysis of TEM images showed that almost half of the PCs in SCA2-58Q mice are at the end-stage of degeneration with markedly shrunken, electron-dense cytosol with similarly darkened nucleus while the rest are moderately degenerated (Fig. 2*G*). This is in contrast to the age-matched wild type mice, where most cells are normal or only moderately affected (Fig 2*G*).

Degeneration does not seem to be limited to PCs in the cerebellum. Granule cells (GCs) in the granule cell layer, which form parallel fibers and serve as excitatory afferents to PCs, also appear to be degenerating in SCA2-58Q with evident cytoplasmic darkening and condensation when compared to those in nontransgenic mice (Fig. 2*D*,*E*). The degeneration of the granule cells are likely to be as a result of secondary toxicity as

Atxn2-58Q transgene is expressed specifically in PC cells in this SCA2-58Q mouse model (Huynh et al., 2000). From these results, I concluded that PC cells in SCA2 transgenic mice undergo DCD form of cell death, consistent with our proposed excitotoxic hypothesis of SCA2 pathogenesis (Fig. 1). Interestingly, by using calbindin staining and unbiased stereology approach in our lab, less than 15% reduction in the number of PC cells in 12 month old SCA2-58Q mice when compared to non-transgenic controls was reported (Liu et al., 2009). From this quantitative comparison it appears that many PCs undergoing DCD are still calbindin-positive. These cells are likely to be dysfunctional and contribute to ataxic symptoms (discussed in chapter 2). From these experiments, I concluded that DCD analysis is a more sensitive way of scoring PC cell degeneration in SCA2 mice than calbindin-staining based stereological method.

The unifying theme for all spinocerebellar ataxias is that purkinje cells begin to degenerate and fire dysfunctionally. Considering this, I hypothesized that preventing or alleviating PC pathology and pathophysiology will be of therapeutic benefit for ataxia patients. The primary focus of this dissertation will be to test this hypothesis by further elucidating the underlying mechanism of SCA2 pathogenesis, characterizing PC dysfunction, identifying therapeutic targets and developing a potential treatment of SCA2. The first part of this dissertation will test the hypothesis that suppressing $InsP_3R$-mediated Ca^{2+} signaling alleviates age-dependent dysfunction, and degeneration of PCs in SCA2 mice. The second part of this dissertation will focus on testing the efficacy of novel compounds that modulate calcium-activated potassium (SK) channels in the symptomatic treatment of SCA2.

Disease subtype	Locus	Protein	Mutation	Normal Repeats	SCA patient Repeats	Pathology	Effect on calcium signaling
SCAl	6p	Ataxin 1	PolyQ exp	6-39	39-82	>75% PC loss	Increase
SCA2	12q	Ataxin 2	PolyQ exp	14-31	33-64	>75% PC loss	Increase
SCA3	14q	Ataxin 3	PolyQ exp	12-42	52-86	<25% PC loss	Increase
SCA5	11q	β-III spectrin	Non-repeat mutations & deletions	N/A	N/A	No data	Increase
SCA6	19p	CACNA1A	PolyQ exp	4-18	19-30	>75% PC loss	Increase/ Decrease
SCA14	19q	PKCγ	Non-repeat mutations	N/A	N/A	No data	Increase/ Decrease
SCA15/ 16	3p	INSPR3	Non-repeat mutations & deletions	N/A	N/A	No data	Decrease

Table 1. **Summary of polyglutamine expansion ataxias.** PolyQ exp., Polyglutamine expansion; N/A, Not applicable; Number of repeats adapted from (Paulson, 2009). SCA pathology adapted from (Schols et al., 2004).

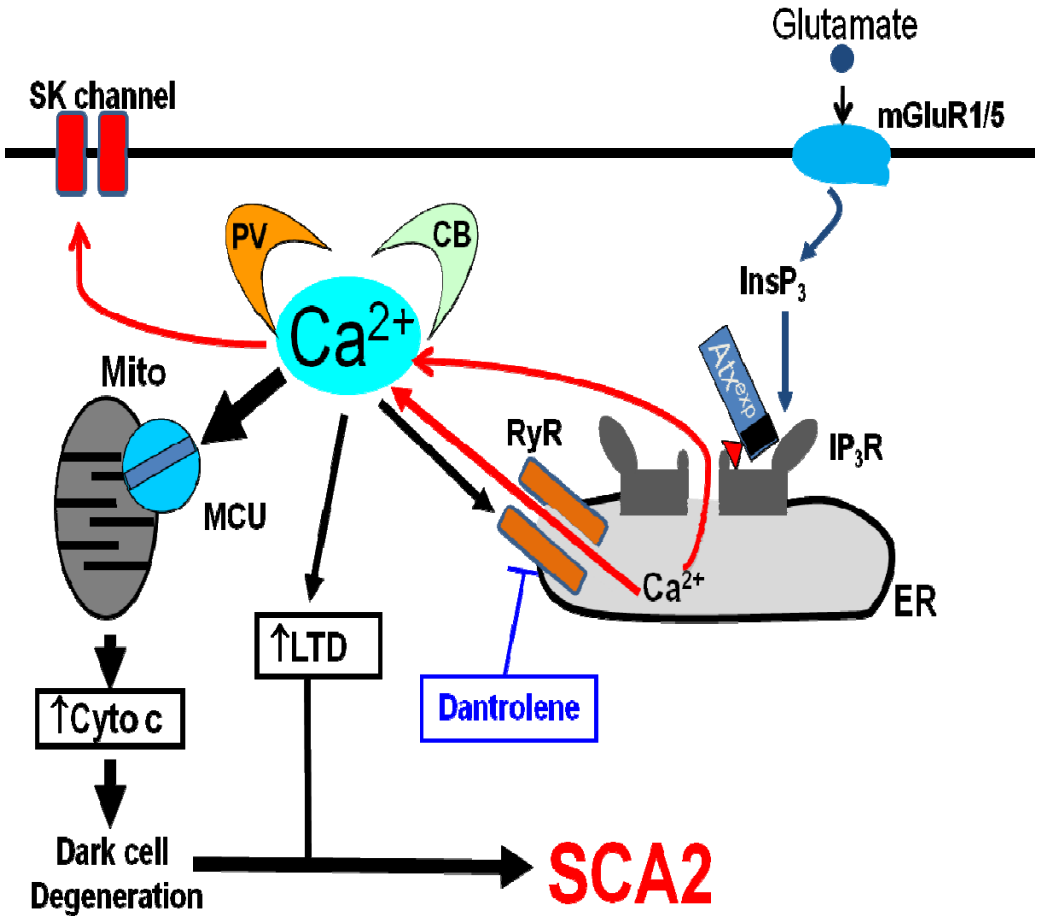

Figure 1. Calcium hypothesis of SCA2 pathogenesis. I propose that the $InsP_3R1$-$ATXN2^{exp}$ association results in increased $InsP_3R1$ activity leading to deranged neuronal calcium signaling. The abnormal cytosolic calcium levels result in mitochondrial Ca^{2+} overload, release of cytochrome c and induction of PC cell death via dark cell degeneration (DCD). Supranormal Ca^{2+} also aberrantly activates Ca^{2+}-activated K^+ channels disrupting precision firing. In addition, abnormal Ca^{2+} signals also disrupt LTD mechanisms, leading to uncoupling of synaptic plasticity mechanisms in SCA2 PC cells from intracellular Ca^{2+} signaling.

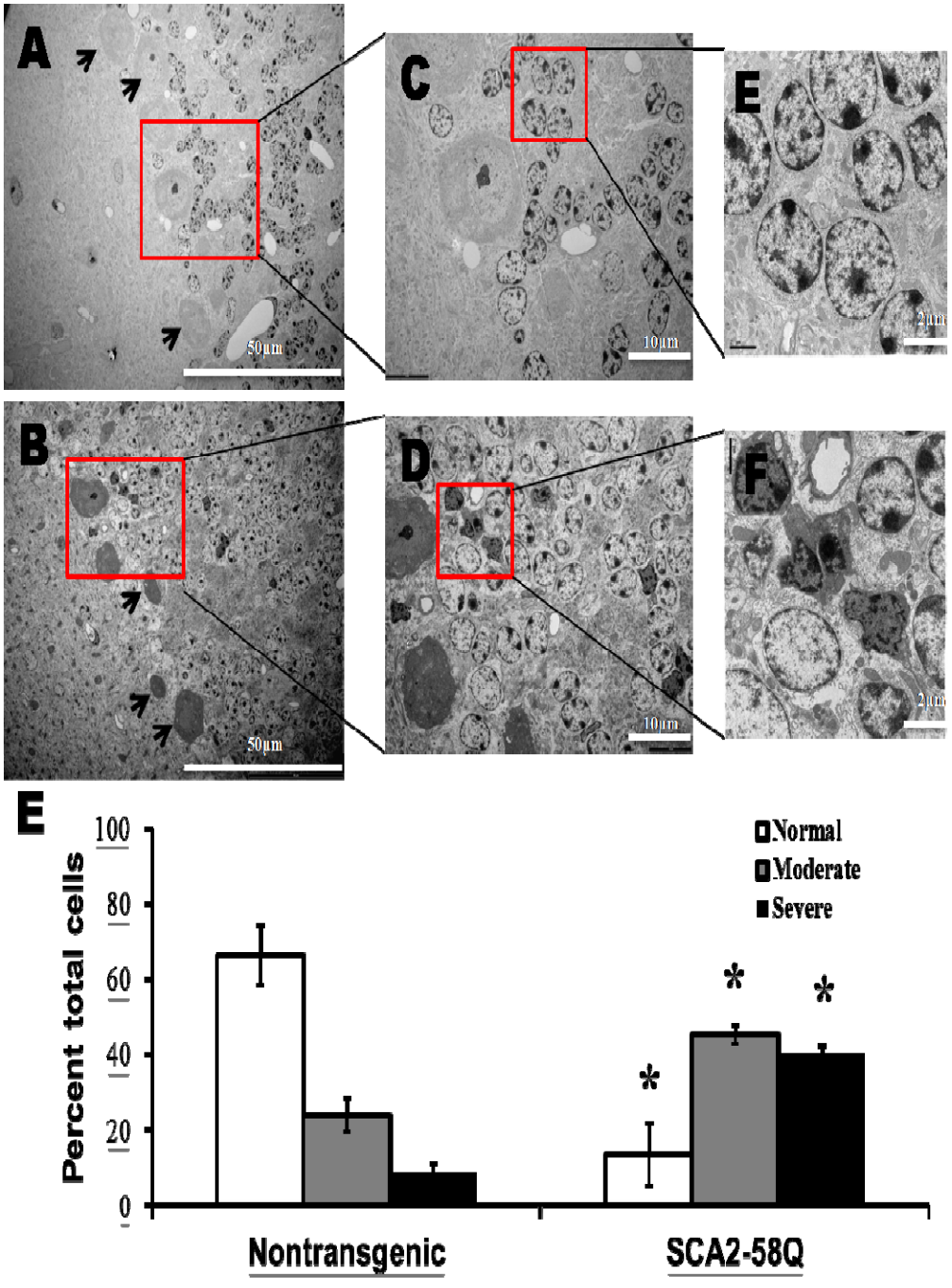

Figure 2. PCs in SCA2 transgenic mice die by dark cell degeneration. Electron micrographs (610X (A,B) and 1700X (C,D) magnification) of the cerebellum from 10-

month old SCA2-58Q mice and age-matched nontransgenic mice. ***A,*** PCs in wildtype mice show regular alignment and arrangement in Purkinje cell layer. ***B,*** PCs in SCA2-58Q mice show defects in spatial alignment of PCs resulting in PCs residing outside of the defined PC layer, evident shrinkage and darkening of the cytoplasm. ***C, D,*** At higher magnification, GCs in the granule cell layer also appear to be degenerating with evident cytoplasmic darkening and condensation. E, Quantification of dark cell degeneration in the PC layer of 10-month old SCA2 transgenic mice and nontransgenic controls (modified from (Custer et al., 2006)). Briefly, PCs were judged to be: normal (spherical, no darkening at all); moderately degenerated (slight shrinkage, moderately electron-dense cytosol not as dark as nucleus); or severely degenerated (markedly shrunken and electron-dense cytosol with similarly darkened nucleus). $P<0.05$, Mann-Whitney U test. Error bars represent s.d. (Adapted from (Kasumu and Bezprozvanny, 2010))

CHAPTER TWO

Chronic suppression of inositol 1,4,5-triphosphate receptor-mediated calcium signaling in cerebellar Purkinje cells alleviates pathological phenotype in Spinocerebellar ataxia 2 mice

Background, Methods, Results, Discussion

Background

A previous publication reported that Atx2-58Q, but not Atx2-22Q, specifically interacts with and increases the sensitivity of inositol 1,4,5-triphosphate receptors ($InsP_3Rs$) to activation by $InsP_3$ (Liu et al., 2009). This was supported by experiments in primary PC cultures from SCA2-58Q transgenic mice that express Atx2-58Q under the control of the PC-specific promoter (Huynh et al., 2000). When compared to PC cultures from their wildtype littermates, SCA2-58Q PC cultures treated with an mGLUR agonist (RS)-3,5-dihydroxyphenylglycine (DHPG) exhibited significantly greater IP3-induced calcium release (IICR) from the endoplasmic reticulum (ER) and higher intracellular calcium (Ca^{2+}) concentrations (Liu et al., 2009). Moreover, the authors demonstrated that long-term feeding of SCA2-58Q mice with the Ca^{2+} stabilizer dantrolene alleviated the motor phenotype of these mice and reduced PC loss (Liu et al., 2009). Based on these findings, it was proposed that the association of polyglutamine-expanded ataxin-2 with $InsP_3Rs$ causes excessive calcium release from the ER, initiates cytoplasmic dysregulation and cellular dysfunction of PCs which eventually results in ataxia (Liu et al., 2009, Kasumu and Bezprozvanny, 2010). In support of this hypothesis, genetic evidence has been used by others to suggest that $InsP_3R$ is the "eye of the storm" of pathogenesis for many SCAs (Schorge et al., 2010).

To specifically test this hypothesis in this study, it is important to explore the functional consequences of the $InsP_3R$-58Q interaction, how this contributes to sensitized $InsP_3Rs$ and the abnormal Ca^{2+} signaling that is alleviated by dantrolene. To do this, I used a specific molecular intervention to normalize $InsP_3R$-mediated Ca^{2+} signals in PC of SCA2-58Q mice. Intracellularly, Inositol 1,4,5-triphosphate 5-phosphatase (5PP)

dephosphorylates IP3 to IP2 (Inositol 1,4-triphosphate) by hydrolyzing the 5' phosphate as soon as IP3 is produced by phospholipase c such that 5PP decreases the lifetime and amount of IP3 available to subsequently activate $InsP_3Rs$. Thus, the expression of 5PP in cells completely blocks IICR.

Two mutant versions of 5PP have been identified. Replacing Arg343 with Ala (RA) in the active site of 5PP decreases the ability of RA to bind and dephosphorylate IP3, thus causing a 10-fold increase in the K_m for IP3 and consequently allowing partial suppression of IICR. A double R343A/R350A (DM) mutation in 5PP creates a null mutant that has a 15-fold greater Km and is unable to suppress IICR (Communi et al., 1996, Kanemaru et al., 2007). RA or DM was overexpressed in SCA2-58Q mice to determine the efficacy of suppressing IICR in restoring normal calcium signaling and preventing or delaying SCA2 pathogenesis. Properly regulated Ca^{2+} signaling is essential for cell survival and function.

Genetic deletion of 5PP in mice results in perinatal lethality, with less than 10% survival past weaning. Mice that did survive presented with an ataxic gait as early as postnatal day 16, as well as loss of PCs and severe cerebellar degeneration at P20 (Andy W Yang; Andrew J Sachs ;Emily M Strunk; Arne M Nystuen, SfN-2011 abstract). In the absence of IICR in $InsP_3R^{-/-}$, PCs are unable to induce cerebellar long-term depression. $InsP_3R^{-/-}$ mice die by postnatal day 23, thus implicating IP3 signaling in survival (Inoue et al., 1998). Dietary supplementation of Lithium in SCA1 mice improved motor performance, learning, memory and alleviated PC pathology, a phenotype that could be explained by the fact that Lithium decreases IP3 levels (Watase et al., 2007). However, it

was reported that the benefit of the Lithium treatment in delaying disease progression is via stimulating autophagy in a mouse model of SCA3 (Menzies et al., 2010).

Consistent with the hypothesis of this study, partial and chronic suppression of IICR in SCA2-58Q mice prevented the onset of PC dysfunction, alleviated motor incoordination and reduced age-dependent PC degeneration in SCA2-58Q mice. These results indicate that partial suppression of IICR is a viable therapeutic strategy for treatment of SCA2 and possibly other SCAs.

Research design and Methods

SCA2-58Q mouse colony.

SCA2-58Q mice were generated previously (Huynh et al., 2000) and used in our previous studies (Liu et al., 2009, Kasumu and Bezprozvanny, 2010). In these mice the expression of Atx2-58Q is driven by the PC-specific L7/pcp2 promoter (FVB strain). SCA2-58Q mice males were bred to wildtype (WT) females to generate mixed litters. For analysis of motor impairment, mice from each litter were genotyped and divided into 3 WT and 3 SCA2-58Q groups, with each group containing 13-19 mice each. All mice were housed in a temperature-controlled room at 22-24°C with a 12hr light/dark cycle. Mice had access to standard chow and water *ad libitum*. All procedures were approved by the Institutional Animal Care and Use Committee (IACUC) of the University of Texas Southwestern Medical Center at Dallas in accordance with the *National Institutes of Health guidelines for the Care and Use of Experimental Animals*.

Cerebellar slice recordings.

Cerebellar slices were prepared from WT and SCA2-58Q mice at 6, 12, 24, and 48 weeks old. Mice were anesthetized with a ketamine/xylazine cocktail and transcardially perfused with ice-cold aCSF containing (in mM): 119 NaCl, 26 NaHCO3, 11 glucose, 2.5 KCl, 2.5 CaCl2, 1.3 MgCl2, 1 NaH2PO4. Solutions were equilibrated with 95% O2/5% CO2. Subsequently, the cerebellum was dissected and 300μm thick sagittal slices were made with a Leica VT1200S vibratome. Slices were allowed to recover in aCSF at 35°C for 30 minutes and then transferred to room temperature before recordings were made.

All recordings were made within 5 hours after dissection. Recordings were made in a chamber (Warner instruments) heated to 34-35°C. Loose-patch cell-attached recordings were made (Hausser and Clark, 1997, Smith and Otis, 2003) to evaluate spontaneous activity of PCs from wildtype and SCA2-58Q at different ages. Briefly, the patch pipette was filled with 140mM NaCl buffered with 10mM HEPES and held at 0 mV. A loose patch (less than 100MΩ) was generated at the PC soma close to the axon hillock. Spontaneous action potential currents were recorded for at least 5 minutes from each cell. These five-minute recordings were analyzed for tonic or burst firing patterns. A cell was characterized as bursting if it was identified that it had more than 5% of the event intervals that fell outside of 3 standard deviations from the mean of all intervals in that cell. Tonically firing cells in all groups were further analyzed for average firing frequency and firing variability (Alvina and Khodakhah, 2010b, a). The proportion of tonically firing PCs for each genotype at each time-point was calculated and plotted as mean percentage of total PCs recorded ± SE. All tonically firing PCs were analyzed further for firing frequency and firing variability. The mean firing frequency in the 5 minute recording duration was calculated for each PC and the average firing frequency for each genotype at each time-point was also calculated and plotted as mean ± SE. To assess firing variability in each PC recording, I calculated the correlation of variation of interspike interval (CV ISI) as the standard deviation divided by the mean interspike interval in a 5 minute recording period for each PC. Although PCs are autonomously active, they do receive excitatory and inhibitory inputs that modulate their firing. To determine if the effects seen were solely spontaneous PC activity, the recordings at 24

and 36 weeks were made in the presence of 100μM Picrotoxin (Sigma) and 10μM DNQX (Sigma) to block fast excitatory and inhibitory synaptic inputs.

Adeno-associated virus production

The inositol 1,4,5-triphosphate 5-phosphatase (5PP) expression constructs were kindly provided to us by Masamitsu Iino (University of Tokyo) (Kanemaru et al., 2007). A hemagglutinin (HA) tag was added to the N-terminus of each 5PP construct by PCR. The 5PP-HA inserts were excised and individually cloned into the pFBGR (pGANCMVBGHpA) plasmid behind the CMV promoter. The inserts now including a CMV promoter were individually cloned into an AAV plasmid in front of the GFP whose expression is driven by a different CMV promoter. These AAV plasmid constructs express HA-tagged versions of wildtype 5PP (AAV-5PP), single mutant 5PP (AAV-RA) or inactive double mutant 5PP (AAV-DM; Fig. 2*A*). Thus, expression of each 5PP construct can be confirmed by antibodies against 5PP and HA, or by GFP fluorescence (Fig. 2*B*). Thus, I could detect exogenous and endogenous 5PP. I generated adeno-associated viral-based vectors (AAV) which have advantages over lentiviral vectors because AAV can be produced with a higher titer, on a larger scale and can integrate into the genome thus have longer-term expression *in vivo* over 12-months (Tang et al., 2009). The 3 AAV-5PP plasmids were sent to the University of Iowa Vector Core where adeno-associated viruses were made using the baculovirus system via Sf9 cell-based AAV production system. To achieve this goal, Bac-to-Bac system was used to generate 5PP baculoviruses. Generated baculoviruses were amplified and used to co-infect 200 ml of Sf9 cells together with BacRep2 and BacCap2 baculoviruses to generate serotype 2

AAV. At 48 hours post-infection, Sf9 cells were lysed and AAV2-5PP/RA/DM and AAV2-GFP viruses were purified by iodixanol gradient centrifugation as previously described followed by Mustang-Q membrane ion exchange (Pall Co). The titer of generated and purified AAV viruses was equal to or greater than 10^{-13}.

Calcium imaging in MEF cells.

Primary PC cultures are difficult to generate and even harder to transduce *in vitro*. Instead of primary PC cultures, Presenilin double knockout mouse embryonic fibroblast (MEF) cells were used to determine the efficacy of the 5PP constructs to suppress IP3-induced calcium release. Due to the absence of Presenilin 1 and 2, these MEF cells have high ER Ca^{2+} levels that can be released via $InsP_3Rs$ with the application of 300nM Bradykinin (according to (Tu et al., 2006)). Bradykinin (BK) was used to stimulate IICR. BK activates phospholipase c-coupled BK receptors which are coupled to the production of IP3 from PIP_2 in the cytoplasm. Cytoplasmic IP3 activates $InsP_3Rs$ releasing Ca^{2+} from the ER. The 5PP enzyme and its derivatives convert IP3 to IP_2, thus decreasing the lifetime of IP3 in the cell, regulating the amount of IP3 available to activate $InsP_3Rs$ and decreasing the amount of Ca^{2+} released from the ER. As a result, we were able to determine the effect that expressing each construct has on BK-induced IP3 signaling. I cultured MEF cells on poly-D-lysine (Sigma) coated 12 mm round glass coverslips and infected with AAV-5PP, AAV-RA, AAV-DM or AAV-GFP. Cytosolic Ca^{2+} imaging experiments with MEF cells were performed 48 hours after viral infection as previously described (Tu et al., 2006). The MEF cells were loaded with the Ca^{2+} indicator Fura-2 for 45 minutes. Cytosolic Ca^{2+} concentration in these experiments was

estimated from the ratio of Fura-2 (Ca^{2+} indicator) signals at 340 nm and 380 nm excitation wavelengths. Baseline (55s) measurements were obtained prior to the bath application of BK, which was dissolved in Ca^{2+} -free aCSF. During analysis, Fura-2 ratio data was collected from only transduced cells. The transduced cells were identified by GFP expression.

Adeno-associated viral injection.

Stereotaxic surgery was performed according to (Dodge et al., 2005). Briefly, 4µl of AAV (10^{13} titer) was bilaterally injected into the deep cerebellar nucleus (DCN) at the coordinates Bregma -5.75; Lateral +1.8; D/V -2.6 mm. PCs project axons into the DCN and retrogradely transport the virus back to the soma where it integrates and is expressed for over 12 months (Kaemmerer et al., 2000, Dodge et al., 2005). AAV GFP expression in PCs is confirmed by scanning cerebellar slices with a fluorescence plate reader or confocal imaging. HA-tag expression was confirmed by western blotting of cerebellar lysates at least 2 weeks after surgery. Infection efficiency was calculated by comparing transduced PCs to PCs from L7-GFP transgenic mice, which express GFP in all PCs driven by the L7/pcp2 PC-specific promoter.

Western blotting.

Each of these viruses was used to transduce MEF cells. Cell lysates were prepared from infected MEF cell cultures was prepared for western blotting. At 2, 6 and 10 months post-DCN injection of these viruses, lysates were prepared from mouse cerebellum for western blotting. The expression of AAV-5PP, AAV-RA, AAV-DM was confirmed by

probing with antibodies against 5PP (Sigma Aldrich) and HA-tag (Sigma Aldrich) (Fig. 2*B*). Actin was used as a loading control (Sigma Aldrich).

Motor coordination assessments in mice.

Rotarod and beamwalk assays were used to assess motor coordination. These were performed as previously described (Liu et al., 2009). For analysis of motor impairment, female mice from each litter were genotyped, weight-matched and divided into 3 WT and 3 SCA2-58Q groups, with each group containing 13-19 mice each. Briefly, SCA2-58Q and WT mice were trained on the accelerating rotarod apparatus (Columbus instruments). Mice were screened on the rotarod running at 5rpm constant speed. Mice that fell off the rod in less than 5 minutes were dismissed. At each time following baseline testing, mice were trained on the rotarod accelerating at 0.2rpm for 4 consecutive days with 3 trials per day. The mean latency to fall off the accelerating rod on day 4 was recorded and analyzed for every animal in all 6 groups. Average group latency was calculated and plotted for all time-points. Three days after rotarod testing, mice were tested on the beam-walk assay using a homemade apparatus. Mice were trained on 3 consecutive days, with 3 consecutive trials on 3 separate beams of 80cm in length but varying diameters. A round plastic 17mm beam, a round plastic 11mm beam and a wooden square 5mm beam were used. The mean latencies to traverse the entire length of the 11mm and 5mm beams on the 3rd day were recorded and analyzed for every animal in all 6 groups. Average group latency was calculated and plotted for all time-points as mean ± SE. These motor coordination tasks were performed at 4, 6, 8, 10 and 12 months of age. Mice that were

found at the 4 month time-point to be severely impaired on both behavioral tasks due to surgery-induced irreversible motor deficits were eliminated from the study.

Pathology

After testing in the motor coordination tasks at the 12 month timepoint was complete, mice were sacrificed for pathological analyses. A subset of mice were transcardially perfused with PBS followed by 4% paraformaldehyde in PBS, brains were dissected out and stored in 30% sucrose. After 1 week in sucrose, whole brains and whole cerebella were weighed. Two brains in each group were sliced into 50μm-thick sections and stained with calbindin antibody (Sigma) for visualizing representative images of PCs.

Dark cell degeneration analysis.

Analysis of Purkinje cell dark cell degeneration (DCD) was performed as previously described (Kasumu and Bezprozvanny, 2010). Briefly, 6-9 mice per group were sacrificed after the analysis of the 12-month motor tasks. Mice were euthanized and transcardially perfused (according to (Custer et al., 2006)) with PBS followed by 2% paraformaldehyde/2% glutaraldehyde in 0.1M cacodylate buffer. The cerebellum was left in fixative overnight. The next day the cerebellum was cut into $1mm^3$ sagittal sections and post-fixed in 1% Osmium Tetroxide. The specimens were subsequently stained en bloc with aqueous 1% uranyl acetate and lead citrate, dehydrated through a graded ethanol series, and embedded in EMbed 812 resin. Each cerebellum was cut into thinner sections (about 70-90 nanometers in thickness) and placed on copper grids. The grids were stained with aqueous 2% uranyl acetate and lead citrate. Two grids from each

animal were examined on a FEI Tecnai G2 Spirit Biotwin transmission electron microscope operated at 120 kV. Digital images were captured with a SIS Morada 11 megapixel side mount CCD camera. At least 6 mice were analyzed per group with 2 grids produced from different cerebellum areas of the same mouse. PCs were judged to be in 1 of 3 stages- normal, moderate or severe. Normal PCs are spherical in shape and have regular alignment in the PC layer. Moderately degenerated PCs have slight shrinkage and moderately electron-dense cytosol that is not as dark as the nucleus. Severely degenerated PCs have markedly shrunken and electron-dense cytosol with similarly darkened nucleus. These PCs are also not regularly aligned in the PC layer. The processing of cerebellar sections for DCD was performed by an independent investigator in the Electron Microscopy core at the University of Texas Southwestern Medical Center at Dallas, who was blind to mouse genotype and treatment. DCD quantification was performed by an investigator that was blind to mouse genotype and treatment. The percentage of normal, moderately and severely degenerated PCs in each mouse was calculated. The average percentage of each group was plotted as mean ± SE.

Statistical analyses

Differences between specific groups were judged by a two-tailed Student's unpaired *t* test using a significance level of $P < 0.05$.

Results

Progressive dysfunction of Purkinje cells in SCA2-58Q mice

PCs are autonomously active neurons in the cerebellum, firing in a clockwise fashion in the absence of synaptic innervation. PCs are the sole output of the cerebellar cortex, and disruption of PC activity impairs cerebellar function in SCAs (Alvina and Khodakhah, 2010b, a, Kasumu and Bezprozvanny, 2010, Mark et al., 2011, Shakkottai et al., 2011). To evaluate the functional state of PCs in SCA2-58Q (58Q) mice, I used well-established protocols (Smith and Otis, 2003, Walter et al., 2006, Mark et al., 2011, Shakkottai et al., 2011) to record spontaneous PC activity in cerebellar slices obtained from the 6, 12, 24, 36 and 48 weeks old 58Q mice and from the age-matched WT littermates. In each experiment the PCs were classified as firing in a tonic or bursting pattern during a 5 minute recording period. The firing pattern of a PC was classified as tonic if it consisted of rarely halting tonic spikes with relatively constant frequency (Fig. 3*A*). A bursting firing pattern was identified by a purely bursting pattern or a repetitive presence of interchanging tonic firing, burst firing and pauses (Fig 3*B*). From analysis of the data we discovered that >80% of PC cells fire in tonic firing pattern in slices obtained from 6 and 12 weeks old mice for both 58Q and WT groups (Fig. 3*C*). To analyze these data further, I determined the mean firing rates and the mean correlation of variation of the interspike intervals (CV ISI) for all tonically firing PCs in both groups of mice. I discovered that both firing frequency and the variability of interspike intervals were similar for 58Q and WT mice at 6 and 12 weeks of age (Fig. 4*A*-*B*). From these results, I concluded that PCs function properly in 6 and 12 weeks 58Q mice, consistent with the

lack of overt phenotype of 58Q mice at these ages in motor coordination assays (Liu et al., 2009).

In contrast to the results obtained with slices from the young mice, the fraction of tonically firing PC cells was significantly lower in 58Q mice than in WT mice at slices from 24-week old mice (Fig. 3*C*). On average, 91 ± 9.4% (n = 4 mice) of WT PCs and only 64 ± 9.4% (n = 7 mice) of 58Q PCs were firing tonically at this age ($p < 0.05$; Fig. 3*C*). Moreover, at 24 weeks of age, the tonically firing PC cells from the 58Q mice were firing less frequently that the tonically firing PC cells from the WT mice at the same age (Fig. 4*A*). On average, tonically active WT cells were firing at 51 ± 3.3 Hz (n = 19 neurons) and tonically active 58Q cells were firing at 37 ± 3.1 Hz (n = 41 neurons) at this age ($p < 0.01$; Fig. 4*A*). The variability of interspike intervals was not significantly different between 58Q and WT mice at this age (Fig 4*B*). The functional differences between 58Q and WT mice became even more dramatic with increased age.

The deficits in PC firing activity seen at 24 weeks old were also confirmed at 36 weeks old. Whereas 86 ± 3.1% (n = 2 mice) of 36-week old WT PCs fired tonically, only 62 ± 5.9% (n = 3 mice; $p < 0.01$) of 58Q PCs fired tonically. On average, tonically firing 58Q PCs also fired with a lower frequency 29 ± 3.5 Hz (n = 22 neurons; $p < 0.001$) when compared to age-matched WT PCs 58 ± 6.8 Hz (n = 14 neurons). The firing variability was also altered with 58Q PCs firing irregularly with a mean CV ISI value of 0.28 ± 0.05 (n= 22 neurons), $p < 0.05$) compared to WT PCs of 0.13 ± 0.03 (n= 14 neurons).

When slices from 48 week old mice were used, the fraction of tonically firing PC cells was reduced to 81 ± 3.4% (n = 4 mice) in WT mice and to 56 ± 9.7% (n = 3 mice) in 58Q mice ($p < 0.01$; Fig. 3*C*). For tonically firing cells the firing frequency of WT cells

remain relatively constant at 55 ± 3.7 Hz (n = 24 neurons) but for 58Q cells the frequency of firing was further reduced to = 25 ± 6.3 Hz (n = 11 neurons; $p < 0.001$; Fig. 4*A*). Moreover, at 48 weeks of age the variability of interspike intervals (CV ISI) for tonically firing cells remain constant for WT cells at 0.20 ± 0.03 (n= 24 neurons) but was significantly increased to 0.49 ± 0.05 (n = 13 neurons) for 58Q cells ($p< 0.0001$, Fig. 4*A*). Thus, I concluded that aging 58Q PC cells increasingly fire in bursting pattern, and even tonically firing cells fire less frequently and with reduced precision when compared to age-matched WT cells. Interestingly, the age of onset of 58Q PC cells electrophysiological abnormalities at 24 weeks of age (Fig. 3*C*) closely mirrors the age of onset of behavioral symptoms in SCA2-58Q mice in motor coordination assays observed in our previous studies (Liu et al., 2009). Based on this coincidence, the data suggest that the reduced precision in PC firing in SCA2-58Q mice is causing the impaired performance of these mice in motor coordination tasks starting at 24 weeks of age. The continuous breakdown of PC cell firing pattern at older ages (Fig. 4*A*-*B*) is likely to cause progressive worsening of motor coordination phenotype of aging SCA2-58Q mice in motor coordination assays (Liu et al., 2009). The lower firing rate and increased irregularity of firing in 58Q PCs is not due to increased inhibition because in the presence of picrotoxin to block fast inhibitory synaptic inputs 24 and 36 weeks, the disruptions in PC pacemaking activity is persistent (Fig. 5*A*-*B*)

Validation of 5PP-mediated suppression of InsP3-induced calcium release

To determine the importance of excessive $InsP_3R$-mediated Ca^{2+} release from the ER for SCA2 pathogenesis, I chose to chronically suppress $InsP_3$-induced-calcium

release (IICR) in PC cells from 58Q mice. To achieve this in a specific way, I used adeno-associated viruses (AAV) to stably express inositol 1,4,5-triphosphate 5-phosphatase (5PP) in PC cells of 58Q mice. $InsP_3R$-mediated Ca^{2+} release from the ER is triggered in response to generation of a cytosolic second messenger IP3. Endogenous 5PP hydrolyzes IP3 by converting IP3 to an inactive form IP2 and terminates the $InsP_3$-induced Ca^{2+} signals. It has been previously demonstrated that stable overexpression of recombinant 5PP can be used to chronically suppress $InsP_3$-mediated Ca^{2+} signals in astrocytes (Kanemaru et al., 2007). I adapted the same approach for chronic suppression of $InsP_3$-mediated Ca^{2+} signals in PC cells of 58Q mice.

Two arginine residues (R343 and R350) have been previously demonstrated to be critical for catalytic activity of 5PP (Communi et al., 1996, Kanemaru et al., 2007). Replacing Arg343 with Ala (R343A) decreases the ability of 5PP to bind $InsP_3$, thus causing a 10-fold increase in the K_m for $InsP_3$ and consequently allowing partial suppression of IICR in cells when RA mutant is overexpressed (Communi et al., 1996, Kanemaru et al., 2007). A double R343A/R350A mutation (DM) creates a null mutant of 5PP that is unable to suppress IICR and can be used as a negative control (Communi et al., 1996, Kanemaru et al., 2007).

I generated AAV viruses encoding HA-tagged versions of wild type 5PP, RA and DM mutants (Fig. 5*A*). In addition to 5PP, these viruses also encoded GFP protein to allow easy identification of infected cells. In validation experiments, mouse embryonic fibroblast (MEF) cell cultures were infected with AAV-5PP viruses. Expression of recombinant 5PP was confirmed by Western blotting of MEF cell lysates with anti-HA and anti-5PP antibodies (Fig. 5*B*). To validate functional effects of 5PP-overexpression, I

performed a series of Fura-2 Ca^{2+} imaging experiments with AAV-5PP infected MEF cells. The AAV-GFP virus was used as an additional control in these experiments. $InsP_3$-coupled hormone Bradykinin (BK) was used to trigger IICR in these experiments. I found that application of 300 nM BK resulted in strong Ca^{2+} responses in MEF cells infected with AAV-GFP or AAV-DM viruses (Fig. 6*A*-*B*). Consistent with the previous report (Kanemaru et al., 2007), IICR was significantly suppressed in cells infected with AAV-RA viruses and completely abolished in cells infected with AAV-5PP viruses (Fig. 6*A*-*B*).

The IP3-mediated signaling is important for Purkinje cell function and genetic deletion of $InsP_3R1$ results in severe epileptic phenotype and early death in mice (Matsumoto et al., 1996). To avoid such problems, I restricted the *in vivo* experiments to the less potent 5PP-RA mutant. The inactive 5PP-DM mutant was used as a negative control in these experiments. The AAV-RA and AAV-DM viruses were delivered by bilateral stereotaxic injection into the deep cerebellar nuclei (DCN) region of 7-week old WT and 58Q mice (Fig. 7*A*). PCs project axonal processes to the DCN and transport the virus load retrogradely to the cell body in the molecular layer of the cerebellar cortex. As previously described, this protocol effectively transduces PCs with recombinant AAV *in vivo* (Kaemmerer et al., 2000, Dodge et al., 2005). Indeed, in my experiments I discovered that 2 weeks after injection AAV-encoded GFP signal that can be detected in an average of 5.8 ± 0.4 cerebellar lobes and 71.1 ± 4.6 % PCs (n = 17 mice) (Fig. 7*B*). The cerebellar expression of HA-tagged recombinant RA and DM constructs was further confirmed by immunohistochemistry using anti-HA antibodies (data not shown). Injection of AAV into the DCN at these coordinates leads to highest expression in the

cerebellar lobules, with some expression in the DCN, pons and medulla (Dodge et al., 2005). The continuous expression of RA and DM constructs in injected mice was confirmed by preparing cerebellar lysates from injected mice and probing with antibodies against the HA-tag (Fig. 14*A*).

Chronic suppression of $InsP_3R$-induced Ca^{2+} release by 5PP overexpression prevents the progressive dysfunction of Purkinje cells in SCA2 mice

To determine the effect of RA expression in preventing the dysfunction of PCs in this SCA2 mouse model, I injected the DCN of 7 week old mice with RA and prepared cerebellar slices from 24- and 48-week old injected mice for the recording of spontaneous PC activity. The transduced cells in these experiments were identified by GFP imaging. At 24 weeks, I found that most 58Q PCs overexpressing RA fired spontaneous action potential currents in a tonic fashion with a firing frequency similar to WT PCs. Specifically, I observed that the overexpression of RA prevented the irregularity in firing patterns of transduced 58Q PCs (89% tonically firing PCs; n = 3 mice) when compared to 58Q-DM PCs (65% tonically firing PCs; n = 4 mice; Fig. 9*A*). The fraction of tonically firing RA-infected 58Q cells was similar to the fraction of tonically firing WT-DM PCs of the same age (83% tonically firing PCs; n = 3 mice; Fig. 9*A*). I also found that RA overexpression restored the firing frequency and precision firing of 58Q PCs (FF = 53 ± 2.5 Hz, $p<0.001$, CV ISI = 0.22 ± 0.07; n = 22 neurons) when compared to 58Q-DM PCs (FF = 37 ± 4.4 Hz; CV ISI = 0.22 ± 0.06; n = 21 neurons; Fig. 9*B,C*). The fraction of tonically-firing PC cells, the frequency of tonically firing cells and the variability of interspike interval were not significantly different between RA-infected 58Q PC cells and

non-infected age-matched WT PC cells (Fig. 9*A-C*). The overexpression of RA slightly did not affect the firing frequency or the regularity of firing of WT PCs (Fig. 9*A-C*) at 24 weeks. I also recorded from non-transduced PCs in the same slices in RA-injected 58Q mice (n = 6 PCs). These PCs still exhibited lower firing frequency (data not shown).

At 48 weeks, I found that most 58Q PCs overexpressing RA fired spontaneous action potential currents in a tonic fashion with a firing frequency similar to WT PCs. Specifically, I observed that the overexpression of 5PP prevented the irregularity in firing patterns of transduced 58Q PCs (81% tonically firing PCs; n = 3 mice) when compared to non-transduced 58Q PCs (55% tonically firing PCs; n = 3 mice; Fig. 10*A*). The fraction of tonically firing RA-infected 58Q cells was similar to the fraction of tonically firing non-infected WT PCs of the same age (76% tonically firing PCs; n = 4 mice; Fig. 10*A*). I also found that RA overexpression restored the firing frequency and precision firing of 58Q PCs (FF = 75 ± 7.4 Hz, $p<0.001$; CV ISI = 0.19 ± 0.04, $p<0.0001$; n = 25 neurons) when compared to non-transduced 58Q PCs (FF = 25 ± 6.3 Hz; CV ISI = 0.68 ± 0.09; n = 11 neurons; Fig. 10*B,C*). The fraction of tonically-firing PC cells, the frequency of tonically firing cells and the variability of interspike interval were not significantly different between RA-infected 58Q PC cells and non-infected age-matched WT PC cells (Fig. 10*B,C*). Interestingly, the overexpression of RA slightly reduced the firing frequency and impaired regularity of firing of WT PCs (Fig. 10*B,C*), but the difference from non-infected WT cells was not statistically significant.

The overexpression of 5PP prevents motor coordination deficits in SCA2 mice

To determine if preventing the PC dysfunction also reverses the motor incoordination in 58Q mice, WT and 58Q mice were divided into 6 groups. One group of WT mice and another group of 58Q mice underwent surgery for the injection of AAV-RA, 2 control groups were included that were injected with AAV-DM and 2 naïve groups of mice were also included that never experienced any surgery (non-injected NI, Table 1). Then, I tested motor coordination over a 10-month period using the beamwalk (11 mm round and 5 mm square beam) and accelerating rotarod behavioral tasks. Both tasks were performed starting at 2 months after surgery, (i.e. at 4, 6, 8, 10 and 12 months old). Previously, our lab reported that the onset of motor incoordination in 58Q is between 6 and 8 months of age (Liu et al., 2009). At 6 months of age, 58Q mice injected with RA made significantly less footslips on 5 mm square beam than NI 58Q and 58Q mice overexpressing DM (Fig. 11*B*). Starting at 8 months of age the SCA2-58Q mice expressing RA made fewer errors while traversing the entire length of the 11 mm or 5 mm beam (Figs. 11*B,* 12*B*) and had a shorter latency to traverse the 11 mm or 5 mm beam (Figs. 11*D* and Fig 12*D*). There was no significant difference between the performance of 58Q-RA, WT-NI and WT-DM mice, demonstrating that suppressing IICR in 58Q prevents the onset of motor deficits (Fig. 11 and Fig. 12). SCA2-58Q mice expressing RA continued to perform significantly better than 58Q mice expressing DM on the 11 mm and 5mm beam at the 8, 10 and 12 month time-points. Overexpression of RA in PC cells of WT mice did not affect its performance on 11 mm beam (Figs 12*A*). However, it increased the number of errors made on the 5mm beam at 10-month and 12-month time-points (Fig. 11*A*) and increased the latency to traverse the entire 5mm beam length at 8 months (Fig. 11*C*).

The same cohort of mice was also tested on the accelerating rotarod task. Also at 6 months old, SCA2-58Q mice injected with RA performed significantly better on the rotarod task than 58Q-DM and 58Q-NI mice (Fig. 13*B*). There was no significant difference between the performance of 58Q mice expressing RA and WT mice expressing DM (Fig. 13*A*-*B*). SCA2-58Q mice expressing RA continued to perform significantly better on the rotarod than 58Q mice expressing DM at the 8, 10 and 12 month time-points. WT mice expressing RA had a trend to perform worse on the rotarod than WT-NI mice and WT-DM mice (Fig. 13*A*). However, this difference was not statistically significant. I also monitored the body weight of all the mice in this study and did not find any significant differences between the 6 groups (Fig. 14*B*).

The overexpression of 5PP alleviates PC cell pathology in SCA2

To assess if the benefit of expressing RA also extended to preventing SCA2-58Q pathology, this cohort of mice was sacrificed at 12 months old for pathological analysis. The brain weights of a subset of mice in each group were measured for quantification of differences in brain weight. Average whole cerebellar weight per group is plotted overtime for the WT and 58Q sub-groups as mean ± SE. When compared to 58Q-DM mice, the overexpression of RA in 58Q mice rescued cerebellar atrophy (*$p < 0.05$; Fig. 15). The overexpression of RA in WT mice did not affect cerebellar weight.

Our lab previously reported that calbindin-staining and stereological counting of PCs only detected a 15% loss of PCs in 12-month old 58Q mice (Liu et al., 2009). An alternative method used to analyze PC health status is by the quantification of dark cell degeneration (DCD). DCD is a form of cell death induced by excitotoxicity (Chapter 1).

Using this method, I had shown that a quantification of DCD is a more sensitive way to analyze PC cell death in SCA2 mice (Fig. 2, (Kasumu and Bezprozvanny, 2010)). I reported that less than 20% of PCs in 58Q mice appear normal, compared to 70% of PCs in age-matched nontransgenic mice (Fig. 2, (Kasumu and Bezprozvanny, 2010)).

DCD has also been used to assess the health state of PCs in mouse models of SCA7 and SCA28 (Barenberg et al., 2001, Strahlendorf et al., 2003, Custer et al., 2006, Maltecca et al., 2009). To analyze DCD, cerebellar sections from each group of mice were processed for transmission electron microscopy and the number of normal, moderately and severely degenerated PCs was quantified. According to (Custer et al., 2006, Kasumu and Bezprozvanny, 2010), PCs spherical in shape and with regular alignment in the PC layer were classified as "normal" (Fig. 8*A*). PCs with slight shrinkage compared to surrounding PCs and with moderately electron-dense cytosol that is not as dark as nucleus were classified as "moderate" (Fig. 16*A*). PCs with markedly shrunken and electron-dense cytosol with similarly darkened nucleus were classified as "severe" (Fig. 16*A*).

In my analysis, I discovered that the expression of RA in 58Q mice significantly increased the percentage of normal PCs when compared to DM-injected 58Q mice (Fig. 16*B*). On average, in samples from RA-injected 58Q mice 54% of PCs were normal, 29% were moderately degenerated and 17% were severely degenerated (n = 218 PCs; Fig. 16*B*, Table 1). In contrast, in samples from DM-injected 58Q mice 12% of PCs were normal, 47% were moderately degenerated and 41% were severely degenerated (n = 185 PCs; Fig. 16*B*; Table 1). When compared to 58Q-DM mice, the increase in the fraction of "normal" cells and the reduction in the fraction of "severely degenerated cells in 58Q-RA

mice were statistically significant ($p < 0.01$; Fig. 16*B*, Table 1). Interestingly, and in sharp contrast to 58Q mice, RA expression in WT PC cells resulted in obvious worsening of DCD phenotype ($p < 0.05$; Fig. 16*B*; Table 1) when compared to DM-expressing WT PCs. Although there is a trend for some loss in PCs in 58Q-RA mice, this is likely due to the partial efficiency of the AAV injection protocol. Only 70% of PCs are transduced at best, and the TEM preparation protocol does not distinguish between transduced and non-transduced PCs. Thus, more than likely non-transduced PCs were counted in the DCD analysis of 58-RA mice.

Discussion

Dysfunction of Purkinje cells in SCA2 and other cerebellar ataxias.

It is generally assumed that neuronal dysfunction prior to symptom presentation is a common occurrence in cerebellar ataxias (Coesmans et al., 2003, Walter et al., 2006, Alvina and Khodakhah, 2010b, a, Kasumu and Bezprozvanny, 2010, Mark et al., 2011, Shakkottai et al., 2011). However, only few functional studies of PC cells in ataxia mouse models have been performed. In a mouse model for SCA3, less than half of PCs exhibited repetitive tonic firing and the rest exhibited burst firing or remained silent for the duration of the recording (Shakkottai et al., 2011). Postnatal deletion of P/Q-type Ca^{2+} channels also decreases the firing frequency and increases the irregularity in firing of PCs, while causing motor deficits at as early as 7 weeks old (Mark et al., 2011). Furthermore, PCs in mouse models of episodic ataxia type 2 (*leaner, ducky, tottering*) fire less regularly than PCs in age-matched wildtype mice (Walter et al., 2006, Alvina and Khodakhah, 2010b, a). These findings agree with results that I obtained for PC spontaneous firing in the SCA2-58Q mouse model (Fig 3). I discovered that the fraction of tonically firing PC cells is lower in SCA2 mice when compared with age-matched wild type mice (Fig 3*C*). Furthermore, I discovered that the frequency of firing in tonically firing SCA2 PCs is reduced (Fig 3*D*) and the correlation of variability of interspike intervals is also increased in these PCs (Fig 3*E*) when compared to age-matched wild type PCs. Interestingly, the age of onset of electrophysiological abnormalities in 58Q PC cells at 24 weeks of age (Fig 3*C-D*) closely mirrors the age of onset of behavioral symptoms in SCA2-58Q mice in previous studies (Liu et al., 2009). The findings

obtained in our study (Fig 3) and previous analyses of ataxic mouse models (Alvina and Khodakhah, 2010b, a, Mark et al., 2011, Shakkottai et al., 2011) support the hypothesis that the irregularity of firing of PCs reflects the dysfunctional state of these cells and is directly linked with the ataxic symptoms. This conclusion is in agreement with the well-established importance of PC firing for maintaining cerebellar timing and function (Walter et al., 2006).

Calcium hypothesis of SCA2 and other cerebellar ataxias

What is the cause of neuronal dysfunction and death in cerebellar ataxias? In previous studies, it was suggested that supranormal IP3-mediated Ca^{2+} release from ER may play an important role in pathogenesis of SCA2 and SCA3 (Chen et al., 2008, Liu et al., 2009). Based on these results, I proposed a "calcium hypothesis" of cerebellar ataxias (Kasumu and Bezprozvanny, 2010). Genetic analysis was used by another group to independently suggest an importance of $InsP_3R$-mediated Ca^{2+} signaling in the pathogenesis of many SCAs (Schorge et al., 2010). Our lab has also demonstrated the neuroprotective effects of dantrolene, a Ca^{2+} stabilizer, in SCA3 and SCA2 mouse models (Chen et al., 2008, Liu et al., 2009). In the present study, I utilized a highly specific molecular tool to test the "Ca^{2+} hypothesis" in the SCA2 mouse model. By using the adeno-associated viral approach, I achieved stable expression of inositol 1,4,5-triphosphate 5-phosphatase (5PP) enzyme in PC cells of SCA2 transgenic mouse model. The 5PP enzyme converts the active messenger IP3 to its inactive $InsP_2$ form. As it has been demonstrated previously (Kanemaru et al., 2007), heterologous overexpression of 5PP results in potent inhibition of IP3-mediated Ca^{2+} signaling in cells. In my

experiments, I used partially active R343A mutant 5PP (RA) with reduced enzymatic activity. I reasoned that chronic expression of RA mutant in SCA2 PCs will normalize supranormal IP3-mediated Ca^{2+} signals in SCA2 PCs without completely suppressing them. The catalytically inactive double mutant 5PP-DM was used in our studies as a negative control. Consistent with our predictions, I found that chronic expression of RA in SCA2 PC cells normalized their electrophysiological phenotype (Fig. 9 and 10), alleviated motor coordination deficit of SCA2 mice in beamwalk and rotarod assays (Fig. 11, 12 and 13), prevented cerebellar atrophy (Fig. 15) and prevented DCD form of PC death in aging SCA2 mice (Fig 16, Table 2). These effects required enzymatic activity of 5PP, as the chronic expression of the catalytically dead R343A/R350A mutant 5PP (DM) had no effect in behavioral assays with SCA2 mice (Fig. 11, 12 and 13) and did not protect SCA2 PC cells in DCD assay (Fig. 16). These findings provided strong support for the "calcium hypothesis of SCA2" and suggested that partial inhibition of IP3-mediated Ca^{2+} signaling could provide therapeutic benefit for the patients afflicted with SCA2 and possibly other SCAs

Importance of $InsP_3R$-mediated Ca^{2+} signaling for PC cell function

Our results indicate that excessive Ca^{2+} release from IP3-sensitive Ca^{2+} stores is likely to play a key role in dysfunction and death of PC cells in SCA2. This conclusion is consistent with early-onset PC degeneration and ataxia phenotype in Inpp5a (5PP) knockout mice (Andy W Yang; Andrew J Sachs ;Emily M Strunk; Arne M Nystuen, SfN-2011 abstract). The 5PP enzyme is highly expressed in cerebellar PCs; thus, it is likely that knockout of 5PP causes delayed termination of IP3 signals and supranormal

Ca^{2+} release. Remarkably, insufficient IP3-mediated Ca^{2+} signaling also leads to the ataxic phenotype and PC degeneration, such as observed in SCA15/16 patients haploinsufficient for the $InsP_3R1$ gene (van de Leemput et al., 2007, Hara et al., 2008, Iwaki et al., 2008). An ataxic phenotype is also observed in *opt* mice with reduced levels of $InsP_3R1$ protein (Street et al., 1997) and a severe ataxia is observed in $InsP_3R1$ knockout mice (Matsumoto et al., 1996). These findings indicate that reduced Ca^{2+} release via $InsP_3R1$ also leads to PC cell dysfunction and ataxic phenotype. Some of the data in the present manuscript support this conclusion. Despite using the RA version of 5PP with reduced activity in our experiments, I observed that chronic expression of RA in wildtype PCs resulted in mild impairment in the precision of PC firing (Fig 10*C*), impaired beam walk and rotarod performance of wild type mice in behavioral studies (Fig 11 and 13) and a reduced fraction of normal cells in DCD analysis of wild type mice (Fig 16*C*, Table 2). Although relatively mild, these effects were in sharp contrast with the beneficial effects of RA expression in SCA2-58Q mice (Fig. 9-16, Table 1). I conclude from these findings that there is a relatively narrow range of optimal IP3-mediated Ca^{2+} signaling that is compatible with proper function and long-term survival of PC cells (Fig. 17). Deviation from this optimal range in either direction of IP3-mediated Ca^{2+} signaling results in PC dysfunction and an ataxic phenotype. This hypothesis agrees well with independent genetic evidence that placed $InsP_3R$ in the "eye of the storm" of pathogenesis for many SCAs (Schorge et al., 2010).

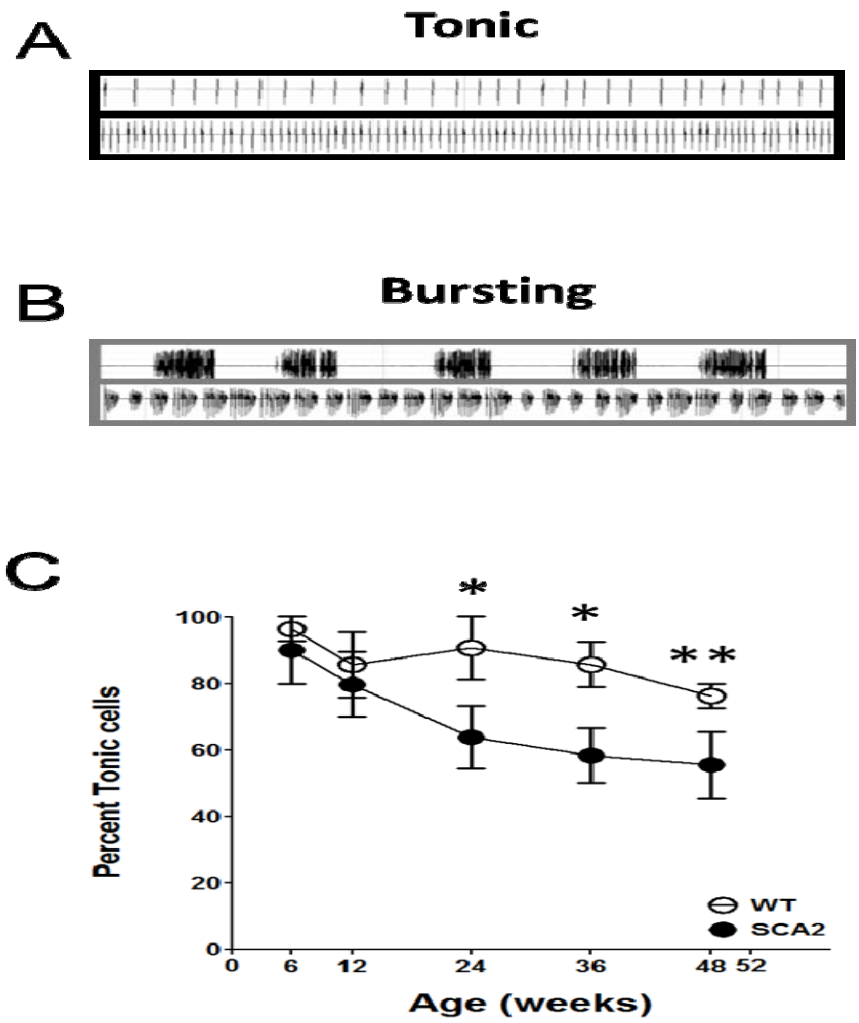

Figure 3. Characterization of PC Spontaneous activity in 58Q mice. Firing activity was analyzed in 6, 12, 24 and 48 weeks old WT and 58Q PCs. PC firing was classified as (A) tonic or (B) bursting based on the firing patter observed during a 5 minute recording. *C,* The proportion of PCs firing tonically was calculated as a percentage of total active cells and plotted. Fewer PCs fire tonically in slices prepared from 24 and 48 weeks old 58Q when compared to age-matched WT mice. (*p < 0.05; **p < 0.01)

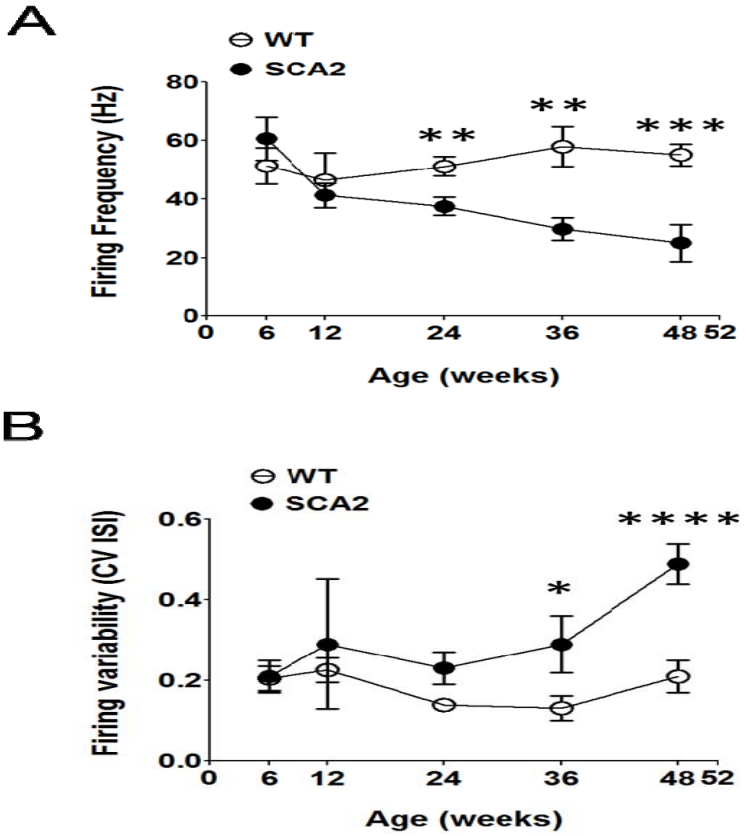

Figure 4. Progressive dysfunction of PCs in SCA2-58Q mice. *A,* Average firing frequency of each PC in the 5 minute duration was analyzed. Mean firing frequency in each group at each time-point was calculated and plotted as mean ± SE. The firing frequency of tonically firing PCs in 24- and 48-week old 58Q mice is lower than in age-matched WT PCs. *B,* Firing variability was represented as the correlation of variation of interspike interval (CV ISI) and calculated for each PC in the 5 minute recording duration. Mean CV ISI in each group at each time-point was calculated and plotted as mean ± SE. Tonically firing PCs in 48-week old 58Q PCs fired more irregularly. **p < 0.01; ***p < 0.001; ****p < 0.0001, whereas no significance is not indicated

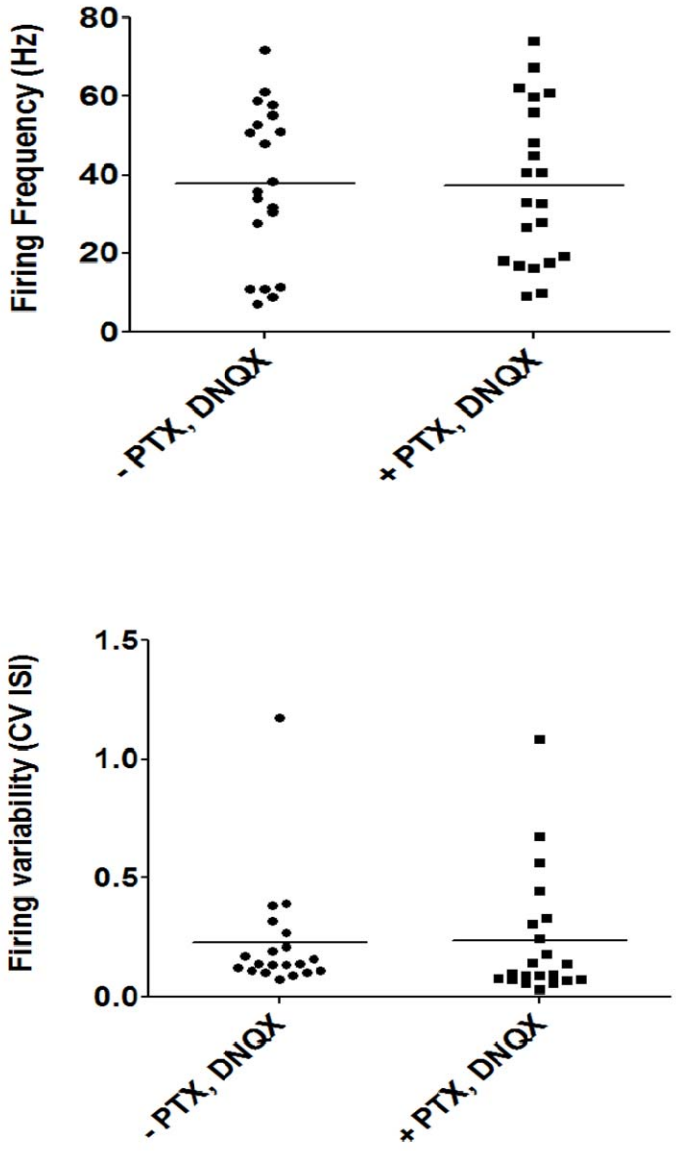

Figure 5. Blocking fast excitatory and inhibitory synaptic inputs had no effect on SCA2 PC activity. *A,* Average firing frequency of each PC in the 5 minute duration was analyzed. Mean firing frequency in each group at each time-point was calculated and

plotted as mean ± SE. The firing frequency of tonically firing PCs in 24-week old 58Q mice is consistent in the absence and presence of synaptic innervation. *B,* Firing variability was represented as the correlation of variation of interspike interval (CV ISI) and calculated for each PC in the 5 minute recording duration. Mean CV ISI in each group at each time-point was calculated and plotted as mean ± SE. The firing variability of tonically firing PCs in 24-week old 58Q mice is consistent in the absence and presence of synaptic innervation.

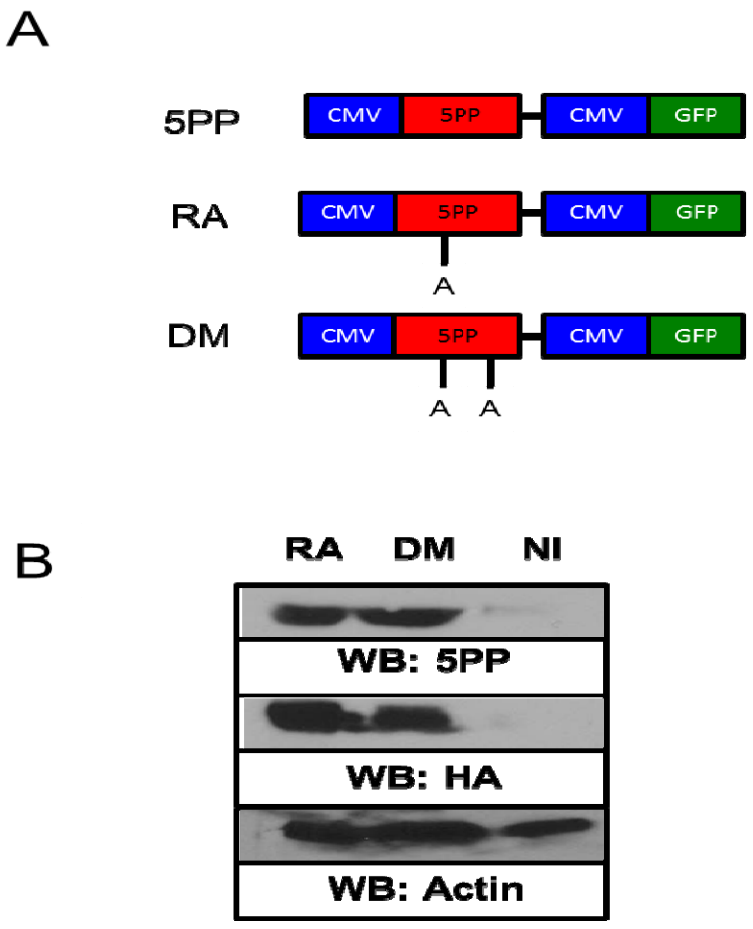

Figure 6. Generation and validation of AAV-5PP viruses. *A,* Cloning strategy for AAV-5PP, AAV-RA, AAV-DM plasmids. Each plasmid contained the 5PP construct and a GFP construct. The expression of both constructs was driven by individual CMV promoters. *B,* After the viruses were generated via the baculovirus system, they were used to infect cell culture to confirm expression. Presenilin 1/2 double knockout MEF cells were infected with ~4 X 10^{13} ip/well AAV-5PP, AAV-RA or AAV-DM viruses. MEF cell lysates were prepared and analyzed by western blotting with antibodies against 5PP, HA and actin.

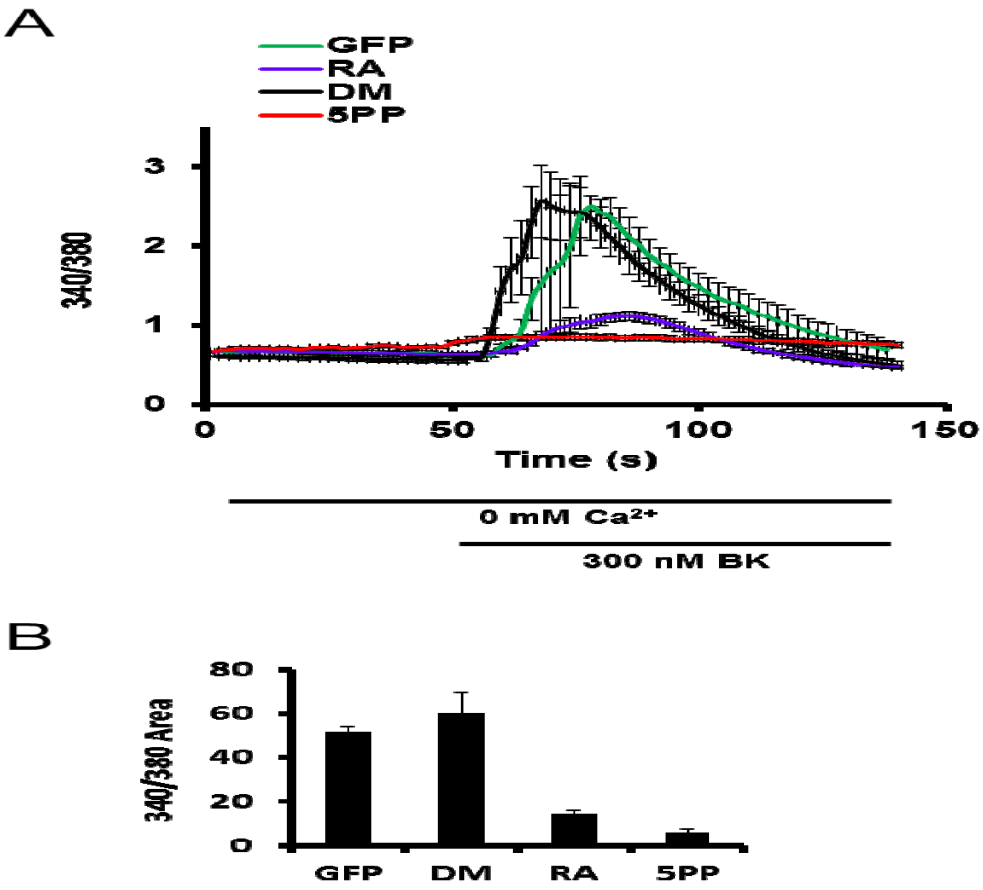

Figure 7. Validation of 5PP viruses in calcium imaging experiments. *A,* MEF cell cultures infected with AAV-5PP, AAV-RA, and AAV-DM were loaded with the calcium indicator, Fura-2. Basal Fura-2 ratio recordings were collected for 55s. 300nM Bradykinin (BK) was added to stimulate BK-coupled IP3-induced calcium release. Fura-2 ratio recordings were collected for 2 minutes to analyze effect of AAV-5PP, AAV-RA, AAV-DM on IP3-induced calcium release. The results are combined from three different batches of cells and shown as mean 340/380 ratio area ± SE. *B,* The area of the Fura-2 340/380 ratios in (A) was calculated and plotted. The BK-induced Ca2+ release in cells expressing RA and 5PP are significantly lower than in cells expressing DM or GFP.

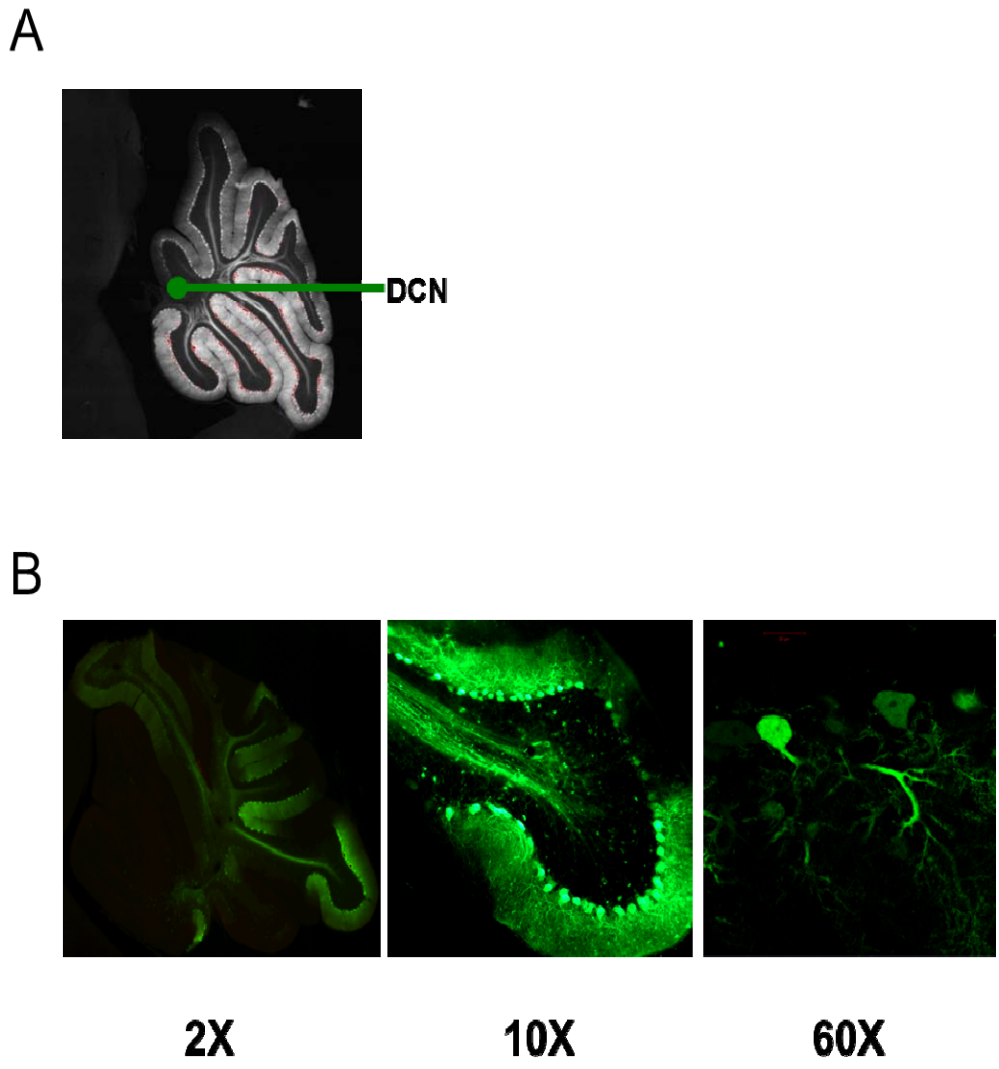

Figure 8. Deep cerebellar nuclei (DCN) injection protocol. ***A,*** 4ul of ~10^{13} ip/ul was injected bilaterally into the DCN in the cerebellum of each mouse. PCs project axons to the DCN where they pick up the viral load and retrogradely transport it to their soma. ***B,*** Three weeks after AAV-5PP-RA virus was injected, mice were sacrificed and expression of the constructs was confirmed 2 weeks after surgery by scanning cerebellar sections

with a florescent plate reader and by confocal imaging (from left to right, 2X, 10X and 60X magnification). Expression of the virus was seen in an average of of 5.8 ± 0.4 lobes and 71.1 ± 4.6 % PCs in 17 mice

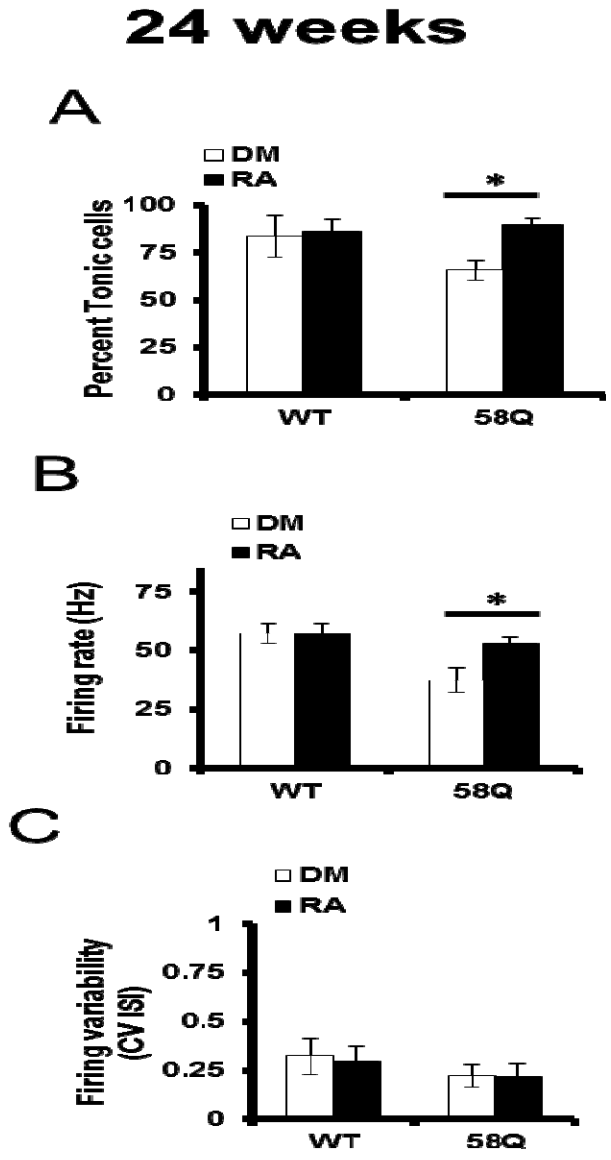

Figure 9. Viral-mediated overexpression of 5PP rescues regular tonic firing in 58Q PCs. The overexpression of RA in SCA2-58Q mice (A) increased the proportion of tonically firing cells (B) increased firing frequency of tonically firing cells and (C) did not affect the firing variability of tonically firing cells. (*$p < 0.05$)

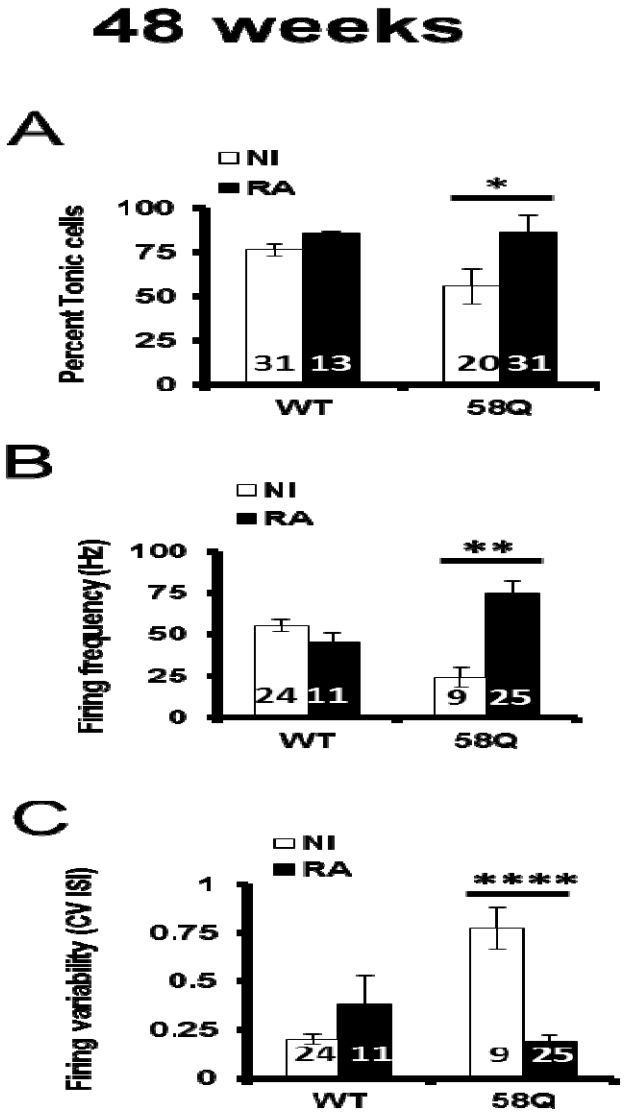

Figure 10. Viral-mediated overexpression of 5PP rescues regular tonic firing in 58Q PCs. The overexpression of RA in SCA2-58Q mice (A) increased the proportion of tonically firing cells (B) increased firing frequency of tonically firing cells and (C) reduced firing variability of tonically firing cells. (*$p < 0.05$; **$p < 0.01$; ****$p < 0.0001$)

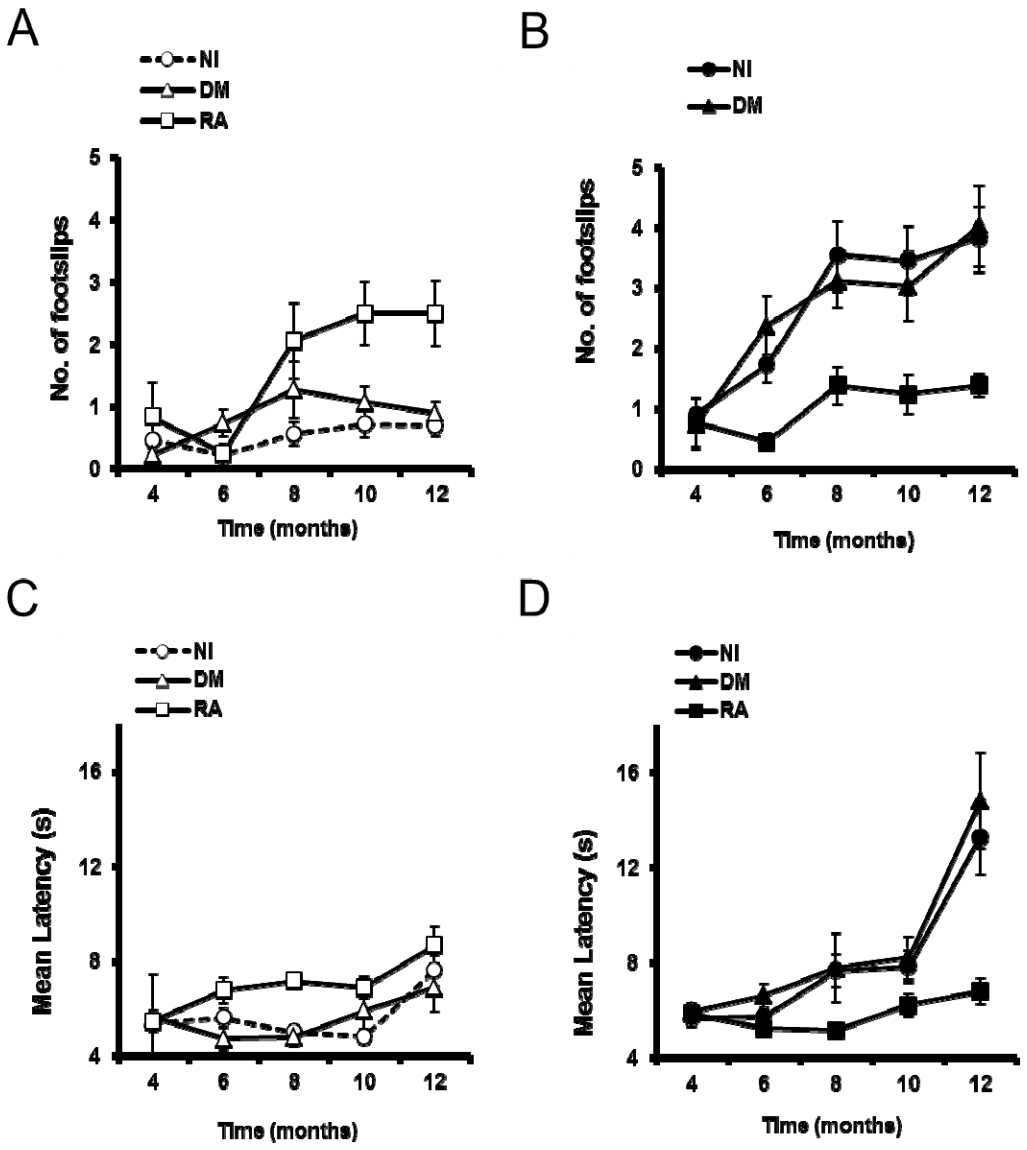

Figure 11. The over-expression of 5PP alleviates the beamwalk deficits in SCA2-58Q mice. Performance on the 5mm beam was analyzed and recorded every 2 months. *A, B,*

Average number of footslips as the mice traverse the entire length of the 5mm beam is plotted for the NI, RA- and DM-injected WT and 58Q mice as mean ± SE from 4 to 12 months. 58Q mice injected with RA made fewer errors on the 5mm beam than 58Q mice injected with DM and NI 58Q mice. *C, D,* Average time to traverse the entire length of the 5mm beam is plotted for all 6 groups as mean ± SE from 4 to 12 months. 58Q mice injected with RA traversed the 5mm beam faster than their 58Q counterparts and as fast as WT mice injected with DM and naïve WT mice. WT-RA mice also showed impairment in beamwalk performance. (e-f) Mice were also tested on the accelerating rotarod at 0.2rpm/s. Average latency to fall from the accelerating rotarod is plotted for all 6 groups as mean ± SE from 4 to 12 months of age. The onset of rotarod deficits in 58Q mice injected with RA was prevented. (*$p < 0.05$; **$p < 0.01$; ***$p < 0.001$)

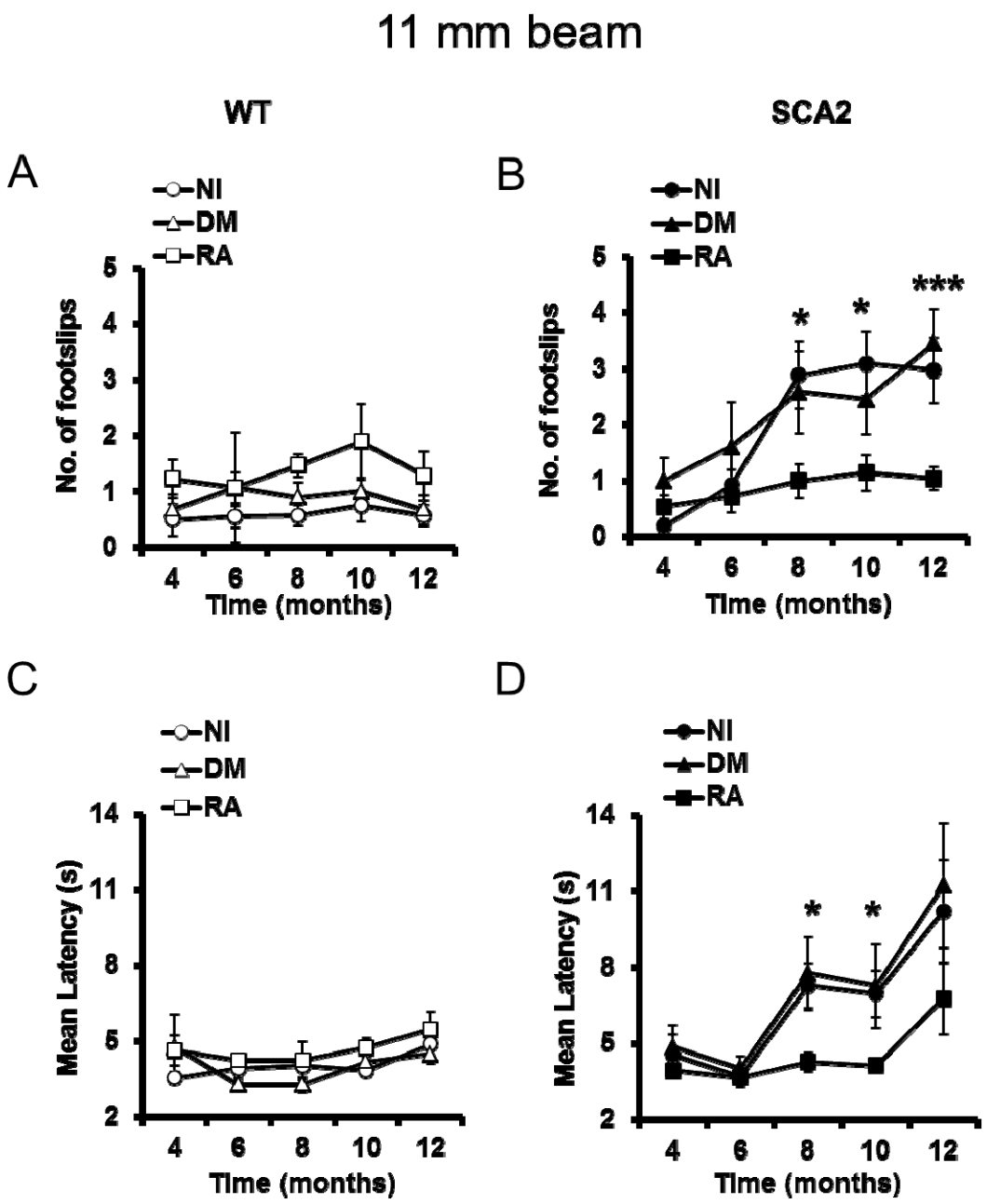

Figure 12. The over-expression of 5PP alleviates the beamwalk deficits in SCA2-58Q mice. Performance on the 11mm beam was analyzed and recorded every 2 months.

A, B, Average number of footslips as the mice traverse the entire length of the 11mm beam is plotted for the NI, RA- and DM-injected WT and 58Q mice as mean ± SE from 4 to 12 months. 58Q mice injected with RA made fewer errors on the 5mm beam than 58Q mice injected with DM and NI 58Q mice. *C, D,* Average time to traverse the entire length of the 5mm beam is plotted for all 6 groups as mean ± SE from 4 to 12 months. 58Q mice injected with RA traversed the 11mm beam faster than their 58Q counterparts and as fast as WT mice injected with DM and naïve WT mice.

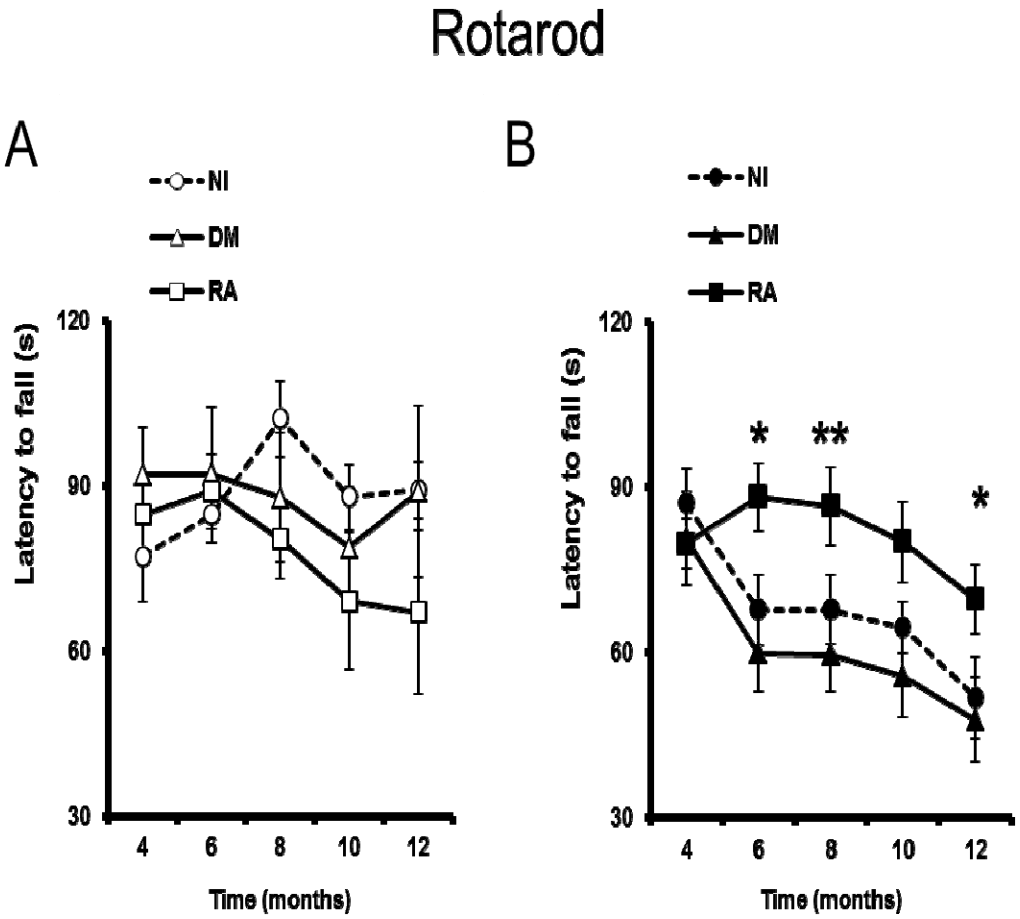

Figure 13. The over-expression of 5PP alleviated the rotarod phenotype of SCA2-58Q mice. Every 2 months, mice are given 3 training trials on the accelerating rotarod at 0.2rpm/s on 4 consecutive days. Average latency to fall from the accelerating rotarod on the 4th day is shown for all 6 groups as mean ± SE from 4 to 12 months of age. The longer the latency to fall off the rod, the better the motor performance. Between 6 to 10 months of age, 58Q-RA mice performed similar to WT, WT-DM and WT-RA mice, as well as significantly better than 58Q and 58Q-DM mice. There is a later onset of motor deficits in 58Q-RA mice at 12 months of age. (*$p < 0.05$; **$p < 0.01$)

A.

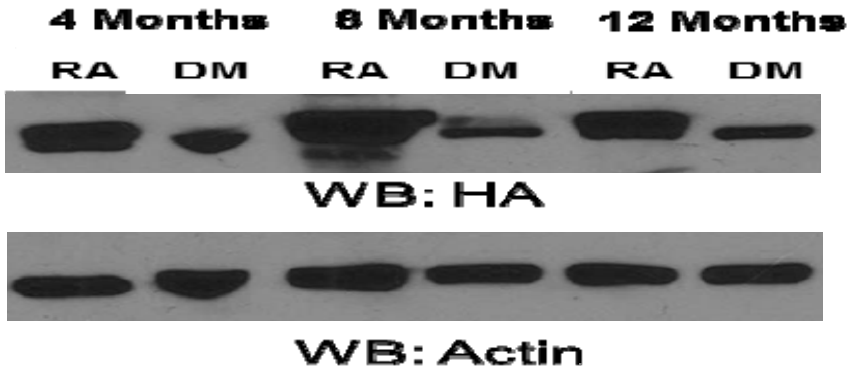

B.

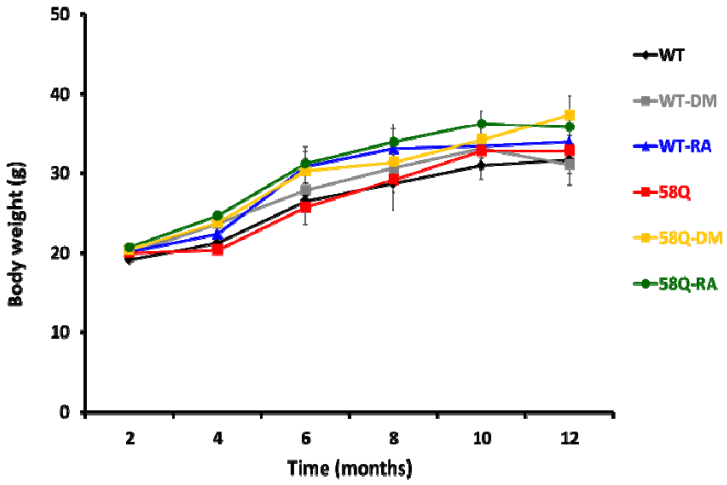

Figure 14. The over-expression of 5PP had no effect on body weight. *A,* Cerebellar lysates were prepared from injected mice at 4, 8 and 12 months of age. Lysates were probed with antibodies against the HA tag and actin, as a loading control. *B,* Mice were weighed every 2 months to ensure that there were no adverse effects of the surgery on weight-gain

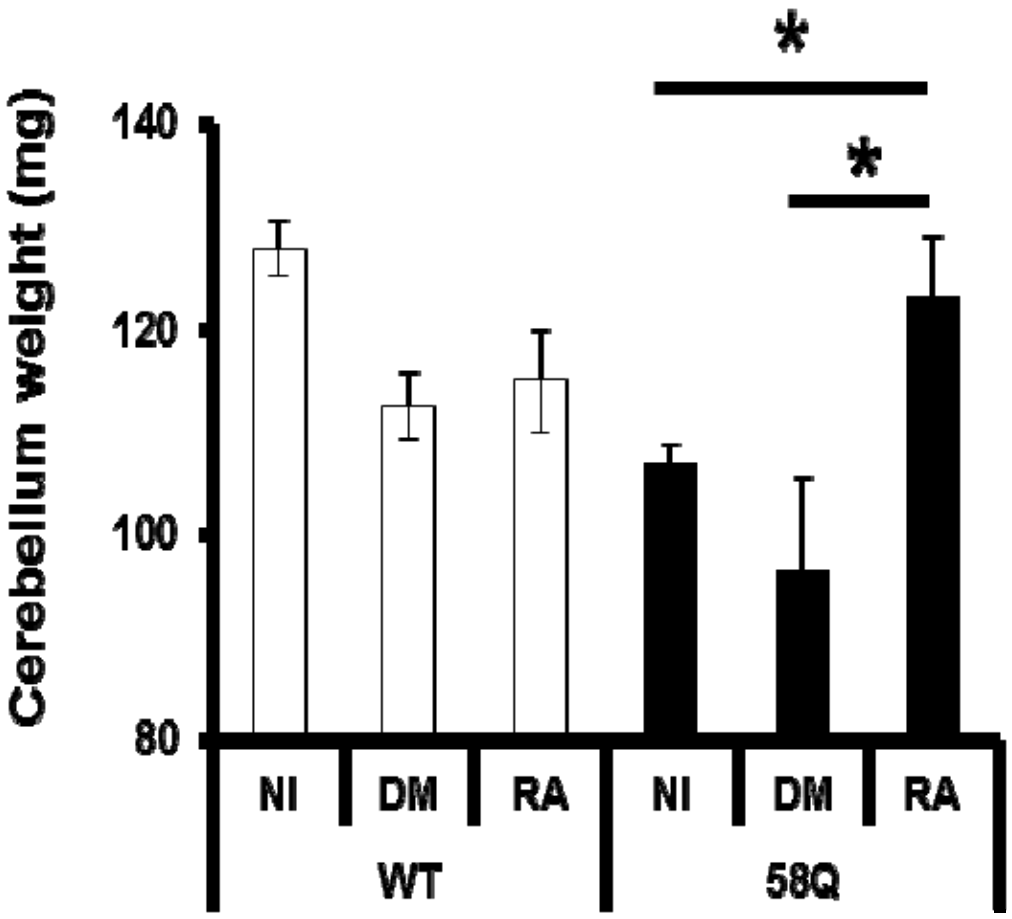

Figure 15. 5PP expression rescues SCA2-58Q pathology. (A) Brain atrophy and (B) Cerebellar atrophy were measured and plotted overtime for all 6 groups as mean ± SE. The overexpression of RA in 58Q mice rescued brain atrophy and cerebellar atrophy. The overexpression of RA in WT mice caused mild brain atrophy without affecting cerebellar weight (*$p < 0.05$)

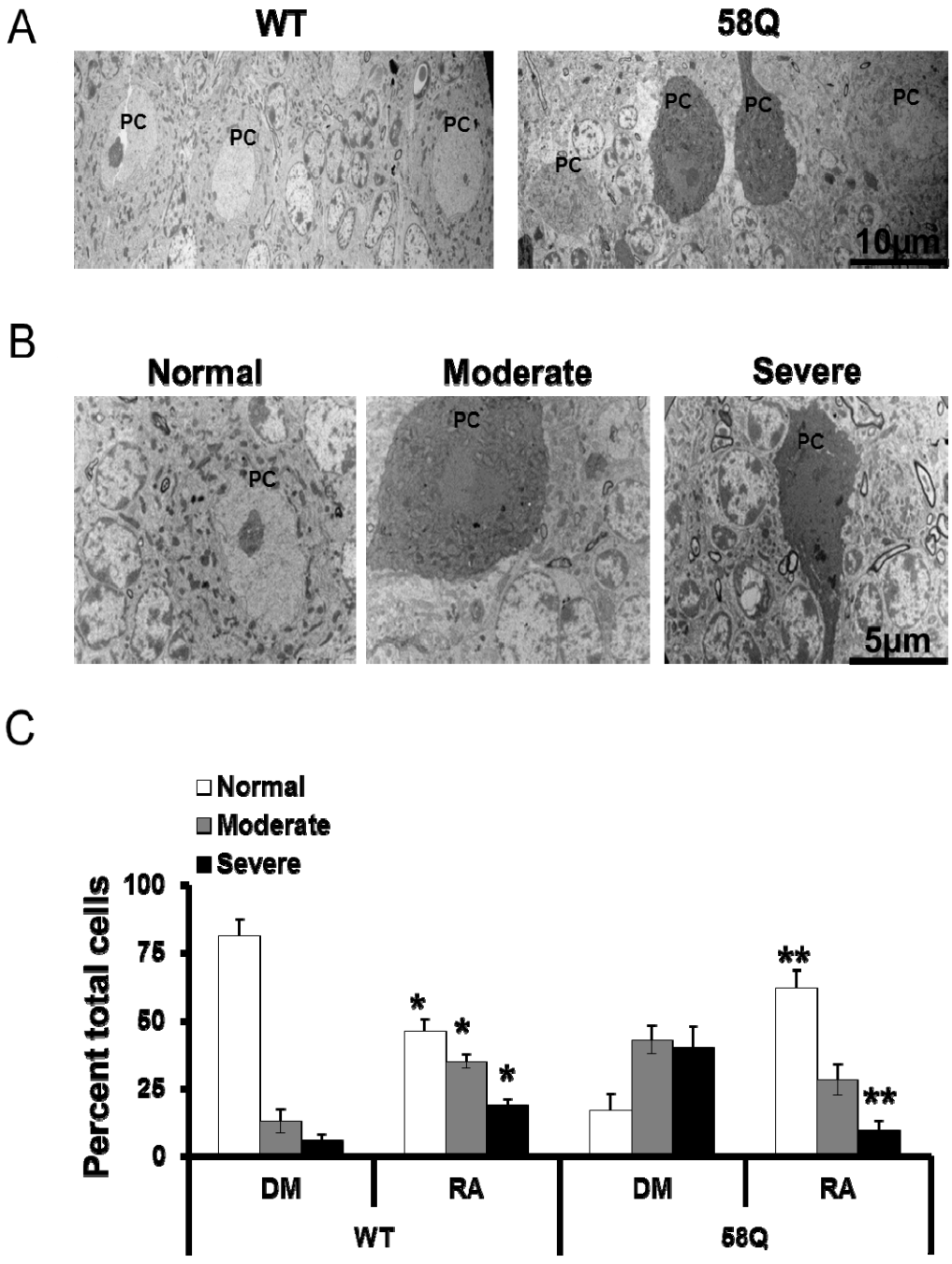

Figure 16. The over-expression of 5PP prevented the dark cell degeneration of SCA2-58Q PCs. *A,* 48-week old cerebellar sections were processed for Transmission

Electron Microscopy and analyzed for changes in Dark cell degeneration status. The number of normal, moderately and severely degenerated PCs in injected mice was quantified. *B,* The overexpression of RA in 58Q mice prevented dark cell degeneration of PCs. The overexpression of RA in WT mice caused slight dark cell degeneration of PCs, which was not significant compared to WT-DM transduced PCs. (**$p < 0.01$)

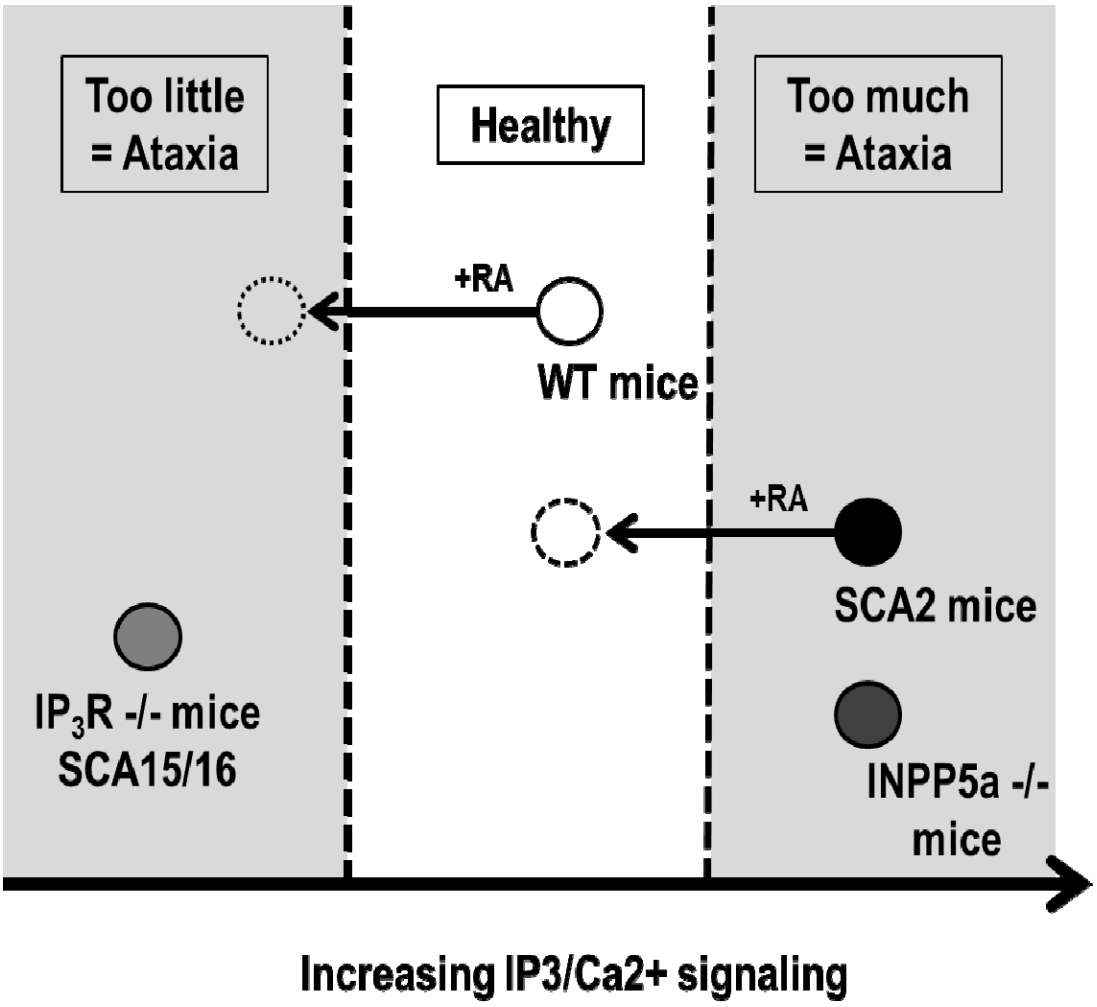

Figure 17. Optimal range of IP3/Ca2+ signaling in PCs.

Group	No. of mice	Brain weight (mg)	DCD measurements		
			Normal (%)	Moderate (%)	Severe (%)
WT-DM	13	528 ± 21	81.1 ± 6	13 ± 4	5.9 ± 2
WT-RA	13	470 ± 10	**46 ± 5***	**35 ± 3***	**19 ± 3***
WT-NI	15	498 ± 18	N/A	N/A	N/A
58Q-DM	12	455 ± 30	17 ± 6	43 ± 5	40 ± 8
58Q-RA	19	532 ± 31*	**62 ± 7****	**28.3 ± 6****	**9.76 ± 4****
58Q-NI	15	436 ± 7.5	N/A	N/A	N/A

Table 2. Summary of *in vivo* study of the effect of 5PP overexpression on SCA2 onset and progression. Eighty-seven mice were genotyped, weight-matched and divided into 6 groups. The allotted AAV virus was injected. The group number, group name, number and genotype of mice in each group and AAV virus injected are shown for each group. Also shown are the mean whole brain weights, cerebellar weights and percentages of DCD status. A two-tailed Student's unpaired *t* test was used to judge differences between groups. There was a significant difference between 58Q-RA transduced PCs and 58Q-DM transduced PCs (**$p < 0.01$). There was no significant difference between the DCD status of WT-DM PCs and 58Q-RA PCs. N/A, not applicable.

CHAPTER THREE

Positive modulators of SK channels reverts irregular cerebellar activity and improves motor function in a mouse model of spinocerebellar ataxia 2.

Background, Methods, Results, Discussion

Background

It has been speculated that the resulting aberrant intracellular Ca^{2+} in SCA2 exerts excitotoxic effects through intracellular Ca^{2+}-dependent signaling and by directly disrupting the functional properties of PCs (Kasumu and Bezprozvanny, 2010). Purkinje cells exert pacemaking activity that is crucial for the projection of cortical cerebellar information to deep cerebellar nuclei and further to other motor coordination areas such as the thalamus, red nucleus and spinal cord. Thus, dysfunctional P C activity could lead to motor incoordination (Walter et al., 2006, Kasumu and Bezprozvanny, 2010, Shakkottai et al., 2011).

Ca^{2+}-activated K^+ channels, both small conductance (the SK2 isoform, $K_{Ca}2.2$ encoded by KCNN2) and big conductance (BK, $K_{Ca}1.1$ encoded by KCNM1) channels, are important regulators of the basic electrophysiology of PCs. Selective deletion of BK or SK2 channels results in ataxic phenotypes, SK2 deficiency being most severe (Szatanik et al., 2008, Chen et al., 2010). SK channels are voltage-independent heterotrimeric potassium channels, which are activated by intracellular calcium. SK channel activation modulates PC firing activity by increasing the hyperpolarization between spikes (after-hyperpolarization, AHP) thus eliminating burst activity (Cingolani et al., 2002, Womack and Khodakhah, 2003).

Four subtypes of SK channels have been identified. SK1, SK2 and SK3 conduct potassium ions on the order of ~10 pS (Kohler et al., 1996). SK4 channels are often referred to as IK because they conduct ions on the order of ~20-80 pS and are thus intermediate between SK and BK channels (Vergara et al., 1998). IK is not expressed in the central nervous system (CNS, (Thompson-Vest et al., 2006)). Of the 3 subtypes of SK

channels, SK2 has the strongest expression in the brain, specifically in the neocortex and hippocampus (Sailer et al., 2002, Patko et al., 2003). Moderate expression of SK1 has been reported in regions parallel to SK2 expression in the brain (Sailer et al., 2002, Patko et al., 2003). Very weak expression of SK3 has been reported in the brain with highest expression in the striatum, basal ganglia and brainstem (Sailer et al., 2002, Patko et al., 2003). However, in the cerebellum, SK1-3 expression varies widely between the different cerebellar neurons. Only SK2 channel expression has been reported in purkinje cells (Cingolani et al., 2002), while high levels of SK3 channels are expressed in granule cells (Stocker and Pedarzani, 2000). Very little, if any, expression of SK3 has been reported in the DCN (Stocker and Pedarzani, 2000, Sailer et al., 2004, Shakkottai et al., 2004).

Functional studies have been performed to study SK channels in neurons and behavior. SK3 single knockout mice lack a behavioral phenotype, likely due to compensation by other SK subtypes (Bond et al., 2000). Furthermore, a naturally occurring SK2 loss-of-function mutation in mice (*frissonant* mice) causes prominent motor deficits (Callizot et al., 2001), while the deletion of SK2 prevents medium I_{AHP} in hippocampal slices (Bond et al., 2004).

The precise "pacemaker" firing of PCs is believed to encode cerebellar timing and function (Walter et al., 2006). SK channels play a role in the establishment of the normal endogenous pacemaking activity of PCs. Thus, SK channels are an interesting target for pharmaceutical intervention in ataxias. In mouse models of episodic ataxia type 2 (EA2) (*tottering, leaner, ducky*), which are ataxic due to missense mutations in the gene encoding the P/Q-type voltage-dependent Ca^{2+} channel, the direct involvement of SK channels is well established (Walter et al., 2006, Alvina and Khodakhah, 2010b, a). In

slices from these mice, the endogenous pacemaking activity of PCs is significantly more irregular compared to age-matched wildtype mice (Alvina and Khodakhah, 2010b, a). This phenomenon is well rationalized by decreased Ca^{2+}-influx during the action potential and less effective activation of the SK channels, causing aberrant medium after-hyperpolarizations (mAHP´s) and irregular firing. 1-EBIO (1-ethyl-2-benzimidazolinone, an SK channel activator), a compound that activates SK channels by directly increasing their Ca^{2+}-sensitivity, corrects this firing anomaly, and intriguingly alleviates the ataxia when administered directly into the cerebellum (Walter et al., 2006).

Follow-up studies confirmed this concept by systemically delivering chlorzoxazone or 4-aminopyridine, weak SK channel-activating drugs, to EA2 mouse models (Alvina and Khodakhah, 2010b, a). Specifically, chronic *in vivo* perfusion of *ducky* mice with 1-EBIO abolished dyskinesia episodes and improved performance on the accelerating rotarod. The *tottering* mouse model of episodic ataxia 2 also displays decreased PC pacemaking without a significant change in firing frequency when compared to wildtype littermates. Treating cerebellar slices prepared from *tottering* mice with 4-Aminopyridine (4-AP, a K^+ channel blocker) or chlorzoxazone (CHZ, a Kca activator) restores the precision of firing. CHZ and 4-AP also improved the motor performance of *tottering* mice (Alvina and Khodakhah, 2010b, a).

It is speculated that SK channels might be involved in hereditary degenerative ataxias by a less direct mechanism and that positive modulators may be of benefit in such disorders. It was recently reported that in SCA3 transgenic mice, abnormal cerebellar activity and motor behavior could be alleviated using SKA-31, a Riluzole analogue optimized for positive modulation of SK channels, further suggesting the possibility that

SK channel modulation may represent a treatment principle in a range of cerebellar ataxias (Shakkottai et al., 2011). Furthermore, promising clinical data have recently been obtained with Riluzole in a phase II study in a mixed population of ataxia patients (Ristori et al., 2010), an effect arguably due to SK channel facilitation.

Recent pharmacological studies have reported 2 SK modulators that increase the sensitivity of SK channels to intracellular calcium (Strobaek et al., 2004, Hougaard et al., 2007). Cyclohexyl-[2-(3,5-dimethyl-pyrazol-1-yl)-6-methyl-pyrimidin-4-yl]-amine (CyPPA) and 3-Oxime-6,7-dichloro-1H-indole-2,3-dione (NS309) bind SK1, SK2 and SK3 with varying selectivity and potency (Fig. 18). CyPPA has a high selectivity for SK3 at 6 μM and SK2 at 14 μM with no selectivity for SK1 or IK channels but has very little potency. At concentrations greater than 5uM, CyPPA also binds and activates BK, Nav1.2, VGCC, voltage-gated sodium channels (Hougaard et al., 2007). Conversely, NS309 is not selective for SK1, SK2, SK3 or IK but has great potency for all 3 channels at 1 μM without binding BK channels (Strobaek et al., 2004). CyPPA and NS309 have more selectivity and potency than the older SK activator 1-EBIO, thus lead the way in potential therapeutic compounds for ataxia.

The same Danish Neurosearch company that identified NS309 and CyPPA recently created another SK channel modulator named (4-Chloro-phenyl)-[2-(3,5-dimethyl-pyrazol-1-yl)-9-methyl-9*H*-purin-6-yl]-amine (NS13001). NS13001 has the selectivity of CyPPA and the potency of NS309. NS13001 binds SK3 at 0.14 μM, SK2 at 1.6 μM and SK1 at 10 μM. Thus, it is the ideal SK modulator.

Here, I addressed whether the abnormal cerebellar activity characterized in SCA2 transgenic mice (Chapter 2), is sensitive to SK modulation. Specifically, I compared

CyPPA, NS13001 and NS309 in alleviating the phenotype of symptomatic SCA2 PCs and mice. I studied the role of SK channels in Purkinje cell function using cerebellar slices from SCA2 mice and age-matched wildtype mice. I tested the hypothesis that pharmacologically unselective as well as subtype selective SK modulators might have the potential to revert irregular Purkinje cell firing and improve pacemaker function. Furthermore, I tested the effect of SK modulators on the motor performance and pathology of SCA2-58Q mice.

Research design and Methods

As described in chapter 2

Loose-patch recordings in mouse cerebellar slices

Loose-patch recordings were made as described in Chapter 2. Spontaneous action potential currents were recorded for 5-60 minutes from each cell. The five-minute recordings were analyzed for tonic or burst firing. Burst firing PCs were characterized by the presence of repetitive bursts. Cells were characterized as firing tonically if they fired repetitive non-halting spike for 5 minutes. Tonically firing cells were further analysed for average firing frequency and the firing variability represented by the correlation of variation of interspike interval (CV ISI). For recordings longer than 5 minutes, once a burst firing pattern was confirmed in the first 5 minutes, the bath solution was switched to aCSF containing 5μM NS309 or 5μM CyPPA for at least 15 minutes after which the drug was washed out to determine the effect of the drug on the firing pattern.

Motor coordination assessments in mice

Rotarod and beamwalk tasks were used to assess motor coordination as described in Chapter 2. SCA2-58Q and WT mice were trained on the accelerating rotarod apparatus (Columbus instruments). At baseline, mice were trained on the beamwalk task to traverse 3 separate beams of differing diameters. A round plastic 17mm beam, a round plastic 11mm beam and a wooden square 5mm beam were used. Mice were given 3 consecutive training trials on 3 consecutive days on each beam. On the 3rd day, the mean latencies to

traverse the entire length of the 11mm and 5mm beams were recorded and analyzed for every animal in all 6 groups. After a 3 day wait period, mice were trained on the accelerating rotarod task. Mice were trained to walk on a rotating rod accelerating at 0.2rpm. Mice were trained for 4 consecutive days with 3 consecutive trials per day. The mean latency to fall off the accelerating rod was recorded and analyzed for every animal in all 6 groups. At each time following baseline testing, mice were only given 2 days on each task. Specifically, mice were trained on the beamwalk with 3 trails per beam on day 1 and tested on day 2. After a 3 day wait, mice were trained on the rotarod with 3 consecutive trials on day 6 and tested on day 7.

Dark cell degeneration analyses

Dark cell degeneration was analyzed as described in Chapter 2.

Statistical Analyses

Differences between groups were judged by a two-tailed Student's unpaired *t* test using a significance level of 0.05.

Results

NS309 regularizes firing activity of SCA2 PCs

It has been suggested that pre-symptomatic PC dysfunction is responsible for motor deficits that develop in ataxia mouse models (Kasumu and Bezprozvanny, 2010). In line with this hypothesis, PC dysfunction has been reported prior to the onset of motor symptoms in a mouse model of Spinocerebellar ataxia 3 (Shakkottai et al., 2011). Similar reports of PC dysfunction have been reported in a mouse model of episodic ataxia 2 (EA2) (Walter et al., 2006, Alvina and Khodakhah, 2010b, a). I also found that there is PC dysfunction in a mouse model of SCA2 (Fig. 3 and 4). In this SCA2-58Q mouse model, PCs fire less tonically at the onset of motor dysfunction. As the disease progresses in this model, a greater proportion of PCs fire in a bursting pattern and tonically firing PCs begin to lose the well-established precision. I believe that the irregularity in PC activity represents the ataxic disease state and the reversal of this irregularity could provide therapeutic benefit. In fact, treatment of EA2 mice with activators of KCa channels restores the precision firing of PCs and alleviates the behavioral deficits (Alvina and Khodakhah, 2010b, a).

The efficacy of SK compounds in reversing the irregularity in PC activity in aged SCA2-58Q mice was tested. I recorded spontaneous PC activity in 24-week old SCA2-58Q mice and age-matched WT mice. A tonically firing cell will maintain a relatively constant firing frequency with rare short-lived bursts (Fig. 3*A*, 19*A*, and 18*A*). Burst firing patterns vary in aged SCA2-58Q PCs. Some PCs exhibit rarely halting burst firing (Fig. 3*B*). Other PCs alternate between tonic spikes with increasing frequency, burst

firing and brief silent periods (Fig. 19*D*) in a pattern termed "trimodal" (Womack and Khodakhah, 2002). The efficacy of SK compounds in restoring precision firing in bursting 58Q PCs was tested. I was unable to test the effects of NS13001 on PC physiology due to its insolubility in solution. Instead, I tested the effect of NS309 and CyPPA on PC firing activity in cerebellar slices. PCs were classified as tonically firing or bursting during an initial 5 minute recording duration. Bursting PCs were perfused with either 5μM NS309 or 5μM CyPPA. After treatment with NS309, PCs that were previously firing in a persistently bursting pattern were reverted to tonic firing (n = 6 of 6 PCs; n = 5 mice; Fig. 19*E* and 19*G*), and PCs that were transiently bursting were reverted to tonic activity (n = 2 of 2 PCs; n = 2 mice; Fig. 19*H*). At 5μM, CyPPA was unable to consistently revert persistently bursting PCs (n = 2 of 5 PCs; n = 4 mice; Fig. 19*F*), but reverted transiently bursting PCs to tonic activity (n = 2 of 4 PCs; n = 2 mice; Fig. 19*H*).

Chronic treatment of mice with SK modulators improves motor performance

In order to test the effect of SK modulators on the motor performance of symptomatic SCA2 mice, 9-month old WT and 58Q mice were subdivided into 6 treatment groups (58Q, 58Q-CyPPA, 58Q-NS13001, WT, WT-CyPPA, WT-NS13001). Baseline motor performance was assessed to confirm symptomatic onset of motor incoordination (Fig. 20*A*-*B*; Fig. 21*A*-*B*). This was subsequently followed by chronic delivery of either NS13001 or CyPPA or vehicle to the mice for 3 consecutive weeks. I found that the oral-route of delivery of these compounds to adult mice was sufficient to deliver the compounds across the blood brain barrier. Blood and brain tissue samples

collected 1 hour after oral dosing of 30mg/kg of NS13001 or 10mg/kg of CyPPA is sufficient to produce an effective concentration of the compounds in the blood and brain (data not shown). After a 3-day washout period following the 3-week treatment, motor performance was re-assessed.

At baseline (Fig. 20*A*, white bars), mice were trained for 3 consecutive days on the 17mm, 11mm and 5mm-diameter beams. Each mouse was given 3 consecutive trials per day. Beam-walk performance data was collected on day 3. Mean latency to traverse the entire length of the 11mm beam (Fig. 20*A*) and 5mm beam (Fig. 21*A*) on day 3 was plotted per group. Mean number of footslips on the 11mm beam (Fig. 20*B*) and 5mm beam (Fig. 21*B*) day 3 was also plotted. Data is shown for all 6 groups as mean ± SE. Three days after beamwalk performance was evaluated at baseline, all mice were trained for 4 consecutive days on the accelerating rotarod at 0.2rpm/sec. Each mouse was given 3 consecutive trials per day. Rotarod performance data was collected on days 2, 3 and 4. The mean latency to fall off the accelerating rotarod on day 4 was plotted per group (Fig. 22). Two days after the last trial on the rotarod, mice were put on the drug regimen of either 10mg/kg CyPPA or 30mg/kg NS13001 or placebo in 0.5% HPMC-Corn flour solution. Mice were fed orally 5 consecutive days (Monday to Friday) with 2 rest days (Saturday and Sunday) for 3 consecutive weeks.

After three weeks on the drug regimen, drug-feeding was halted for 3 days. After this brief washout period, mice were re-tested on the beamwalk and rotarod tasks with 3 consecutive trials each (black). Three weeks of chronic feeding of symptomatic SCA2 mice with NS13001 improved beamwalk performance (Fig. 20*A*-*B*; Fig. 21*A*-*B*). 58Q-

NS13001 mice showed significant improvement on the 11mm beam task with a decrease in the latency to traverse the beam-length (Fig. 20A; $p < 0.01$, black bars) and a decreased number of footslips (Fig. 20B; $p < 0.01$, black bars) while traversing the entire beam-length. This effect was also replicated on the 5mm beam. 58Q-NS13001 mice showed significant improvement on the 5mm beam task with a decrease in the latency to traverse the beam-length (Fig. 21*A*; $p < 0.01$, black bars) and a decreased number of footslips (Fig. 21*B*; $p < 0.01$, black bars) while traversing the entire beam-length. There was also a significant difference between the latency to fall off the accelerating rod before and after chronic drug-feeding of 58Q mice fed with NS13001 (Fig. 20*A*, $p < 0.05$, black bars). In all tasks, 58Q mice fed with NS13001 performed as well as WT mice.

Three weeks of chronic feeding of symptomatic SCA2 mice with CyPPA did not improve rotarod performance. There was no significant difference between the latency to fall off the accelerating rod before and after chronic drug-feeding of SCA2 mice fed with CyPPA (Fig. 22, black bars). However, these mice performed better on the beamwalk after 3 weeks of chronic feeding. This effect was not consistent, as 58Q –CyPPA mice had improved latency to complete the 11mm and 5mm task (Fig. 20*B*; Fig. 21*A*, black bars; $p < 0.05$), without having decreased number of footslips (Fig. 20*B*; Fig. 21*B*). There was also no significant difference in the post-drug treatment performance of 58Q mice compared to WT mice fed with CyPPA on the 5mm beam. All groups showed a trend to perform better on the beam-walk task except the SCA2 placebo group.

After testing on the rotarod and beamwalk tasks were completed, mice were returned to their home cages and left alone for 2 months to determine if the therapeutic

benefits of the compounds were reversible. Two months after the post-drug behavioral testing, mice were re-tested on the rotarod and beamwalk again. We found that this effect was reversible as these mice were impaired on the rotarod and beamwalk again after a 2 month wash-out period (Fig. 20*A*-*B*; Fig. 21*A*-*B*, grey bars). At this time-point, the mice were 13 months old and found it difficult to complete the tasks. Some fell off the beams or rod and suffered hind limb paralysis. Body weight was also assessed at all time-points to monitor any changes across the treatment groups that could account for changes in motor performance. Body weight data is shown for all 6 groups as mean ± SE (Fig. 23). There was no significant difference across all groups.

Chronic treatment of SCA2-58Q mice with SK compounds alleviates brain pathology

After the two-month wait period, all mice were sacrificed for the analysis of pathological changes as a result of chronic treatment with SK channel modulating drugs. A subset of the mice in each group were sacrificed, brains were collected and weighed to determine overall changes in whole cerebellar weight. There were no statistically significant effects of the drug treatment on SCA2 whole cerebellar weight. However, there was a trend for SK channel compounds to alleviate cerebellar atrophy (Fig. 24). The lack of statistical significance in cerebellum weight data is likely due to the small number of mice used in the analysis. Most of the mice were processed for transmission electron microscopy.

The rest of the mice in each of the 6 groups were sacrificed and their cerebella were processed for dark cell degeneration analysis. Dark cell degeneration (DCD) is a

form of PC death characterized by morphological changes in PCs identifiable by transmission electron microscopy. It is thought to reflect excitatory cell death as it can be induced by treating cerebellar slices with AMPA (Strahlendorf et al., 2003). DCD has been used to quantify PC degeneration in models of SCA2, SCA7 and SCA28 (Custer et al., 2006, Maltecca et al., 2009, Kasumu and Bezprozvanny, 2010)

In my analysis, I discovered that treatment of 58Q mice with NS13001 and CyPPA shifted the distribution in the DCD status of PCs. On average, in samples from NS13001-treated 58Q mice 43% of PCs were normal, 38% were moderately degenerated and 19% were severely degenerated (n = 218 PCs; Fig. 25*B*, Table 1). Similarly, in samples from CyPPA-treated 58Q mice 32% of PCs were normal, 35% were moderately degenerated and 33% were severely degenerated (n = 218 PCs; Fig. 25*B*, Table 1). In contrast, in samples from 58Q control mice, 12% of PCs were normal, 47% were moderately degenerated and 41% were severely degenerated (n = 185 PCs; Fig. 25*B*; Table 1). When compared to 58Q control mice, the increase in the fraction of "normal" cells in 58Q-13001 and 58Q-CyPPA mice was statistically significant ($p < 0.001$; Fig. 25*B*, Table 1). There was a trend for 58Q-13001 treated mice to have a reduced fraction of "severely" degenerated cells (Fig. 25*B*). However, this was not statistically significant. WT mice treated with SK compounds also had a trend to have more normal PCs.

Discussion

Target of SK channel modulators in purkinje cells

In this study, oral-delivery of NS13001 was effective in improving the beam-walk and rotarod performance of 10-month old symptomatic SCA2 mice while CYPPA only improved beam-walk performance (Fig. 19-21). This treatment also improved SCA2 pathology (Fig. 23). Thus, it seems that the higher potency of NS13001 (SK3 at 0.14 μM, SK2 at 1.6 μM and SK1 at 10 μM) over CyPPA (SK3 at 6 μM and SK2 at 14 μM) was very essential to alleviating the SCA2 motor and pathological phenotype.

In slices, the 5 μM dose of CyPPA was only able to revert transient bursting while the same dose of NS309 reverts persistent and transient bursting in SCA2 PCs (Fig. 18). Since, only SK2 channel expression has been reported in purkinje cells (Cingolani et al., 2002), I speculate that the likely target of CyPPA, NS309 and NS13001 is on SK2 channels and not SK1, SK3 or IK. Thus, the higher potency afforded for by NS309 (SK1, SK2 and SK3 at 1 μM) over CyPPA in slices was very essential to alleviating the SCA2 electrophysiological phenotype.

PCs receive excitatory inputs from granule cells and provide inhibitory output to DCN neurons. Since, high levels of SK3 has been reported in granule cells (Stocker and Pedarzani, 2000), with some expression in the DCN (Stocker and Pedarzani, 2000, Sailer et al., 2004, Shakkottai et al., 2004), a secondary effect of NS13001, CyPPA and NS309 could be via SK3 channels. NS13001 has a 10-fold higher affinity for SK3 channels than for SK2 channels. An effect of NS13001 in dopaminergic neurons (DN) of the substantia nigra cannot be ruled out, as SK3 channels are highly expressed in these neurons. *In*

vitro, blocking SK channels in DN primary culture with apamin caused neuronal loss that was not synergistic to death induced by AMPA stimulation. Thus, stimulating AMPAR in DNs decreases SK3 current density and activating SK3 channels in DNs with 1-EBIO or CyPPA protects against apamin and AMPA-induced excitotoxicity (Benitez et al., 2011). CyPPA also activates non-SK channels at higher doses (Hougaard et al., 2007). Thus, the effects of CyPPA in slices and animals could be attributed to non-SK targets.

Selective neuronal vulnerability in purkinje cells

The proteins mutated in SCAs are ubiquitously expressed in different neuronal and non-neuronal cell types but pathology is mainly localized to PCs. Why are PCs mostly affected in these disorders? Does the unique physiology of affected PCs make them preferentially vulnerable to dysfunction? PCs are pacemakers like dopaminergic neurons (DN) in the substantia nigra. DNs also exhibit firing patterns similar to PCs, albeit with a slower frequency (2-4Hz). DNs also fire in 3 distinct patterns: single spikes with regular frequency, single spikes with irregular frequency or burst firing (Grace and Bunney, 1984a, b, Freeman et al., 1985). Thus, the studies of vulnerability in these unique DNs could be extended to PCs.

Studies have reported the involvement of SK channels in the switch from single-spike to burst firing pattern in DNs (Waroux et al., 2005, Ji and Shepard, 2006). It is suggested that burst firing prevents proper release of neurotransmitters to downstream targets, leading to overall dysfunction (Riegel and Lupica, 2004, Pedarzani and Stocker, 2008). Accordingly, the bursting of subthalamic neurons has been associated with the phenotype in Parkinson's disease patients (Levy et al., 2000). It has also been suggested

that pacemaking makes neurons vulnerable to stress as each action potential fired requires opening of voltage-gated calcium channels (VGCCs) (Surmeier, 2007, Chan et al., 2009, 2010, Surmeier et al., 2010). Thus, the more spikes fired the more these channels have to be opened and the more stressed these neurons become. Normalizing PC firing in irregularly and stressed PCs could function in decreasing stress; thus, slowing down the pathology in SCA2 PCs.

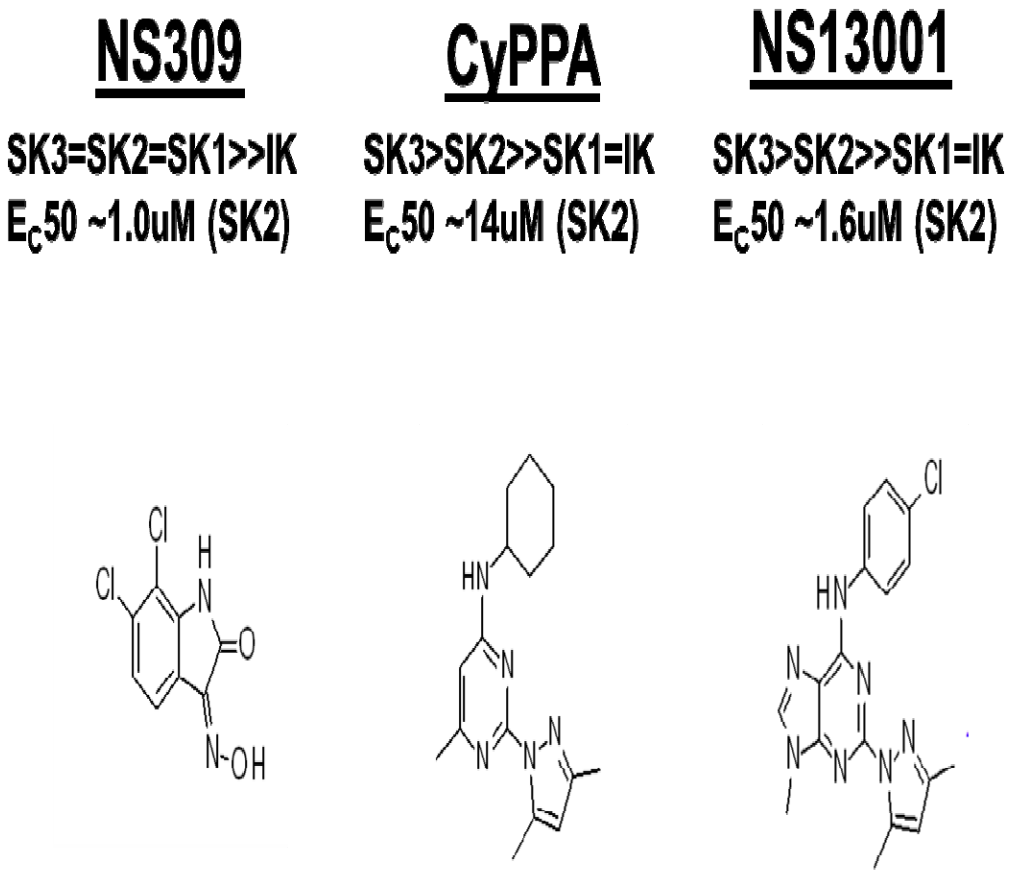

Figure 18. Structure of SK channel modulators. The molecular structures of all 3 compounds are shown. The selectivity of each SK compound for all 4 SK channel subtypes is shown. The potency of each subtype for the SK2 channel subtype is also shown. As seen, NS309 has no selectivity but high potency for SK2. CyPPA has high selectivity but low potency while the novel NS13001 has very high selectivity and high potency.

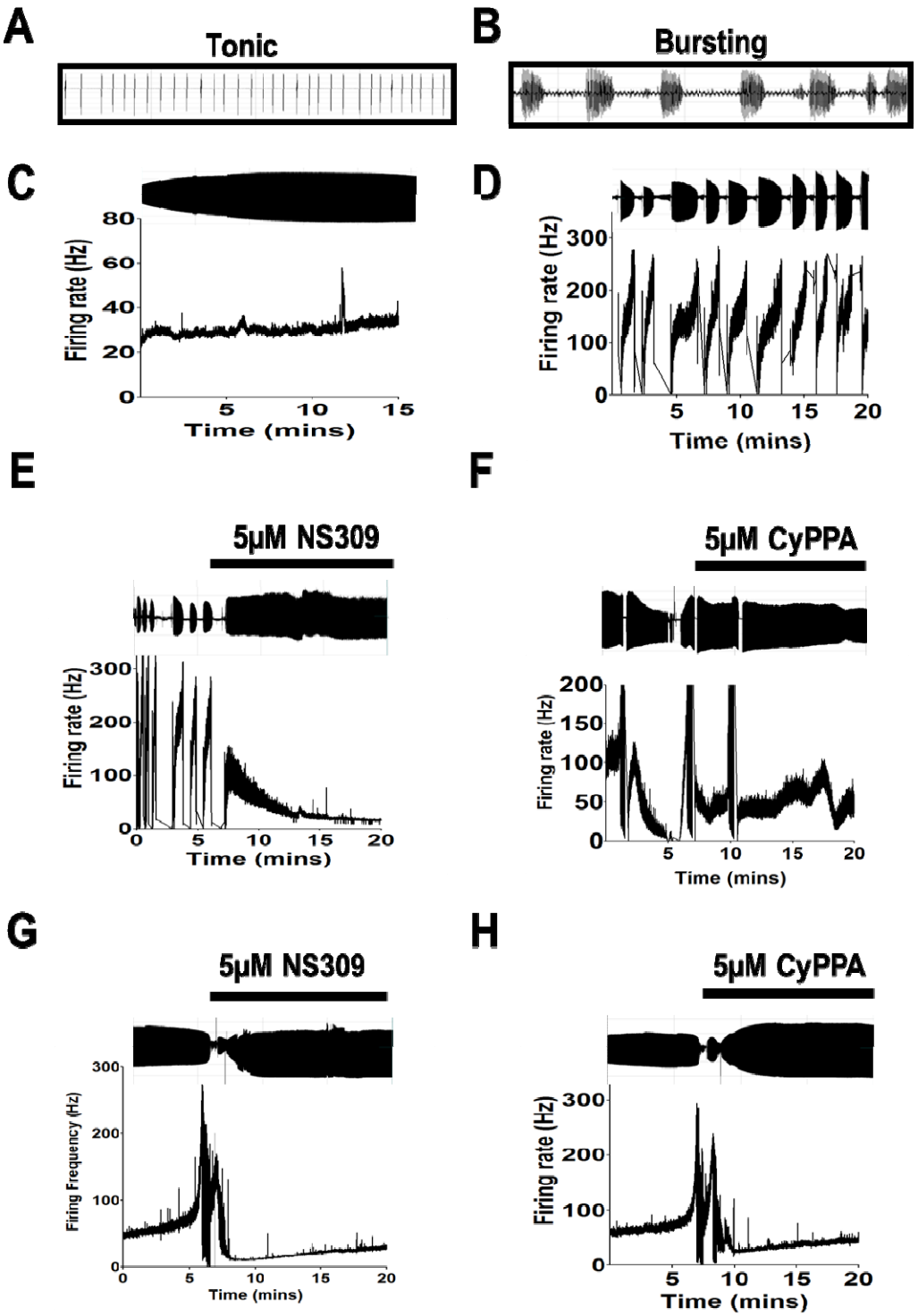
A
Tonic
B
Bursting
C
Firing rate (Hz)
80
60
40
20
0
5
10
15
Time (mins)
D
Firing rate (Hz)
300
200
100
0
5
10
15
20
Time (mins)
E
5μM NS309
Firing rate (Hz)
300
200
100
0
0
5
10
15
20
Time (mins)
F
5μM CyPPA
Firing rate (Hz)
200
150
100
50
0
5
10
15
20
Time (mins)
G
5μM NS309
Firing Frequency (Hz)
300
200
100
0
0
5
10
15
20
Time (mins)
H
5μM CyPPA
Firing rate (Hz)
300
200
100
0
5
10
15
20
Time (mins)

Figure 19. The spontaneous action potential firing of Purkinje neurons is sensitive to SK channel modulators. (A) sample 1-second trace of a Tonically firing PC. (B) sample 1-second trace of a bursting PC. This particular cell exhibited a trimodal firing patter with individual segments of tonic, bursting and silence. (C) sample 15-minute plot of a Tonically firing SCA2-58Q PC. (D) sample 20-minute plot of a bursting SCA2-58Q PC. (E) A SCA2-58Q PC persistently fired in a bursting pattern for 7 minutes and reverted to tonic firing after treatment with 5μM NS309. (F) A SCA2-58Q PC reverted to tonic firing after treatment with 5μM CyPPA**.** (G) A SCA2-58Q PC transiently fired in a bursting pattern and was reverted to tonic firing after treatment with 5μM NS309. (H) A SCA2-58Q PC transiently fired in a bursting pattern and was reverted to tonic firing after treatment with 5μM CyPPA**.**

	No. of 15-35 min recordings of PCs	No. of bursting PCs reverted to Tonic
Tonic-No drug	6	N/A
Tonic-CyPPA	1	N/A
Tonic-NS309	1	N/A
Burst-No drug	7	N/A
Burst-CyPPA	5	3
Burst-NS309	8	8

Table 3. Summary of the effect of SK channel modulators on PC firing activity in slices. Spontaneous PC activity was recorded for 15-30 minutes in the presence of picrotoxin and DNQX. When bursting activity was detected in the recording during the first 5 minutes, the allotted SK channel drug (CyPPA or NS309) was added to determine the effect of the compounds in reverting the burst firing to tonic firing.

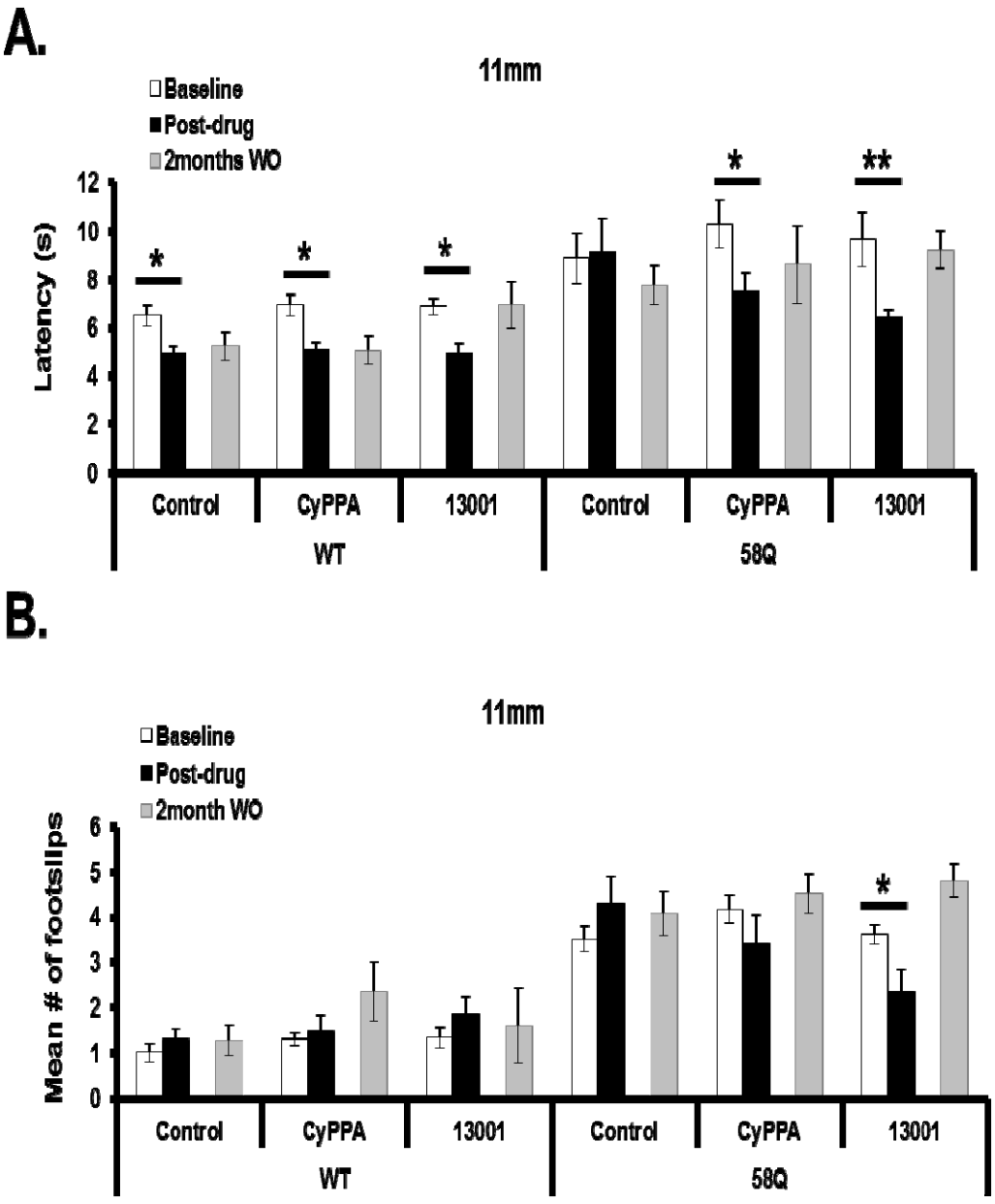

Figure 20. Chronic treatment of SCA2 mice with SK Channel modulators improves motor coordination on the beamwalk task. **(A-B) At baseline, after drug treatment and after a two-month washout (WO) period, mice from all 6 groups were trained on the**

17mm, 11mm and 5mm beams. Average time to traverse the entire length of each beam is recorded. Mean latency to traverse 11mm beams before (white bars) and after (black bars) 3 weeks of chronic drug treatment is plotted for each group of mice as mean ± SE. The WT control mice (WT), WT mice fed with CyPPA (WT-CyPPA), WT mice fed with 13001 (WT-13001), 58Q control mice (58Q), the 58Q mice fed with CyPPA (58Q-CyPPA), and the 58Q mice fed with 13001 (58Q-13001) (A). Average number of footslips as the mice traverse the entire length of the 11mm beam was also recorded. Mean number of footslips as the mice traverse the 11mm beams before (white bars) and after (black bars) 3 weeks of chronic drug treatment is also plotted for each group of mice (B). Mice were trained on the accelerating rotarod. Mean latency to fall off rotarod before (white bars) and after (black bars) 3 weeks of chronic drug treatment is plotted for each group of mice as mean ± SE.

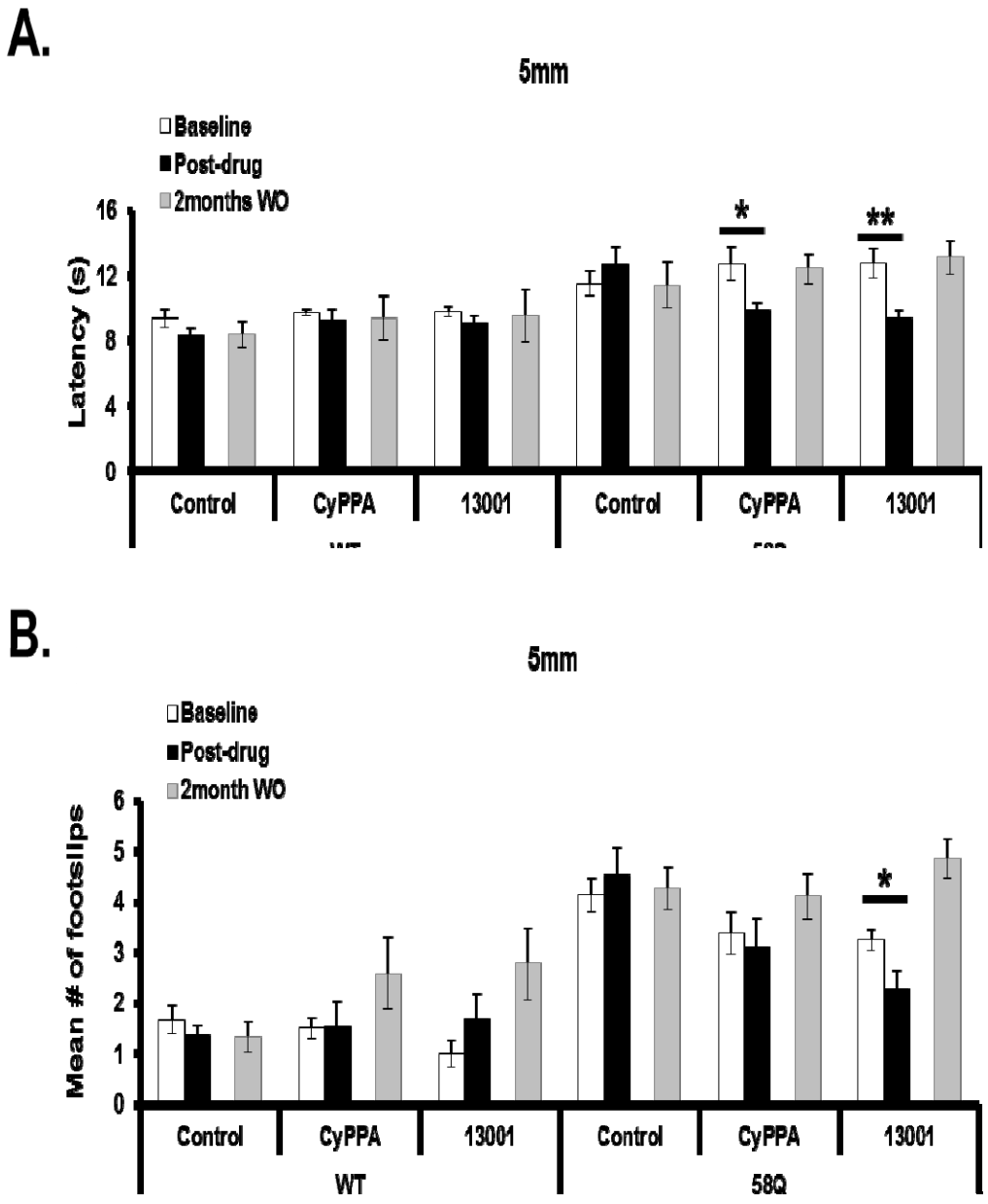

Figure 21. Chronic treatment of SCA2 mice with SK Channel modulators improves motor coordination on the 5mm beamwalk task. (A-B) At baseline, after drug treatment and after a two-month washout (WO) period, mice from all 6 groups were

trained on the 17mm, 11mm and 5mm beams. Average time to traverse the entire length of each beam is recorded. Mean latency to traverse 5mm beam before (white bars) and after (black bars) 3 weeks of chronic drug treatment is plotted for each group of mice as mean ± SE. The WT control mice (WT), WT mice fed with CyPPA (WT-CyPPA), WT mice fed with 13001 (WT-13001), 58Q control mice (58Q), the 58Q mice fed with CyPPA (58Q-CyPPA), and the 58Q mice fed with 13001 (58Q-13001) (A). Average number of footslips as the mice traverse the entire length of the 5mm beam was also recorded. Mean number of footslips as the mice traverse the 5mm beams before (white bars) and after (black bars) 3 weeks of chronic drug treatment is also plotted for each group of mice (B).

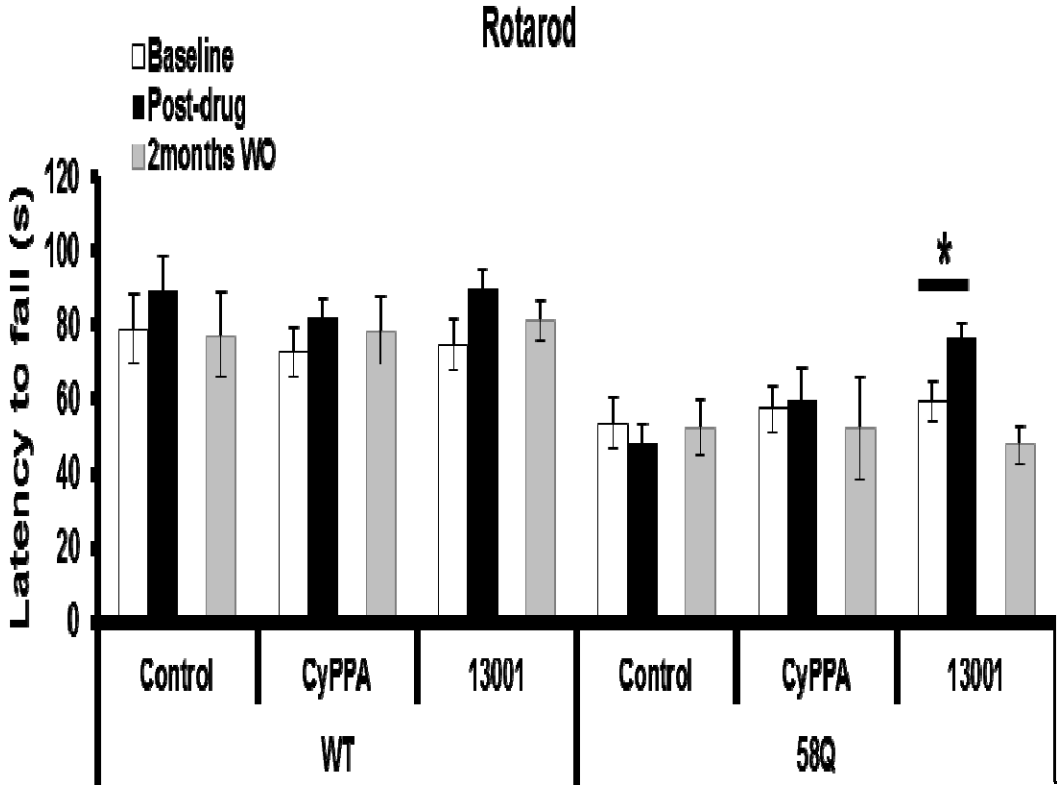

Figure 22. Chronic treatment of SCA2 mice with SK Channel modulators improves rotarod performance.. *A,* At baseline and after drug treatment, mice are trained on the accelerating rotarod. Mean latency to fall off rotarod before (black) and after (red) 3weeks of chronic drug treatment is plotted for each group of mice the WT control mice (WT), WT mice fed with CyPPA (WT-CyPPA), WT mice fed with 13001 (WT-13001), 58Q control mice (58Q), the 58Q mice fed with CyPPA (58Q-CyPPA), and the 58Q mice fed with 13001 (58Q-13001) as mean ± SE.

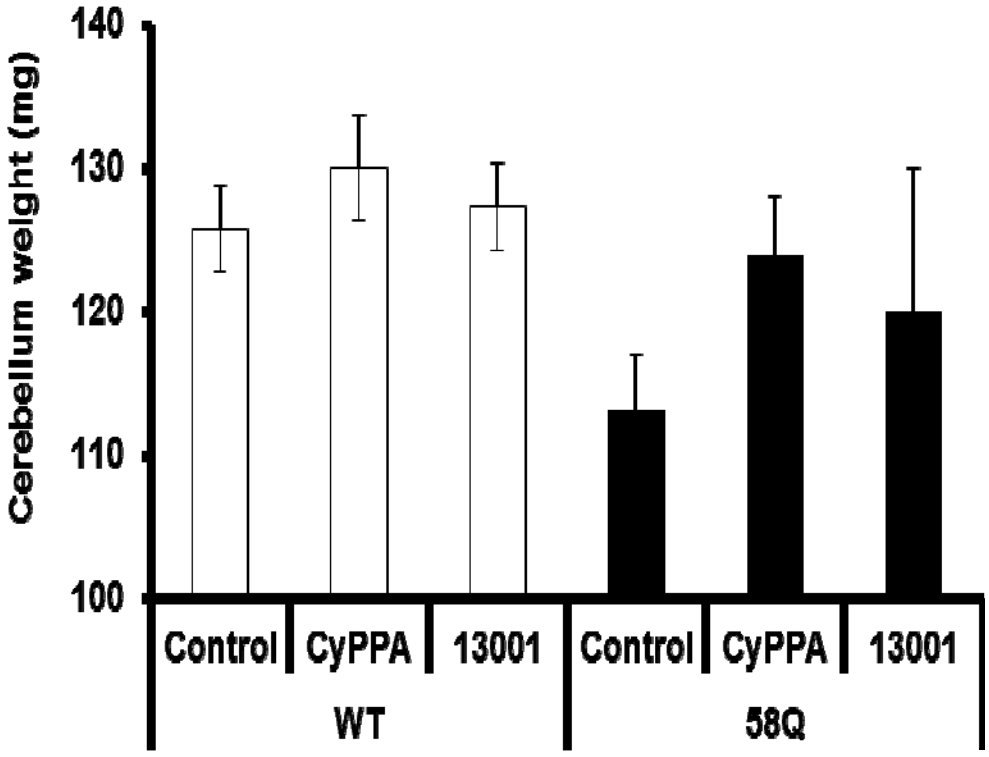

Figure 23. Chronic treatment of mice with SK modulators improves SCA2 pathology. *A.* At the end of the acute study, all mice were sacrificed for pathological analysis. Some of the mice in each group were perfused for determining brain atrophy. The rest of the mice were perfused for DCD analysis. Whole cerebella weight were measured.. There was a trend for SK compounds to reverse the cerebellar atrophy of SCA2-58Q mice. However, this was not significant. SK compounds had no adverse effect on cerebellar weight of WT mice (B).

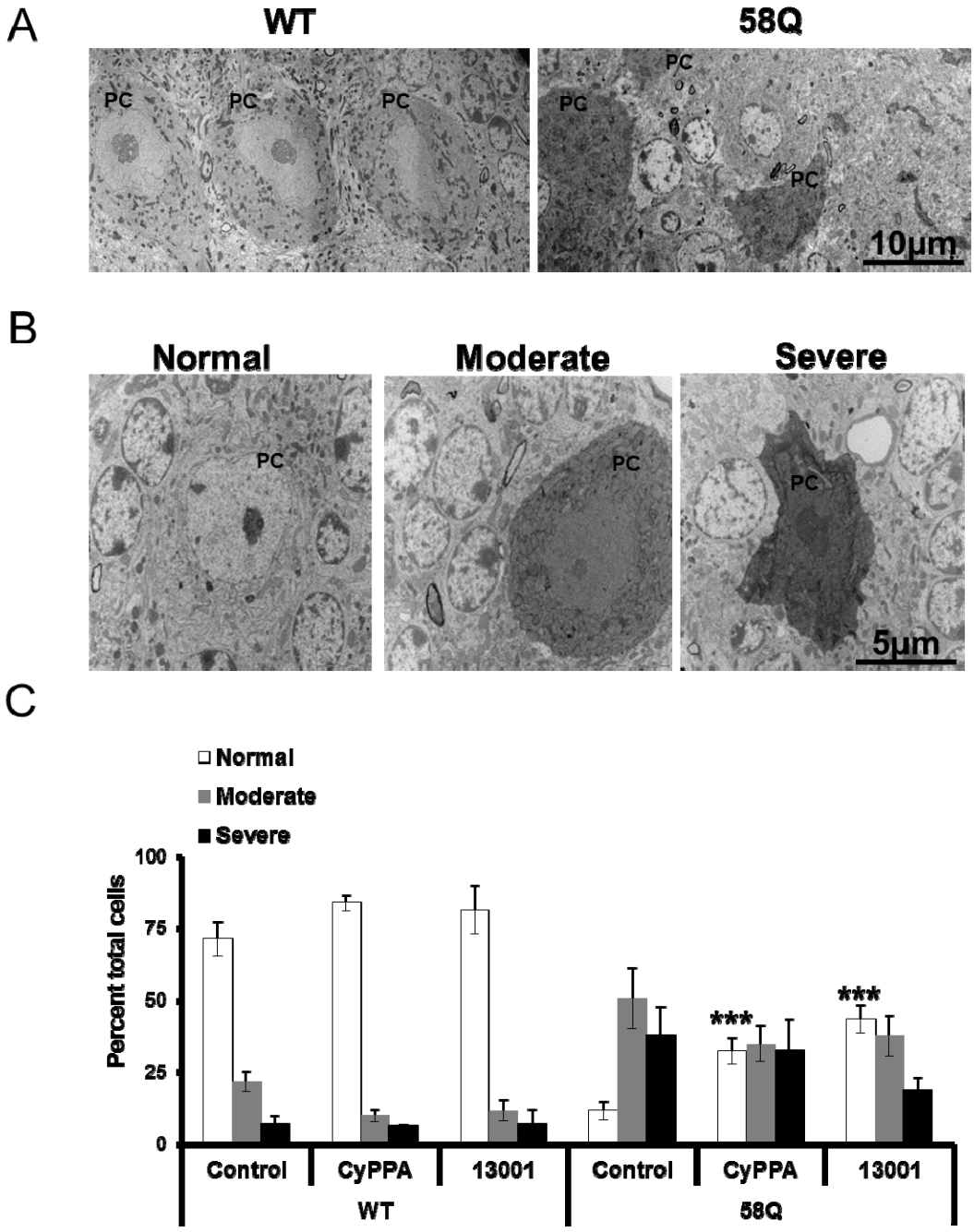

Figure 24. Chronic treatment of mice with SK modulators improves Dark Cell Degenration status of SCA2 PCs *A,* Cerebellar sections were processed for

Transmission Electron Microscopy for the analysis of Dark cell degeneration (DCD). After processing, the percentages of normal, moderately and severely degenerated PCs were calculated. (D) Average percentage of normal, moderate and severely degenerated PCs in each group is plotted as mean ± SE. The treatment of 58Q mice had a trend to rescue PCs from DCD. (n = 222-296 PCs counted). ***$p < 0.05$; ***$p < 0.01$; ***$p < 0.001$

Table 3

	No. of animals	Cerebellum (mg)	DCD measurements			
			No. of PCs counted	Normal (%)	Moderate (%)	Severe (%)
WT	10 (7)	126 ± 3	258	71.4 ± 6	21.6 ± 3	7 ± 3
WT-CyPPA	13 (9)	130 ± 4	245	83.9 ± 3	9.85 ± 2	6.23
WT-13001	10 (7)	127 ± 3	255	81.5 ± 8	11.7 ± 4	6.83 ± 5
58Q	15 (11)	113 ± 4	296	11.6 ± 3	50.7 ± 11	37.7 ± 10
58Q-CyPPA	14 (10)	124 ± 4	222	32.4 ± 5***	34.9 ± 6	32.7 ± 11
58Q-13001	20 (16)	120 ± 10	288	43.4 ± 5***	37.6 ± 7	18.9 ± 4

Table 4. Summary of in vivo study of the effect of SK channel modulators on SCA2 progression. The number of mice at the end of the study is in parentheses. Two-tailed Student's unpaired *t* test was used to judge differences between drug-treated groups and the placebo groups. P values, ***$p < 0.001$

CHAPTER FOUR

Conclusions and Future experiments.

Conclusions

Altered calcium homeostasis underlies SCA2

The PC degeneration common to the polyQ SCAs is believed to result from a toxic gain-of-function associated with the polyQ expanded protein but the pathogenic mechanisms are not well understood. Based on work in mouse models of Huntington's disease and SCA2 and SCA3, our lab has suggested that aberrant Ca^{2+} signaling secondary to binding of polyQ expanded protein to the type 1 inositol 1,4,5-trisphosphate receptor ($InsP_3R1$) at intracellular Ca^{2+} stores may be a common pathogenic mechanism in polyQ disorders (Tang et al., 2003, Chen et al., 2008, Liu et al., 2009). Normalizing intracellular Ca^{2+} in mouse models of these polyQ disorders alleviated the expected ataxia and pathology associated with the expression of the polyQ-expanded proteins (Tang et al., 2003, Chen et al., 2008, Liu et al., 2009).

Here, I characterized the neuronal dysfunctional in SCA2. Spontaneously firing PCs exemplify 4 modes of firing- a never-ending tonic spiking pattern with relatively constant frequency, brief segments of tonic spikes separated into bursts by brief random pauses, a trimodal pattern with initial tonic spikes followed by volley of bursts and a brief pause; or a bimodal state with brief bursts and pauses (Abrams et al., 2010). It is not understood why a PC fires in a certain pattern but I speculate that certain patterns may be related to ataxia. If the firing rate and precision of PCs encode any kind of information then a lack of precision demonstrates disrupted information encoding and processing in cerebellar function. I found that more PCs in SCA2 mice fire less frequently, less regularly and even burst in a significant number of cases. Thus, an irregularity in PC

firing activity is related to or causes the ataxic phenotype. The reversion of bursting to tonic firing alleviated ataxia in already symptomatic SCA2 mice while preventing the development of supranormal intracellular calcium levels prevents the onset of SCA2.

I also provided evidence for the suggestion that PC dysfunction rather than death leads to ataxia (Kasumu and Bezprozvanny, 2010). A lack of cell death in the presence of motor deficits was also reported in a mouse model for SCA14, where PCs exhibited electrophysiological deficits without any obvious morphological changes or degeneration (Shuvaev et al., 2011). Also, the delivery of auto-antibodies against mGluR1 receptors to wildtype mice causes immediate cerebellar ataxia in the absence of any cell death (Coesmans et al., 2003). In the SCA2-58Q mouse model, obvious PC degeneration is not reported until 10- to 12-months of age (Liu et al., 2009, Kasumu and Bezprozvanny, 2010). Here, I showed that PC dysfunction starts as early as 6 months of age, around the same time that motor deficits begin.

Calcium influx through voltage-gated Ca^{2+} channels (VGCC) is responsible for pacemaking (Yanovsky et al., 2005), by coupling to SK channels. Calcium-induced Ca^{2+} release (CICR) through ryanodine receptors has been shown to also activate SK channels (Seutin et al., 2000, Yanovsky et al., 2005). However, there have been no reports of IP3-induced calcium release (IICR) coupling to SK channel activation. Thus, IICR should not modulate pacemaking in a healthy cell because IICR is transient and normally well-controlled. However, in SCA2 where there is supranormal IICR (Liu et al., 2009), the IICR Ca^{2+} pool most likely disturbs the VGCC Ca^{2+} pool, disrupts pacemaking and causes irregular PC firing activity. This would be the basis of the neuroprotective abilities of chronic 5PP overexpression in SCA2 mice. 5PP prevents the onset of global Ca^{2+}

dysregulation due to Atx2-58Q interaction with InsP3Rs. It would also be interesting to determine if there are any changes in the expression of VGCCs and SK channels in 5- to 6-month old SCA2 mice. It would be logical that chronic overexpression of 5PP prevents these putative changes.

Future directions:

1. Are the beneficial effects of NS13001 attributable to off-target effects?

In order to move forward with testing the efficacy of NS13001 in patients, it would be important to validate that the beneficial effects of NS13001 in symptomatic SCA2 is not due to off-target effects of this compound. Such off-targets would be the binding of channels other than SK channels. Such a compound should have a similar structure to NS13001 but lack biologically activity. The analog should be used in a drug-trial side-by-side with NS13001 in 10-month old SCA2 mice. It is more than likely that there will be no off target effects based on the very high potency and selectivity achieved with the creation of this new compound.

2. What channels are involved in the electrophysiological phenotype?

In Chapter 3, I showed that modulation of SK channels provides therapeutic benefit for SCA2-58Q mice. It is not known however if the SCA2 phenotype involves a dysregulation of SK channel activity. It would be beneficial to do a quantitative analysis of SCA2-58Q mice and age-matched WT mice to determine if there are any changes in the mRNA or protein expression of SK1, SK2 and SK3 channels. Electrophysiological analyses can also determine if SK current is actually reduced. Taken, together the results could explain the mechanism of the benefits attributed to SK modulators; whether these compounds compensate for a decrease in overall SK activity by increasing the sensitivity of SK channels.

3. Is Long term depression disrupted in SCA2-58Q mice?

As discussed in Chapter 1, $InsP_3R$ activation is necessary for the induction of LTD.LTD requires a coincident and simultaneous influx of Ca2+ via VGCC induced by climbing fiber inputs and the activation of mGLUR-IP3 signaling via parallel fibers inputs. My hypothesis posits that there is excessive IP3 signaling in SCA2 mice and so it is expected that LTD is also affected in SCA2. This can be tested in acute slices at different ages as in Chapter 2, using parallel fiber stimulation paired with PC depolarization to 0 mV. If LTD is in fact altered, it would also be interesting to test if the chronic expression of 5PP restores normal LTD induction.

4. Is calcium buffering important in the onset and progression of SCA2?

It has been reported that the deletion of calcium buffers in Spinocerebellar ataxia 1 (SCA1) mice accelerates the ataxic and neurodegenerative phenotype (Vig et al., 2011). I hypothesized that the excessive Ca^{2+} release from IP3-sensitive Ca^{2+} stores plays an important role in SCA2 pathogenesis. I believe that the resulting supranormal Ca^{2+} signals lead to mitochondrial Ca^{2+} overload, activation of calpain and caspases, and eventual dark cell degeneration of PCs. If this idea is correct, then I expect that endogenous cytosolic Ca^{2+} buffers play a significant protective role in SCA2.

By chelating cytosolic Ca^{2+}, the endogenous buffers reduce the amount of Ca^{2+} that enters mitochondria and prevent activation of calpains and caspases. To test these assumptions, it would be interesting to evaluate the importance of endogenous cytosolic Ca^{2+} buffers in the context of SCA2. There are 3 major cytosolic Ca^{2+}-binding proteins (CaBPs) – calbindin d-28k (CB, fast Ca^{2+} buffer), calretinin (CR), and parvalbumin (PV, slow Ca^{2+} buffer). These proteins differ in their Ca^{2+} binding properties and expression

pattern. Cerebellar purkinje cells contain extremely high amounts of dendritic CB (200 – 300 μm) and somatic PV (50 – 100 μm). In contrast, CR is expressed predominantly in cerebellar granule cells and not in purkinje cells. Thus, CB and PV are the most relevant CaBPs for understanding the role of endogenous Ca^{2+} buffering in the context of SCA2. I took a genetic approach in order to address the role of CB and PV in SCA2. Both CB and PV knockout mice have been generated and extensively characterized. These mice were obtained from Dr. Beat Schwaller (University of Fribourg, Switzerland).

To understand the importance of endogenous PC Ca^{2+} buffering in SCA2 pathogenesis, I have crossed SCA2-58Q mice with $CB^{-/-}$ mice and $PV^{-/-}$ mice. The double mutant mice (SCA2-58Q:$CB^{-/-}$ and SCA2-58Q:$PV^{-/-}$) were generated on B6 background. These mice should be characterized by following procedures described in the methods section (Chapter 2). Preliminary electrophysiology data (Figure 24) suggests that PCs in single knockout calbindin mice at 12 weeks old may have less spontaneous activity compared to WT mice (not statistically significant). It is possible that the phenotype of generated double mutant lines will not be very different from the phenotype of SCA2-58Q line. In this scenario, a triple mutant SCA2 mouse line that lacks both CB and PV proteins (SCA2-58Q:$CB^{-/-}$:$PV^{-/-}$) should be generated. The double knockout $CB^{-/-}$:$PV^{-/-}$ mouse line is viable but displays a more severe ataxic phenotype and alterations in PC morphology than a single CB knockout. Therefore, the phenotype of SCA2-58Q:$CB^{-/-}$:$PV^{-/-}$ mice is also expected to be more severe. The generated triple mutant mice should be characterized as described (Chapter 2). The results obtained in these studies will provide unique information about an importance of endogenous Ca^{2+} buffers for PC neuroprotection in SCA2. These data should also provide an understanding of the relative

importance of "fast Ca^{2+} buffering" and "slow Ca^{2+} buffering" for a neurodegenerative disease process. As an additional benefit, it is highly likely that the behavioral phenotype will develop faster in at least one of these double mutant lines or in triple mutant line. The generated mutant line will represent an "accelerated" model of SCA2 pathology which would have a significant value for preclinical studies and testing of therapeutic agents for SCA2 treatment.

5. Are therapeutic targets in SCA2 beneficial in the treatment of Amyotrophic lateral sclerosis and Progressive supranuclear palsy?

There is a strong association between ATXN2 repeat-length and Amyotrophic lateral sclerosis (ALS), as well as a moderate association with progressive supranuclear palsy (PSP) (Ross et al., 2011). ALS patients have longer repeats in the ATXN2 gene than controls, and so expanded ATXN2 repeats are a genetic risk factor for (Ross et al., 2011). Thus, maybe some SCA2 therapy could be advantageous for these patients as well to relieve shared symptoms between these 3 disorders, especially PSP patients who have impaired gait and balance and ALS patients that present with difficulty speaking and swallowing.

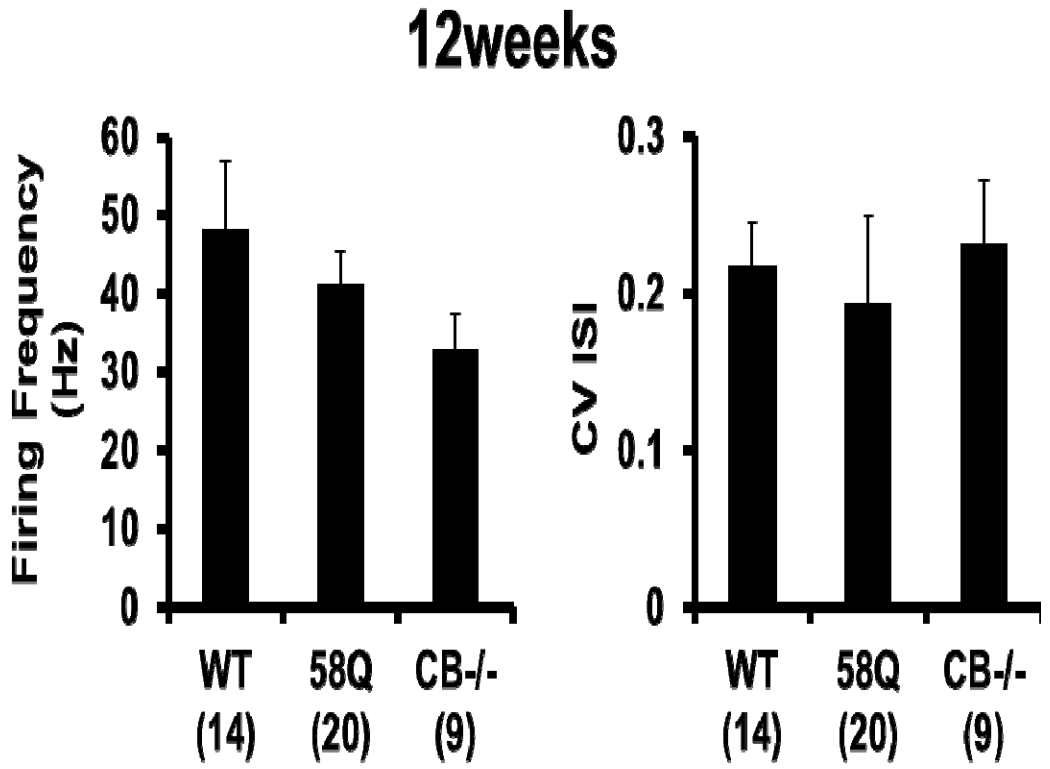

Figure 25. Electrophysiological comparison of wildtype, SCA2 and calbindin knockout mice at 12 weeks. *A,* Average firing frequency of each PC in the 5 minute duration was analyzed. Mean firing frequency in each group at each time-point was calculated and plotted as mean ± SE. There is a trend for the firing frequency of tonically firing PCs in 12-week old $CB^{-/-}$ to be lower than in age-matched WT and 58Q PCs. *B,* Firing variability was represented as the correlation of variation of interspike interval (CV ISI) and calculated for each PC in the 5 minute recording duration. Mean CV ISI in each group at each time-point was calculated and plotted as mean ± SE. The number of PCs recorded from in each group is in parentheses.

BIBLIOGRAPHY

Abrams ZR, Warrier A, Trauner D, Zhang X (2010) A Signal Processing Analysis of Purkinje Cells in vitro. Front Neural Circuits 4:13.

Adachi N, Kobayashi T, Takahashi H, Kawasaki T, Shirai Y, Ueyama T, Matsuda T, Seki T, Sakai N, Saito N (2008) Enzymological analysis of mutant protein kinase Cgamma causing spinocerebellar ataxia type 14 and dysfunction in Ca2+ homeostasis. J Biol Chem 283:19854-19863.

Airaksinen MS, Eilers J, Garaschuk O, Thoenen H, Konnerth A, Meyer M (1997) Ataxia and altered dendritic calcium signaling in mice carrying a targeted null mutation of the calbindin D28k gene. Proc Natl Acad Sci U S A 94:1488-1493.

Alvina K, Khodakhah K (2010a) KCa channels as therapeutic targets in episodic ataxia type-2. J Neurosci 30:7249-7257.

Alvina K, Khodakhah K (2010b) The therapeutic mode of action of 4-aminopyridine in cerebellar ataxia. J Neurosci 30:7258-7268.

Barenberg P, Strahlendorf H, Strahlendorf J (2001) Hypoxia induces an excitotoxic-type of dark cell degeneration in cerebellar Purkinje neurons. Neurosci Res 40:245-254.

Benitez BA, Belalcazar HM, Anastasia A, Mamah DT, Zorumski CF, Masco DH, Herrera DG, de Erausquin GA (2011) Functional reduction of SK3-mediated currents precedes AMPA-receptor-mediated excitotoxicity in dopaminergic neurons. Neuropharmacology 60:1176-1186.

Bezprozvanny I (2009) Calcium signaling and neurodegenerative diseases. Trends Mol Med 15:89-100.

Bezprozvanny I, Klockgether T (2010) Therapeutic prospects for spinocerebellar ataxia type 2 and 3 Drugs of the Future 34:991-999.

Bond CT, Herson PS, Strassmaier T, Hammond R, Stackman R, Maylie J, Adelman JP (2004) Small conductance Ca2+-activated K+ channel knock-out mice reveal the identity of calcium-dependent afterhyperpolarization currents. J Neurosci 24:5301-5306.

Bond CT, Sprengel R, Bissonnette JM, Kaufmann WA, Pribnow D, Neelands T, Storck T, Baetscher M, Jerecic J, Maylie J, Knaus HG, Seeburg PH, Adelman JP (2000) Respiration and parturition affected by conditional overexpression of the Ca2+-activated K+ channel subunit, SK3. Science 289:1942-1946.

Brasnjo G, Otis TS (2001) Neuronal glutamate transporters control activation of postsynaptic metabotropic glutamate receptors and influence cerebellar long-term depression. Neuron 31:607-616.

Callizot N, Guenet JL, Baillet C, Warter JM, Poindron P (2001) The frissonnant mutant mouse, a model of dopamino-sensitive, inherited motor syndrome. Neurobiol Dis 8:447-458.

Campisi A, Caccamo D, Li Volti G, Curro M, Parisi G, Avola R, Vanella A, Ientile R (2004) Glutamate-evoked redox state alterations are involved in tissue transglutaminase upregulation in primary astrocyte cultures. FEBS Lett 578:80-84.

Carlson KM, Andresen JM, Orr HT (2009) Emerging pathogenic pathways in the spinocerebellar ataxias. Curr Opin Genet Dev 19:247-253.

Chan CS, Gertler TS, Surmeier DJ (2009) Calcium homeostasis, selective vulnerability and Parkinson's disease. Trends Neurosci 32:249-256.

Chan CS, Gertler TS, Surmeier DJ (2010) A molecular basis for the increased vulnerability of substantia nigra dopamine neurons in aging and Parkinson's disease. Mov Disord 25 Suppl 1:S63-70.

Chan SL, Mattson MP (1999) Caspase and calpain substrates: roles in synaptic plasticity and cell death. J Neurosci Res 58:167-190.

Chen X, Kovalchuk Y, Adelsberger H, Henning HA, Sausbier M, Wietzorrek G, Ruth P, Yarom Y, Konnerth A (2010) Disruption of the olivo-cerebellar circuit by Purkinje neuron-specific ablation of BK channels. Proc Natl Acad Sci U S A 107:12323-12328.

Chen X, Tang TS, Tu H, Nelson O, Pook M, Hammer R, Nukina N, Bezprozvanny I (2008) Deranged calcium signaling and neurodegeneration in spinocerebellar ataxia type 3. J Neurosci 28:12713-12724.

Cingolani LA, Gymnopoulos M, Boccaccio A, Stocker M, Pedarzani P (2002) Developmental regulation of small-conductance Ca2+-activated K+ channel expression and function in rat Purkinje neurons. J Neurosci 22:4456-4467.

Coesmans M, Smitt PA, Linden DJ, Shigemoto R, Hirano T, Yamakawa Y, van Alphen AM, Luo C, van der Geest JN, Kros JM, Gaillard CA, Frens MA, de Zeeuw CI (2003) Mechanisms underlying cerebellar motor deficits due to mGluR1-autoantibodies. Ann Neurol 53:325-336.

Coesmans M, Weber JT, De Zeeuw CI, Hansel C (2004) Bidirectional parallel fiber plasticity in the cerebellum under climbing fiber control. Neuron 44:691-700.

Communi D, Motte S, Boeynaems JM, Pirotton S (1996) Pharmacological characterization of the human P2Y4 receptor. Eur J Pharmacol 317:383-389.

Custer SK, Garden GA, Gill N, Rueb U, Libby RT, Schultz C, Guyenet SJ, Deller T, Westrum LE, Sopher BL, La Spada AR (2006) Bergmann glia expression of polyglutamine-expanded ataxin-7 produces neurodegeneration by impairing glutamate transport. Nat Neurosci 9:1302-1311.

Dodge JC, Clarke J, Song A, Bu J, Yang W, Taksir TV, Griffiths D, Zhao MA, Schuchman EH, Cheng SH, O'Riordan CR, Shihabuddin LS, Passini MA, Stewart GR (2005) Gene transfer of human acid sphingomyelinase corrects neuropathology and motor deficits in a mouse model of Niemann-Pick type A disease. Proc Natl Acad Sci U S A 102:17822-17827.

Farre-Castany MA, Schwaller B, Gregory P, Barski J, Mariethoz C, Eriksson JL, Tetko IV, Wolfer D, Celio MR, Schmutz I, Albrecht U, Villa AE (2007) Differences in locomotor behavior revealed in mice deficient for the calcium-binding proteins parvalbumin, calbindin D-28k or both. Behav Brain Res 178:250-261.

Filla A, De Michele G, Santoro L, Calabrese O, Castaldo I, Giuffrida S, Restivo D, Serlenga L, Condorelli DF, Bonuccelli U, Scala R, Coppola G, Caruso G, Cocozza S (1999) Spinocerebellar ataxia type 2 in southern Italy: a clinical and molecular study of 30 families. J Neurol 246:467-471.

Finch EA, Augustine GJ (1998) Local calcium signalling by inositol-1,4,5-trisphosphate in Purkinje cell dendrites. Nature 396:753-756.

Freeman AS, Meltzer LT, Bunney BS (1985) Firing properties of substantia nigra dopaminergic neurons in freely moving rats. Life Sci 36:1983-1994.

Furuichi T, Simon-Chazottes D, Fujino I, Yamada N, Hasegawa M, Miyawaki A, Yoshikawa S, Guenet JL, Mikoshiba K (1993) Widespread expression of inositol 1,4,5-trisphosphate receptor type 1 gene (Insp3r1) in the mouse central nervous system. Receptors Channels 1:11-24.

Grace AA, Bunney BS (1984a) The control of firing pattern in nigral dopamine neurons: burst firing. J Neurosci 4:2877-2890.

Grace AA, Bunney BS (1984b) The control of firing pattern in nigral dopamine neurons: single spike firing. J Neurosci 4:2866-2876.

Greer PL, Greenberg ME (2008) From synapse to nucleus: calcium-dependent gene transcription in the control of synapse development and function. Neuron 59:846-860.

Hara K, Shiga A, Nozaki H, Mitsui J, Takahashi Y, Ishiguro H, Yomono H, Kurisaki H, Goto J, Ikeuchi T, Tsuji S, Nishizawa M, Onodera O (2008) Total deletion and a missense mutation of ITPR1 in Japanese SCA15 families. Neurology 71:547-551.

Hausser M, Clark BA (1997) Tonic synaptic inhibition modulates neuronal output pattern and spatiotemporal synaptic integration. Neuron 19:665-678.

Hof PR, Glezer, II, Conde F, Flagg RA, Rubin MB, Nimchinsky EA, Vogt Weisenhorn DM (1999) Cellular distribution of the calcium-binding proteins parvalbumin, calbindin, and calretinin in the neocortex of mammals: phylogenetic and developmental patterns. J Chem Neuroanat 16:77-116.

Hougaard C, Eriksen BL, Jorgensen S, Johansen TH, Dyhring T, Madsen LS, Strobaek D, Christophersen P (2007) Selective positive modulation of the SK3 and SK2 subtypes of small conductance Ca2+-activated K+ channels. Br J Pharmacol 151:655-665.

Huynh DP, Figueroa K, Hoang N, Pulst SM (2000) Nuclear localization or inclusion body formation of ataxin-2 are not necessary for SCA2 pathogenesis in mouse or human. Nat Genet 26:44-50.

Imbert G, Saudou F, Yvert G, Devys D, Trottier Y, Garnier JM, Weber C, Mandel JL, Cancel G, Abbas N, Durr A, Didierjean O, Stevanin G, Agid Y, Brice A (1996) Cloning of the gene for spinocerebellar ataxia 2 reveals a locus with high sensitivity to expanded CAG/glutamine repeats. Nat Genet 14:285-291.

Inoue T, Kato K, Kohda K, Mikoshiba K (1998) Type 1 inositol 1,4,5-trisphosphate receptor is required for induction of long-term depression in cerebellar Purkinje neurons. J Neurosci 18:5366-5373.

Ito M (1984) The Cerebellum and Neural Control.

Iwaki A, Kawano Y, Miura S, Shibata H, Matsuse D, Li W, Furuya H, Ohyagi Y, Taniwaki T, Kira J, Fukumaki Y (2008) Heterozygous deletion of ITPR1, but not SUMF1, in spinocerebellar ataxia type 16. J Med Genet 45:32-35.

Ji H, Shepard PD (2006) SK Ca2+-activated K+ channel ligands alter the firing pattern of dopamine-containing neurons in vivo. Neuroscience 140:623-633.

Jorntell H, Hansel C (2006) Synaptic memories upside down: bidirectional plasticity at cerebellar parallel fiber-Purkinje cell synapses. Neuron 52:227-238.

Kaemmerer WF, Reddy RG, Warlick CA, Hartung SD, McIvor RS, Low WC (2000) In vivo transduction of cerebellar Purkinje cells using adeno-associated virus vectors. Mol Ther 2:446-457.

Kanemaru K, Okubo Y, Hirose K, Iino M (2007) Regulation of neurite growth by spontaneous Ca2+ oscillations in astrocytes. J Neurosci 27:8957-8966.

Kano M, Hashimoto K, Tabata T (2008) Type-1 metabotropic glutamate receptor in cerebellar Purkinje cells: a key molecule responsible for long-term depression, endocannabinoid signalling and synapse elimination. Philos Trans R Soc Lond B Biol Sci 363:2173-2186.

Kasumu A, Bezprozvanny I (2010) Deranged Calcium Signaling in Purkinje Cells and Pathogenesis in Spinocerebellar Ataxia 2 (SCA2) and Other Ataxias. Cerebellum.

Kiehl TR, Nechiporuk A, Figueroa KP, Keating MT, Huynh DP, Pulst SM (2006) Generation and characterization of Sca2 (ataxin-2) knockout mice. Biochem Biophys Res Commun 339:17-24.

Kiehl TR, Shibata H, Pulst SM (2000) The ortholog of human ataxin-2 is essential for early embryonic patterning in C. elegans. J Mol Neurosci 15:231-241.

Kimura T, Sugimori M, Llinas RR (2005) Purkinje cell long-term depression is prevented by T-588, a neuroprotective compound that reduces cytosolic calcium release from intracellular stores. Proc Natl Acad Sci U S A 102:17160-17165.

Kohler M, Hirschberg B, Bond CT, Kinzie JM, Marrion NV, Maylie J, Adelman JP (1996) Small-conductance, calcium-activated potassium channels from mammalian brain. Science 273:1709-1714.

Lastres-Becker I, Rub U, Auburger G (2008) Spinocerebellar ataxia 2 (SCA2). Cerebellum 7:115-124.

Levy R, Hutchison WD, Lozano AM, Dostrovsky JO (2000) High-frequency synchronization of neuronal activity in the subthalamic nucleus of parkinsonian patients with limb tremor. J Neurosci 20:7766-7775.

Lin X, Antalffy B, Kang D, Orr HT, Zoghbi HY (2000) Polyglutamine expansion down-regulates specific neuronal genes before pathologic changes in SCA1. Nat Neurosci 3:157-163.

Liu J, Tang TS, Tu H, Nelson O, Herndon E, Huynh DP, Pulst SM, Bezprozvanny I (2009) Deranged calcium signaling and neurodegeneration in spinocerebellar ataxia type 2. J Neurosci 29:9148-9162.

Maltecca F, Magnoni R, Cerri F, Cox GA, Quattrini A, Casari G (2009) Haploinsufficiency of AFG3L2, the gene responsible for spinocerebellar ataxia type 28, causes mitochondria-mediated Purkinje cell dark degeneration. J Neurosci 29:9244-9254.

Mark MD, Maejima T, Kuckelsberg D, Yoo JW, Hyde RA, Shah V, Gutierrez D, Moreno RL, Kruse W, Noebels JL, Herlitze S (2011) Delayed postnatal loss of P/Q-type calcium channels recapitulates the absence epilepsy, dyskinesia, and ataxia phenotypes of genomic Cacna1a mutations. J Neurosci 31:4311-4326.

Matilla-Duenas A, Sanchez I, Corral-Juan M, Davalos A, Alvarez R, Latorre P (2009) Cellular and Molecular Pathways Triggering Neurodegeneration in the Spinocerebellar Ataxias. Cerebellum.

Matsumoto M, Nakagawa T, Inoue T, Nagata E, Tanaka K, Takano H, Minowa O, Kuno J, Sakakibara S, Yamada M, Yoneshima H, Miyawaki A, Fukuuchi Y, Furuichi T, Okano H, Mikoshiba K, Noda T (1996) Ataxia and epileptic seizures in mice lacking type 1 inositol 1,4,5-trisphosphate receptor. Nature 379:168-171.

Menzies FM, Huebener J, Renna M, Bonin M, Riess O, Rubinsztein DC (2010) Autophagy induction reduces mutant ataxin-3 levels and toxicity in a mouse model of spinocerebellar ataxia type 3. Brain 133:93-104.

Miyata M, Finch EA, Khiroug L, Hashimoto K, Hayasaka S, Oda SI, Inouye M, Takagishi Y, Augustine GJ, Kano M (2000) Local calcium release in dendritic spines required for long-term synaptic depression. Neuron 28:233-244.

Neher E, Sakaba T (2008) Multiple roles of calcium ions in the regulation of neurotransmitter release. Neuron 59:861-872.

Nicholls DG, Vesce S, Kirk L, Chalmers S (2003) Interactions between mitochondrial bioenergetics and cytoplasmic calcium in cultured cerebellar granule cells. Cell Calcium 34:407-424.

Nixon RA (2003) The calpains in aging and aging-related diseases. Ageing Res Rev 2:407-418.

Patko T, Vassias I, Vidal PP, De Waele C (2003) Modulation of the voltage-gated sodium- and calcium-dependent potassium channels in rat vestibular and facial nuclei after unilateral labyrinthectomy and facial nerve transsection: an in situ hybridization study. Neuroscience 117:265-280.

Paulson HL (2009) The spinocerebellar ataxias. J Neuroophthalmol 29:227-237.

Pedarzani P, Stocker M (2008) Molecular and cellular basis of small--and intermediate-conductance, calcium-activated potassium channel function in the brain. Cell Mol Life Sci 65:3196-3217.

Perkins EM, Clarkson YL, Sabatier N, Longhurst DM, Millward CP, Jack J, Toraiwa J, Watanabe M, Rothstein JD, Lyndon AR, Wyllie DJ, Dutia MB, Jackson M (2010) Loss of beta-III

spectrin leads to Purkinje cell dysfunction recapitulating the behavior and neuropathology of spinocerebellar ataxia type 5 in humans. J Neurosci 30:4857-4867.
Pirker W, Back C, Gerschlager W, Laccone F, Alesch F (2003) Chronic thalamic stimulation in a patient with spinocerebellar ataxia type 2. Mov Disord 18:222-225.
Potts MB, Adwanikar H, Noble-Haeusslein LJ (2009) Models of traumatic cerebellar injury. Cerebellum 8:211-221.
Pulst SM, Nechiporuk A, Nechiporuk T, Gispert S, Chen XN, Lopes-Cendes I, Pearlman S, Starkman S, Orozco-Diaz G, Lunkes A, DeJong P, Rouleau GA, Auburger G, Korenberg JR, Figueroa C, Sahba S (1996) Moderate expansion of a normally biallelic trinucleotide repeat in spinocerebellar ataxia type 2. Nat Genet 14:269-276.
Pulst SM, Santos N, Wang D, Yang H, Huynh D, Velazquez L, Figueroa KP (2005) Spinocerebellar ataxia type 2: polyQ repeat variation in the CACNA1A calcium channel modifies age of onset. Brain 128:2297-2303.
Riegel AC, Lupica CR (2004) Independent presynaptic and postsynaptic mechanisms regulate endocannabinoid signaling at multiple synapses in the ventral tegmental area. J Neurosci 24:11070-11078.
Ristori G, Romano S, Visconti A, Cannoni S, Spadaro M, Frontali M, Pontieri FE, Vanacore N, Salvetti M (2010) Riluzole in cerebellar ataxia: a randomized, double-blind, placebo-controlled pilot trial. Neurology 74:839-845.
Ross OA, Rutherford NJ, Baker M, Soto-Ortolaza AI, Carrasquillo MM, DeJesus-Hernandez M, Adamson J, Li M, Volkening K, Finger E, Seeley WW, Hatanpaa KJ, Lomen-Hoerth C, Kertesz A, Bigio EH, Lippa C, Woodruff BK, Knopman DS, White CL, 3rd, Van Gerpen JA, Meschia JF, Mackenzie IR, Boylan K, Boeve BF, Miller BL, Strong MJ, Uitti RJ, Younkin SG, Graff-Radford NR, Petersen RC, Wszolek ZK, Dickson DW, Rademakers R (2011) Ataxin-2 repeat-length variation and neurodegeneration. Hum Mol Genet 20:3207-3212.
Sailer CA, Hu H, Kaufmann WA, Trieb M, Schwarzer C, Storm JF, Knaus HG (2002) Regional differences in distribution and functional expression of small-conductance Ca2+-activated K+ channels in rat brain. J Neurosci 22:9698-9707.
Sailer CA, Kaufmann WA, Marksteiner J, Knaus HG (2004) Comparative immunohistochemical distribution of three small-conductance Ca2+-activated potassium channel subunits, SK1, SK2, and SK3 in mouse brain. Mol Cell Neurosci 26:458-469.
Sanpei K, Takano H, Igarashi S, Sato T, Oyake M, Sasaki H, Wakisaka A, Tashiro K, Ishida Y, Ikeuchi T, Koide R, Saito M, Sato A, Tanaka T, Hanyu S, Takiyama Y, Nishizawa M, Shimizu N, Nomura Y, Segawa M, Iwabuchi K, Eguchi I, Tanaka H, Takahashi H, Tsuji S (1996) Identification of the spinocerebellar ataxia type 2 gene using a direct identification of repeat expansion and cloning technique, DIRECT. Nat Genet 14:277-284.
Satterfield TF, Jackson SM, Pallanck LJ (2002) A Drosophila homolog of the polyglutamine disease gene SCA2 is a dosage-sensitive regulator of actin filament formation. Genetics 162:1687-1702.
Schols L, Bauer P, Schmidt T, Schulte T, Riess O (2004) Autosomal dominant cerebellar ataxias: clinical features, genetics, and pathogenesis. Lancet Neurol 3:291-304.
Schorge S, van de Leemput J, Singleton A, Houlden H, Hardy J (2010) Human ataxias: a genetic dissection of inositol triphosphate receptor (ITPR1)-dependent signaling. Trends Neurosci 33:211-219.
Serra HG, Duvick L, Zu T, Carlson K, Stevens S, Jorgensen N, Lysholm A, Burright E, Zoghbi HY, Clark HB, Andresen JM, Orr HT (2006) RORalpha-mediated Purkinje cell development determines disease severity in adult SCA1 mice. Cell 127:697-708.

Seutin V, Mkahli F, Massotte L, Dresse A (2000) Calcium release from internal stores is required for the generation of spontaneous hyperpolarizations in dopaminergic neurons of neonatal rats. J Neurophysiol 83:192-197.

Shakkottai VG, Chou CH, Oddo S, Sailer CA, Knaus HG, Gutman GA, Barish ME, LaFerla FM, Chandy KG (2004) Enhanced neuronal excitability in the absence of neurodegeneration induces cerebellar ataxia. J Clin Invest 113:582-590.

Shakkottai VG, do Carmo Costa M, Dell'Orco JM, Sankaranarayanan A, Wulff H, Paulson HL (2011) Early changes in cerebellar physiology accompany motor dysfunction in the polyglutamine disease spinocerebellar ataxia type 3. J Neurosci 31:13002-13014.

Sharp AH, Nucifora FC, Jr., Blondel O, Sheppard CA, Zhang C, Snyder SH, Russell JT, Ryugo DK, Ross CA (1999) Differential cellular expression of isoforms of inositol 1,4,5-triphosphate receptors in neurons and glia in brain. J Comp Neurol 406:207-220.

Shuvaev AN, Horiuchi H, Seki T, Goenawan H, Irie T, Iizuka A, Sakai N, Hirai H (2011) Mutant PKCgamma in spinocerebellar ataxia type 14 disrupts synapse elimination and long-term depression in Purkinje cells in vivo. J Neurosci 31:14324-14334.

Smith SL, Otis TS (2003) Persistent changes in spontaneous firing of Purkinje neurons triggered by the nitric oxide signaling cascade. J Neurosci 23:367-372.

Stocker M, Pedarzani P (2000) Differential distribution of three Ca(2+)-activated K(+) channel subunits, SK1, SK2, and SK3, in the adult rat central nervous system. Mol Cell Neurosci 15:476-493.

Strahlendorf J, Box C, Attridge J, Diertien J, Finckbone V, Henne WM, Medina MS, Miles R, Oomman S, Schneider M, Singh H, Veliyaparambil M, Strahlendorf H (2003) AMPA-induced dark cell degeneration of cerebellar Purkinje neurons involves activation of caspases and apparent mitochondrial dysfunction. Brain Res 994:146-159.

Street VA, Bosma MM, Demas VP, Regan MR, Lin DD, Robinson LC, Agnew WS, Tempel BL (1997) The type 1 inositol 1,4,5-trisphosphate receptor gene is altered in the opisthotonos mouse. J Neurosci 17:635-645.

Strobaek D, Teuber L, Jorgensen TD, Ahring PK, Kjaer K, Hansen RS, Olesen SP, Christophersen P, Skaaning-Jensen B (2004) Activation of human IK and SK Ca2+ -activated K+ channels by NS309 (6,7-dichloro-1H-indole-2,3-dione 3-oxime). Biochim Biophys Acta 1665:1-5.

Surmeier DJ (2007) Calcium, ageing, and neuronal vulnerability in Parkinson's disease. Lancet Neurol 6:933-938.

Surmeier DJ, Guzman JN, Sanchez-Padilla J (2010) Calcium, cellular aging, and selective neuronal vulnerability in Parkinson's disease. Cell Calcium 47:175-182.

Szatanik M, Vibert N, Vassias I, Guenet JL, Eugene D, de Waele C, Jaubert J (2008) Behavioral effects of a deletion in Kcnn2, the gene encoding the SK2 subunit of small-conductance Ca2+-activated K+ channels. Neurogenetics 9:237-248.

Tang TS, Guo C, Wang H, Chen X, Bezprozvanny I (2009) Neuroprotective effects of inositol 1,4,5-trisphosphate receptor C-terminal fragment in a Huntington's disease mouse model. J Neurosci 29:1257-1266.

Tang TS, Tu H, Chan EY, Maximov A, Wang Z, Wellington CL, Hayden MR, Bezprozvanny I (2003) Huntingtin and huntingtin-associated protein 1 influence neuronal calcium signaling mediated by inositol-(1,4,5) triphosphate receptor type 1. Neuron 39:227-239.

Thompson-Vest N, Shimizu Y, Hunne B, Furness JB (2006) The distribution of intermediate-conductance, calcium-activated, potassium (IK) channels in epithelial cells. J Anat 208:219-229.

Tu H, Nelson O, Bezprozvanny A, Wang Z, Lee S-F, Hao YH, Serneels L, De Strooper B, Yu G, Bezprozvanny I (2006) Presenilins form ER calcium leak channels, a function disrupted by mutations linked to familial Alzheimer's disease. Cell 126:981-993.

van de Leemput J, Chandran J, Knight MA, Holtzclaw LA, Scholz S, Cookson MR, Houlden H, Gwinn-Hardy K, Fung HC, Lin X, Hernandez D, Simon-Sanchez J, Wood NW, Giunti P, Rafferty I, Hardy J, Storey E, Gardner RJ, Forrest SM, Fisher EM, Russell JT, Cai H, Singleton AB (2007) Deletion at ITPR1 underlies ataxia in mice and spinocerebellar ataxia 15 in humans. PLoS Genet 3:e108.

van de Loo S, Eich F, Nonis D, Auburger G, Nowock J (2009) Ataxin-2 associates with rough endoplasmic reticulum. Exp Neurol 215:110-118.

Vecellio M, Schwaller B, Meyer M, Hunziker W, Celio MR (2000) Alterations in Purkinje cell spines of calbindin D-28 k and parvalbumin knock-out mice. Eur J Neurosci 12:945-954.

Vergara C, Latorre R, Marrion NV, Adelman JP (1998) Calcium-activated potassium channels. Curr Opin Neurobiol 8:321-329.

Vig PJ, Subramony SH, Qin Z, McDaniel DO, Fratkin JD (2000) Relationship between ataxin-1 nuclear inclusions and Purkinje cell specific proteins in SCA-1 transgenic mice. J Neurol Sci 174:100-110.

Vig PJ, Wei J, Shao Q, Lopez ME, Halperin R, Gerber J (2011) Suppression of Calbindin-D28k Expression Exacerbates SCA1 Phenotype in a Disease Mouse Model. Cerebellum.

Walter JT, Alvina K, Womack MD, Chevez C, Khodakhah K (2006) Decreases in the precision of Purkinje cell pacemaking cause cerebellar dysfunction and ataxia. Nat Neurosci 9:389-397.

Wang SS, Denk W, Hausser M (2000) Coincidence detection in single dendritic spines mediated by calcium release. Nat Neurosci 3:1266-1273.

Waroux O, Massotte L, Alleva L, Graulich A, Thomas E, Liegeois JF, Scuvee-Moreau J, Seutin V (2005) SK channels control the firing pattern of midbrain dopaminergic neurons in vivo. Eur J Neurosci 22:3111-3121.

Watase K, Barrett CF, Miyazaki T, Ishiguro T, Ishikawa K, Hu Y, Unno T, Sun Y, Kasai S, Watanabe M, Gomez CM, Mizusawa H, Tsien RW, Zoghbi HY (2008) Spinocerebellar ataxia type 6 knockin mice develop a progressive neuronal dysfunction with age-dependent accumulation of mutant CaV2.1 channels. Proc Natl Acad Sci U S A 105:11987-11992.

Watase K, Gatchel JR, Sun Y, Emamian E, Atkinson R, Richman R, Mizusawa H, Orr HT, Shaw C, Zoghbi HY (2007) Lithium therapy improves neurological function and hippocampal dendritic arborization in a spinocerebellar ataxia type 1 mouse model. PLoS Med 4:e182.

Welsh JP, Yamaguchi H, Zeng XH, Kojo M, Nakada Y, Takagi A, Sugimori M, Llinas RR (2005) Normal motor learning during pharmacological prevention of Purkinje cell long-term depression. Proc Natl Acad Sci U S A 102:17166-17171.

Werth JL, Thayer SA (1994) Mitochondria buffer physiological calcium loads in cultured rat dorsal root ganglion neurons. J Neurosci 14:348-356.

Womack M, Khodakhah K (2002) Active contribution of dendrites to the tonic and trimodal patterns of activity in cerebellar Purkinje neurons. J Neurosci 22:10603-10612.

Womack MD, Khodakhah K (2003) Somatic and dendritic small-conductance calcium-activated potassium channels regulate the output of cerebellar Purkinje neurons. J Neurosci 23:2600-2607.

Yanovsky Y, Zhang W, Misgeld U (2005) Two pathways for the activation of small-conductance potassium channels in neurons of substantia nigra pars reticulata. Neuroscience 136:1027-1036.

Zhu LP, Yu XD, Ling S, Brown RA, Kuo TH (2000) Mitochondrial Ca(2+)homeostasis in the regulation of apoptotic and necrotic cell deaths. Cell Calcium 28:107-117.

Zhuchenko O, Bailey J, Bonnen P, Ashizawa T, Stockton DW, Amos C, Dobyns WB, Subramony SH, Zoghbi HY, Lee CC (1997) Autosomal dominant cerebellar ataxia (SCA6)

associated with small polyglutamine expansions in the alpha 1A-voltage-dependent calcium channel. Nat Genet 15:62-69.